A Mechanistic Insight into Yeast Chemotropism and the Development of New Tools to Study This Phenomenon

BY

REAGAN E. DEFLORIO
B.S., Butler University, 2003

THESIS

Submitted as partial fulfillment of the requirements
for the degree of Doctor of Philosophy in
Biological Sciences
in the Graduate College of the
University of Illinois at Chicago, 2012

Chicago, Illinois

Defense Committee:

Axia Alfonso, Chair
David Stone, Advisor
Ronald Dubreuil
Teresa Orenic
Robert Arkowitz, Université de Nice

This thesis is dedicated to my family and friends

for their constant love and support,

without which this would never

have been accomplished.

"They can call me crazy if I fail. All the chance that I need is one in a million,

and they can call me brilliant if I succeed."

~ Ani DiFranco

ACKNOWLEDGEMENTS

I would like to thank the following individuals for their advice, support, guidance, and experimental contributions, which have made this possible:

Dr. David Stone and the Stone Lab at the University of Illinois at Chicago: Amber Ismael, Dmitry Suchkov, Madhu Sukumar, Nik Waszczak, Dr. Edward Draper, Dr. E Li, Dr. Metodi Metodiev, and Liz Apollinari

Dr. Robert Arkowitz and the Arkowitz Lab at the Université de Nice-Sophia Antipolis: Aurélia Vernay, Dr. Martine Bassalina, Dr. Vincent Corvest, Béatrice Polo, and Dr. Sebastien Schaub

Dr. David Eddington and Marie-Elena Brett at the University of Illinois at Chicago, Bioengineering Department

My committee members at the University of Illinois at Chicago: Dr. Aixa Alfonso, Dr. Ronald Dubreuil, Dr. Teresa Orenic, and Dr. Jennifer Schmidt

Dr. Daniel Lew and Jayme Johnson at Duke University

I would also like to thank the following individuals for being the most wonderful and brilliant family and friends one could ever have:

Kristin Allen, Dr. Karin Anderson, Dr. Nathalie Arquier, Dr. Roberto Bandiera, Rachel Barnett, Dr. Lynn Clary, Ralph and Christina DeFlorio, Rachel Foster, Nica Gonzalez, Amber Ismael, Patrick Jouandin, Rita Keeling, Hsiao-Lei Lai, Giovanni Marchetti, Dr. Paco Martin, Dana McKinney, Laetitia Paganelli, Dr. Sandrine Pizette, Dr. Nadia Ranieri, Dr. Nuria Romero, Lindsey Rosen, Aurélia Vernay, Rémi and Annick Vernay, Nik Waszczak, Catrina Won, Zi Yang

Thank you all! I never would have made it without you.

RED

TABLE OF CONTENTS

TABLE OF CONTENTS (continued)

CHAPTER PAGE

LIST OF TABLES

LIST OF FIGURES

LIST OF ABBREVIATIONS

cAMP	3', 5'-cyclic Adenosine MonoPhosphate
cAR1	cAMP Receptor 1
CDC24	Cell Division Cycle 24, Cdc42 GEF
CDC42	Cell Division Cycle 42, Rho-like GTPase
BEM1	Bud EMergence 1, polarisome component
BUD1	BUD site selection 1, Ras-family GTPase
DCC	Deleted in Colorectal Cancer, Netrin receptor
FAR1	Factor ARrest 1, cyclin-dependent kinase inhibitor
FRAP	Fluorescence Recovery After Photo-bleaching
FUS3	MAPK required for cell FUSion
Gα	G protein α subunit encoded by *GPA1*
$G\alpha^{DSD}$	Mutant Gα unable to bind Fus3, encoded by $gpa1^{K21E\ R22E}$
Gβ	G protein β subunit encoded by *STE4*
$G\beta^{P-}$	Mutant Gβ unable to be phosphorylated, encoded by $ste4^{T320A\ S335A}$
Gγ	G protein γ subunit encoded by *STE18*
GEF	Guanine nucleotide Exchange Factor
GFP	Green Fluorescent Protein
GPCR	G Protein Coupled Receptor
GSK-3	Glycogen Synthase Kinase-3
GTP	Guanosine-5'-triphosphate
GTPase	Enzyme that hydrolyzes GTP to GDP
iFRAP	inverse Fluorescence Recovery After Photo-bleaching
LEGI	Local Excitation-Global Inhibition

LIST OF ABBREVIATIONS (continued)

MAPK	Mitogen-Activated Protein Kinase
MAT	MATing type locus
Netrin	Attractive axon guidance cue
PAK	p21 Activated Kinase
PH	Pleckstrin Homology
PI3K	Phosphatidyl-Inositol 3-Kinase
PIP_2	Phosphatidyl-Inositol (4,5)-bisPhosphate
PIP_3	Phosphatidyl-Inositol (3,4,5)-triPhosphate
PTEN	Phosphatase and TENsin homolog
Rac	Subfamily of Rho GTPases
Ras	RAt Sarcoma superfamily of small GTPases
Rho	Subfamily of Ras GTPases
ROBO	ROundaBOut family cell adhesion molecule
ROCK	Rho-associated protein kinase
SEM	Standard Error of Mean
SMP	Small Multiple Protrusions
Slit	Repulsive axon guidance cue
SPA2	Spindle Pole Antigen 2, polarisome component
STE2	STErile 2, *MAT***a** pheromone receptor
WT	Wild Type

SUMMARY

Chemotaxis and chemotropism are important biological processes required throughout eukaryotic development. Understanding how cells interpret complex signaling gradients and direct their movement or growth in response to such gradients is a fundamental question of cell biology. The mating response of *Saccharomyces cerevisiae* is chemotropic. Mating yeast interpret gradients of pheromone secreted by cells of the opposite mating type and are able to orient their growth in the direction of the closest mating partner. The mating response is mediated by a transmembrane receptor and its associated heterotrimeric G protein. Upon binding of pheromone by the receptor, the G protein dissociates into its active Gα subunit and its free Gβγ dimer. The Gβγ dimer is anchored to the membrane via lipid moieties that are covalently attached to the Gγ subunit. The Gβ subunit is rapidly phosphorylated at multiple sites and interacts with several downstream effectors to transmit the mating signal throughout the cell and mark the site on the membrane where chemotropic growth will occur.

My results show that this phosphorylation event is critical for proper communication between the pheromone receptor and polarity establishment proteins that direct polarized growth in a pheromone gradient. Pheromone-stimulated cells unable to phosphorylate Gβ mislocalize Gβ and other polarity proteins, and the phosphorylation state of Gβ affects the dynamics of its interactions with these proteins. Gβ phosphorylation is also required for stable growth of a mating projection. In cells unable to phosphorylate Gβ, the axis of polarity exhibits constrained wandering within the area of receptor localization causing formation of abnormal mating projections. I also demonstrate that Gβ phosphorylation is important for initial orientation and reorientation in a pheromone gradient.

SUMMARY (continued)

Pheromone gradients in mating mixtures are dynamic. Therefore, cells must employ mechanisms to redirect their growth as the direction of the gradient changes. Although the ability to reorient is necessary for chemotaxing and chemotroping cells, very little is known about this phenomenon. I began investigating the mechanisms underlying reorientation by following the movement fluorescently-tagged proteins in reorienting cells. My results suggest that Gβ and Spa2 are early regulators of this process, as these proteins localize to the new growth site prior to morphogenesis. To advance future studies aimed at elucidating the mechanisms guiding cell reorientation, I developed and validated a novel genetic screen to uncover mutants specifically defective in this process. In collaboration with Dr. Eddington's laboratory at the University of Illinois, I developed a microfluidic device that can generate stable pheromone gradients and rapidly rotate them in 90° increments, mimicking the dynamic gradients yeast are exposed to *in situ*. Collectively, my research has advanced our understanding of the mechanisms guiding yeast chemotropism and generated powerful new tools to facilitate future research of the reorientation process.

1. INTRODUCTION

1.1 Chemotaxis and Chemotropism

Chemotaxis is directed cell movement in response to a chemical gradient. Cells are able to interpret external signaling gradients and translate these into intracellular signals that guide cell movement toward the source of a chemoattractant or away from the source of a repellent. The ability of cells to move directionally underlies many important biological processes. During embryogenesis, cells migrate in response to chemical stimuli to form organized tissues and organs (Thiery, 1984). In adults, chemotaxis is essential for the movement of leukocytes during the immune response and migration of fibroblasts to sites of wound healing (Mrass and Weninger, 2006; Postlethwaite et al., 1976). Recent studies have shown that the migration of stem cells is also directional (Laird et al., 2008). In addition to its role in normal physiology, chemotaxis also plays an important role in many pathological conditions. Directed movement of tumor cells in response to chemokines is required for cancer metastasis, and improper movement of chemotactic immune cells leads to chronic inflammatory diseases such as asthma and arthritis (Jin et al., 2008).

The related phenomenon of chemotropism is polarized cell growth in response to a chemical gradient. The directional growth exhibited by neuronal cells during development and maintenance of the nervous system is dependent on the ability of these cells to interpret signaling gradients and polarize their growth properly in response (Raper and Mason, 2010). The growing axon of a nerve cell is able to interpret both attractive and repulsive guidance cues (O'Donnell et al., 2009). Survival of metastatic

tumors requires invasion of healthy tissue by vascularization through angiogenesis. (Klagsbrun and Eichmann, 2005). The mating response of *Saccharomyces cerevisiae* is also chemotropic (Arkowitz, 2009), and this highly conserved eukaryotic system is a convenient model for studying signal induced cell polarization.

Although chemotactic and chemotropic cells differ fundamentally in their mode of cellular displacement, there exists a common set of problems cells undergoing either process must overcome. Both cell types must be able to interpret complex signaling gradients and convert these external guidance cues into intracellular signals that will guide cell polarity. They must be able to sense the direction of the gradient and decide if they will be drawn toward it or away from it. Once cells have properly read the signal and a directional decision has been made, they must then recruit proteins responsible for polarizing growth to the site on the membrane facing the specified direction. This site becomes the leading or front edge of the cell while the opposite side of the cell becomes the back. As cell growth or migration is occurring, the dynamic chemical gradient is changing. Therefore, cells must also employ mechanisms allowing an update of the external signal. Once the cell has sensed a shift in the gradient, it must be able to reorient its direction of growth or movement in response to this change.

1.2 Molecular models of directional sensing

Although many cell types rely on directional sensing to perform their necessary functions, this process has been studied most in the eukaryotic chemotactic systems of *Dictyostelium discoideum* and mammalian leukocytes, and in the eukaryotic chemotropic systems of growing axons and mating *Saccharomyces cerevisiae*.

Chemotactic and chemotropic cells display an impressive ability to interpret external signaling gradients. It has been shown that these cells can interpret gradients that vary as little as 0.5-10% across the width of the cell (Fisher et al., 1989; Lohof et al., 1992; Mato et al., 1975; Moore et al., 2008; Segall, 1993; Zigmond, 1977). How these cells are able to convert very slight differences in receptor occupancy across the cell surface into a robust directional response culminating in cell polarization is an important question. Due to the high conservation of proteins involved in these processes across species, we have been able to gain most of our knowledge of how cells interpret chemical gradients from research on chemotaxis and chemotropism using the above-mentioned eukaryotic models.

1.2.1 Chemotactic movement of amoebae and neutrophils

Our current knowledge of how directional sensing occurs in chemotactic cells has largely come from the study of the amoebae *D. discoideum* and mammalian leukocytes. *D. discoideum* moves in response to gradients of folic acid secreted by bacterial cells during normal growth and to gradients of 3', 5'-cyclic adenosine monophosphate (cAMP) secreted by neighboring cells under starvation conditions; the latter stimulates cells to migrate toward each other to enable formation of a multicellular aggregate that can undergo differentiation and morphogenesis (Wang et al., 2011). Neutrophils are a key component of the immune system, and these cells migrate to sites of infection by responding to gradients of various chemokines in the blood and tissues (Williams et al., 2011). Although these two cell types are highly divergent, the mechanisms underlying their chemotactic responses are quite similar.

Guidance cues from the environment are bound by G protein coupled receptors (GPCRs) that are uniformly distributed across the surface of the cell (Franca-Koh et al., 2009; Servant et al., 1999; Xiao et al., 1997). Occupation of the receptor induces activation and dissociation of the heterotrimeric G protein into its Gα and Gβγ subunits and initiates a signaling response that is amplified to reflect the external gradient. This ultimately leads to a reorganization of signaling components and the cytoskeleton so that the cell is divided into a gradient-sensitive leading edge and subordinate lagging edge (Franca-Koh et al., 2009; Wang et al., 2011; Williams et al., 2011). Chemotactic cells keep the receptor and the G protein uniformly distributed on the cell surface to enable quick and frequent changes in direction. Thus, there is likely an asymmetric redistribution of downstream signaling components that reflects the external gradient (Jin et al., 2000; Servant et al., 2000). Activation of the G protein leads to recruitment of pleckstrin homology (PH) domain-containing proteins from the cytosol to the leading edge of the cell (Comer and Parent, 2002; Servant et al., 2000), and accumulation of the lipid kinase phosphatidylinositol 3-kinase (PI3K) facilitates the conversion of phosphatidylinositol (4,5)-bisphosphate (PIP_2) to phosphatidylinositol (3,4,5)-triphosphate (PIP_3) (Franca-Koh et al., 2009). Once generated, this intracellular signaling gradient must be linked to polymerization of the actin cytoskeleton toward the leading edge and suppression of growth at the lagging edge, but how this is achieved is not clearly understood.

In *D. discoideum*, chemotaxis is primarily mediated by the GPCR, cAR1, and binding of cAMP leads to activation of the receptor and its associated G protein (Chen et al., 1996; Milne et al., 1997). Following gradient exposure, cAR1 remains uniformly

distributed across the cell surface, but the interaction between cAR1 and cAMP is prolonged at the leading edge compared to the lagging edge of the cell (Ueda et al., 2001; Xiao et al., 1997). This suggests there may be asymmetric activation of cAR1 and the G protein, but this is likely not sufficient to amplify the external gradient and direct actin polymerization to this site. There have been several pathways, downstream of the receptor and G protein, implicated in amplification of the intracellular signal (Wang et al., 2011).

The first pathway discovered to play a role in this process involves the production and degradation of the second messenger, PIP_3. Activation of cAR1 results in recruitment of PI3Ks to the leading edge where they phosphorylate PIP_2, generating a gradient of PIP_3 (Funamoto et al., 2002; Parent et al., 1998). This gradient might be enhanced through a positive feedback loop involving PI3K and the GTPase, Ras. Continuous activation of PI3K requires Ras activity, and continuous activation of Ras requires PI3K activity (Sasaki and Firtel, 2006). Ras remains uniformly distributed around the cell, but it is locally activated prior to PI3K activation at the leading edge in response to a gradient of chemoattractant (Kae et al., 2004; Sasaki et al., 2007). The phosphatase and tensin homologue (PTEN) is responsible for converting PIP_3 to PIP_2, and exposure to a gradient of cAMP results in an inverse gradient of PTEN at the rear of the cell (Funamoto et al., 2002; Iijima and Devreotes, 2002). As membrane localization of PTEN is dependent on PIP_2 binding, PTEN accumulation at the rear of the cell may by a consequence of enhanced PI3K activity at the leading edge (Iijima et al., 2004). This exclusion of PTEN from the leading edge results in even more PIP_3 accumulation at this site. Thus, the combination of PI3K and Ras activity at the leading

edge of the cell and restricted PTEN phosphatase activity at the back of the cell generates a steep intracellular gradient of PIP_3, which reflects the external cAMP gradient (Kortholt et al., 2007). Several PH domain-containing proteins and GEFs for small GTPases, which regulate actin polymerization, are known to be downstream effectors of PIP_3 (Wang et al., 2011). Therefore, it is possible that the role of accumulation at the leading edge is to recruitment these proteins to direct actin polymerization toward the front of the cell.

Although the PIP_3 pathway is an important mediator of chemotaxis in *D. discoideum*, there must be other pathways capable of generating intracellular signaling gradients and directed actin polymerization because chemotaxis is still observed in cells lacking all PI3Ks and PTEN (Hoeller and Kay, 2007). To date, there have been three additional pathways proposed to mediate chemotaxis in *D. discoideum*, including PLA2 signaling, guanylyl cyclase regulation of cGMP, and Ras regulation of the TorC2 complex (Wang et al., 2011). The Ca^{2+}-sensitive phospholipase A2 (PLA2A) is responsible for converting phosphatidylcholine to arachidonic acid and has been shown to mediate actin polymerization during chemotaxis (Kolsch et al., 2008; Wang et al., 2011). While loss of either the PIP_3 pathway or the PLA2 pathway only slightly impairs chemotaxis, inactivation of both pathways results in an inability of cells to polymerize their actin cytoskeletons in response to gradients of cAMP (Wang et al., 2011). This suggests there is redundancy between these two lipid-mediated signaling pathways.

Regulation of chemotactic movement by soluble guanylyl cyclase involves production of cGMP. Upon cAMP stimulation, guanylyl cyclase produces cGMP at the back of the cell and mediates a pathway that both facilitates and represses pseudopod

formation (Veltman and Van Haastert, 2006). cGMP regulates myosin II filaments at the rear of the cell, thereby suppressing pseudopod extension at the lagging edge and allowing cells to restrict pseudopod extension to the leading edge (Goldberg et al., 2002). The final pathway implicated in chemotaxis involves Ras regulation of the protein kinase TORC2. As discussed above, Ras GTPases are activated downstream of the receptor and G protein and promote activation of PI3Ks. RasC and RasG have been shown to mediate chemotactic signaling (Khosla et al., 2000; Lim et al., 2001). RasC activates the protein kinase TORC2 (Cai et al., 2010; Charest et al., 2010). TORC2 phosphorylates PIP_3-responsive PH domain-containing PKB proteins at the leading edge of the cell (Kamimura et al., 2008). Therefore, RasC likely mediates crosstalk between PIP_3-mediated and TORC2-mediated activation of PH domain-containing proteins at the leading edge of the cell during chemotaxis.

Directional sensing in neutrophils is mediated by a more diverse set of GPCRs, but it is still important for these cells to localize PIP_3 to the leading edge during chemotaxis (Williams et al., 2011). Addition of PIP_3 to cells induces front-like morphological changes in cultured cells, and it is involved in a positive feedback loop that leads to increased self-production through recruitment of PI3K (Weiner et al., 2002). One difference between neutrophils and *D. discoideum* is that the positive feedback loop established to generate accumulation of PIP_3 is dependent on Rac activity not Ras activity (Wang et al., 2002). Activation of Rac is mediated by the guanine nucleotide exchange factor (GEF) DOCK2 whose membrane recruitment depends on PIP_3 (Nishikimi et al., 2009), and activation of Rac facilitates production of PIP_3. Chemotaxing neutrophils also employ a mechanism to negatively regulate PIP_3

accumulation at the sides and rear of the cell, but this is carried out by the SHIP1 phosphatase instead of PTEN as in *D. discoideum* (Nishio et al., 2007).

Directional sensing occurs independent of actin polymerization, exhibited by the formation of PIP_3 gradients in cells with disrupted actin cytoskeletons (Janetopoulos et al., 2004; Jin et al., 2000; Sasaki et al., 2004; Servant et al., 2000). However, actin is required for the directed movement of eukaryotic cells (Berzat and Hall, 2010). As in directional sensing, polarization of the actin cytoskeleton during neutrophil chemotaxis also requires activation of the G protein and release of the Gβγ subunit. It has been shown that Gβγ directly binds the p-21 activated kinase PAK1, which is coupled to the PAK1-associated protein PIXα (Li et al., 2003). PIXα is a GEF that activates Cdc42, which in turn promotes PAK1 kinase activity. While Rac is required for formation of F-actin cables, Cdc42 restricts actin polymerization to the leading edge of the cell (Srinivasan et al., 2003). This implicates Gβγ as the earliest positional determinant downstream of the occupied receptor in selection of a polarized growth site during chemotaxis.

1.2.2 Chemotropic growth of neurons

Like chemotaxing cells, chemotropic cells interpret chemical gradients via membrane bound surface receptors. During chemotaxis, cells must be able to change direction quickly and often as they move rapidly. It is probably for this reason that they keep their receptors uniformly distributed across the cell surface. Chemotropism is a more long-term, committed response. These cells usually polarize their receptors on the side of the cell facing the gradient to allow a more exclusive input from one direction. In

rat neurons, a gradient of GABA (γ-aminobutyric acid) induces an asymmetric lateral redistribution of GABA receptors (Bouzigues et al., 2007). This is thought to initiate a positive-feedback loop in which receptor activation results in an increase in Ca^{2+}, which stabilizes microtubules and allows stable delivery of more receptors. This phenomenon of receptor redistribution is also observed during yeast chemotropism, which will be discussed in greater detail in section 1.3.

Axon pathfinding during neuronal development is a well-studied chemotropic process (Raper and Mason, 2010). At the tip of a growing axon there is an actin-rich region called the growth cone. The growth cone receives attractive and repulsive signals that influence microtubule-driven growth of the axon. Prior to chemotropic elongation of an axon, a developing neuron is composed of many thin protrusions called neurites. Axon formation begins by selection of a single neurite to become the growing axon while growth of the remaining neurites is inhibited (Dottie et al., 1988). Although there may exist external signals that influence which neurite is selected for growth, our current knowledge suggests that this selection process is based on intrinsic signals within the cell. One such cue is thought to be the localization of the centrosome and the Golgi. These structures are situated next to the first neurite formed after mitotic cell division and act as positional determinants that mark this neurite for growth (de Anda et al., 2005; Zmuda and Rivas, 1998). Localization of the Golgi at this site suggests there is likely differential delivery of proteins that promote axonal growth specifically targeted to the chosen neurite. As in chemotaxing cells, PIP_3 accumulation is observed in the neurite tip, and inhibition of PI3K disrupts axon formation suggesting PIP_3 is a key regulator of axon formation (Menager et al., 2004; Shi et al., 2003). One way that PIP_3

might influence neurite outgrowth is by activating the Akt kinase, which phosphorylates and thereby inactivates the kinase GSK-3 (Jiang et al., 2005; Salcedo-Tello et al., 2011; Shi et al., 2004). Localized inhibition of GSK-3 activity prevents phosphorylation of the tumor suppressor protein APC, and unphosphorylated APC stabilizes microtubule plus ends promoting elongation of the neurite (Salcedo-Tello et al., 2011; Shi et al., 2004; Zumbrunn et al., 2001). Cdc42 also localizes to the neurite tip, along with other members of both the Ras and Rho-families of small GTPases, and its activation is required for axon formation (Hall and Lalli, 2010; Schwamborn and Puschel, 2004). Cdc42 is regulated by the Par6-aPKC complex in many polarity pathways (Etienne-Manneville, 2004; Shi et al., 2003). This complex is also found at the neurite tip where it interacts with the Rac exchange factor Stef (Nishimura et al., 2005). Rac activates PI3K, which promotes further PIP_3 accumulation. Currently there are no known Cdc42 exchange factors required for axon formation, but if there exist PIP_3-sensitve exchange factors, this would support a positive-feedback loop resulting in localized Cdc42 activation at the tip of the forming axon. In addition to Cdc42, GTP-Ras accumulates at the tip of the neurite as a result of targeted vesicular transport (Fivaz et al., 2008). Ras activation requires PI3K, and PI3K is a target of Ras, suggesting a positive feedback loop leading to activation of Ras at the neurite (Hall and Lalli, 2010; Yoshimura et al., 2006). The selective positioning of the Golgi ensures Ras delivery is confined to the neurite selected for axonal growth.

Once a single neurite has been selected to elongate, the growing axon must be able to interpret guidance cues from the environment to grow in the appropriate direction. Some of the most well studied guidance cues include: Netrins, Slits,

Semaphorins, and Ephrins (O'Donnell et al., 2009). These small molecules are bound by receptors in the growth cone. Axon turning is thought to occur by simultaneous stabilization of actin in the direction of the gradient and actin destabilization in distal areas of the cell. Actin dynamics influence microtubule plus ends to elongate toward the attractant. Growing axons respond to both attractive and repulsive cues. Signaling from activated Rho and its target kinase ROCK is important for inducing actomyosin contractions that collapse axon growth in response to repulsive cues (Narumiya et al., 2009; Wahl et al., 2000), while Rac and Cdc42 mediate growth in response to attractive cues. In cultured neurons, the DCC receptor activates Cdc42 and Rac upon binding of Netrin-1 (Hall and Lalli, 2010; Li et al., 2002a; 2002b). Activated Cdc42 and Rac promote Arp2/3-dependent actin polymerization and stabilization of actin and microtubules through PAK activity (Daub et al., 2001; Shekarabi et al., 2005).

1.2.3 Mechanistic models of chemotaxis

As discussed above, chemotactic and chemotropic cells have a common set of problems to solve when sensing the direction of a gradient and orienting their movement or growth in response. These cells must interpret complex signaling gradients accurately by responding to activation of GPCRs and their associated G proteins. The induced signal must be strong enough to direct polymerization of actin cables or microtubules, via Ras and Rho-family GTPase activity, to the site on the membrane where polarized growth should occur. Although little is known about how cells reorient in dynamic gradients, cells must also employ mechanisms to continually update the signal to maintain or change direction as the gradient changes. Several

models have been proposed to explain how chemotactic cells are able to generate such robust responses in very shallow gradients of chemoattractant (Iglesias and Devreotes, 2008), but a similar mechanistic understanding is lacking in chemotropic cells.

One of the most popular mechanistic models of gradient sensing is the local excitation-global inhibition (LEGI) model (Kutscher et al., 2004; Levchenko and Iglesias, 2002; Parent and Devreotes, 1999). In a LEGI mechanism, receptor activation leads to a rapid local activation of the response and is followed by a slower global inhibition of the response throughout the cell. This model accurately predicts cellular responses to increasing steps and gradients of chemoattractant, but it does not account for intracellular amplification of the external gradient observed by accumulation of signaling molecules at the leading edge (Iglesias and Devreotes, 2008; Xiong et al., 2010). The 'balanced inactivation model' was proposed to address this shortcoming in the LEGI model (Levine et al., 2006). This model is based on the LEGI model but includes an inactivator, which is mutually antagonistic to the response. This additional component increases the extent of intracellular gradient amplification.

Several models increase the amplification potential even further by incorporating positive-feedback loops (Iglesias and Devreotes, 2008). As in the LEGI model, these models rely on local receptor activation but also include the presence of a local inhibitor that slowly diffuses away from the site of activated receptor (Meier-Schellersheim et al., 2006; Xu et al., 2007). More importantly, these models propose the employment of mechanisms that allow activated components of the response to positively regulate their own production via autocatalytic effects (Meier-Schellersheim et al., 2006; Postma and Van Haassert, 2001), substrate delivery (Skupsky et al., 2005; Xu et al., 2007), or

degradation inhibition (Gamba et al., 2005). Due to the high signal amplification in these models, the actual shape of the gradient can be lost. Therefore, it is likely that these models more accurately reflect downstream polarization events rather than initial detection of the gradient (Iglesias and Devreotes, 2008). Finally, there are the models of spontaneous polarization, which rely on the steady state of response components being unstable (Narang, 2006; Subramanian and Narang, 2004). This allows subtle noise-induced asymmetries to be amplified by mutual inhibition of antagonistic components leading to eventual separation into 'front' and 'back' of the cell components (Iglesias and Devreotes, 2008).

Although each of these models can account for some aspects of gradient sensing and cell polarization, none of them can fully explain how both processes occur within the same cell. The mechanisms guiding these processes likely combine different components from these models at various steps during the response. Even though a complete, accurate gradient sensing model has not yet been defined for chemotactic cells, even less is known about how yeast interpret signaling gradients and generate amplified intracellular signaling gradients. Previous research on the mating response of *S. cerevisiae* has led to an in depth understanding of how these cells are able to polarize their growth in the presence of a gradient, but a mechanistic understanding of how yeast convert small asymmetries in receptor occupancy into a robust intracellular signal that leads to directional growth remains largely unknown.

1.3 The mating response of *S. cerevisiae*

The budding yeast *S. cerevisiae* exists as one of two mating types in its haploid state, *MAT***a** or *MAT*α (Fig. 1). Cells of each mating type constitutively secrete a peptide pheromone capable of being bound by GPCRs on the surface of cells of the opposite mating type. *MAT***a** cells secrete **a**-factor and *MAT*α cells secrete α-factor. Upon binding of pheromone to the receptor, a signaling cascade is initiated that ultimately leads to arrest in the G1 phase of the cell cycle, transcription of mating-specific genes, directed growth toward the closest mating partner (*i.e.* toward the strongest source of pheromone), and finally, cellular and nuclear fusion resulting in the formation of a *MAT***a**/α diploid zygote (Arkowitz, 2009; Jones and Bennett, 2011). By examining cells exposed to pheromone gradients, it has been calculated that yeast cells can detect a difference in ligand concentration varying as little as 0.5% across the length of the cell and that there is only a 1.3% increase in occupied receptors on the side of the cell facing the gradient compared to the back (Moore et al., 2008; Segall, 1993). Uncovering the mechanisms that allow yeast cells to convert these very slight asymmetries of ligand and activated receptor into robust intracellular signaling gradients is necessary to advance our knowledge of signal-induced cell polarization in all chemotropic eukaryotes.

Figure 1. Life cycle of the yeast *S. cerevisiae*.
Haploid yeast exist as two mating types: *MAT***a** and *MAT*α. Each cell type constitutively secretes a peptide pheromone that can be bound by surface receptors on cells of the opposite mating type. Binding of pheromone initiates a signaling cascade that leads to cell cycle arrest in the G1 phase and induction of mating-specific gene transcription. Cells are able to interpret the complex pheromone gradients in mating mixtures and determine the direction of the closest potential mating partner. They then reorient their actin cytoskeletons and grow in that direction. Ultimately, this polarized growth leads to morphogenesis of a mating projection, cell fusion, and the formation of a diploid zygote.

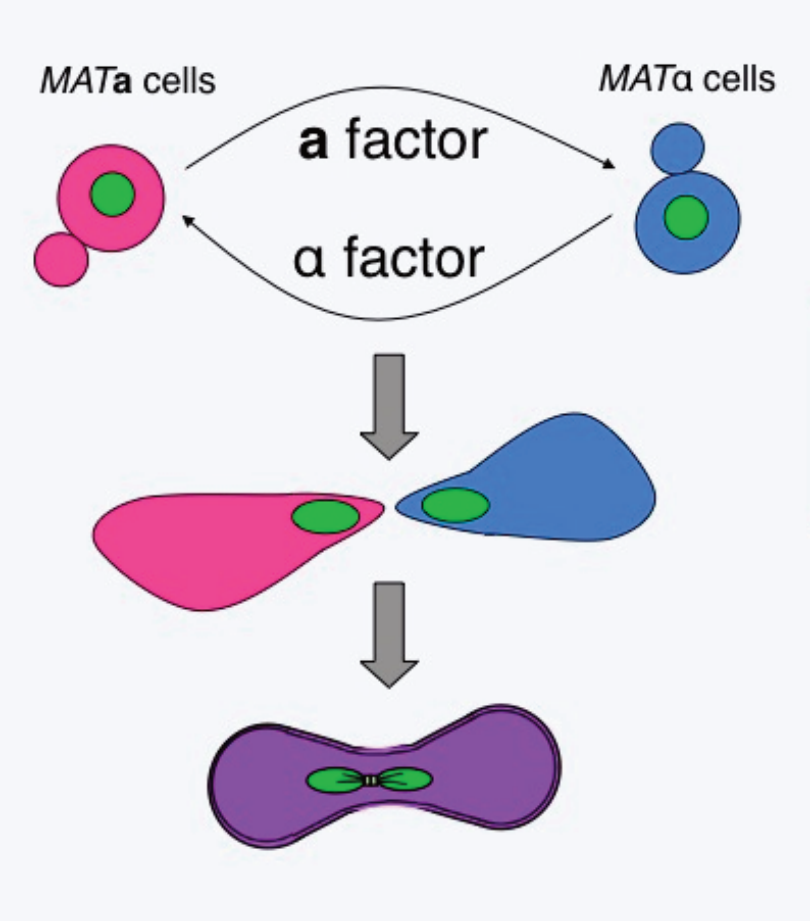
*MAT***a** cells
*MAT*α cells
a factor
α factor

1.3.1 Signaling from the receptor to the nucleus

As in chemotactic cells, directional sensing in both yeast mating types is mediated by a seven transmembrane receptor and its associated heterotrimeric G protein (Fig. 2; Xue et al., 2008). The pheromone-bound receptor acts as a GEF that activates Gα by catalyzing the exchange of GDP for GTP (Blumer and Thorner, 1990). Gα-GTP dissociates from the Gβγ dimer, and Gβ is rapidly phosphorylated at multiple sites (Cole and Reed, 1991). Once dissociated, Gα-GTP and Gβγ are free to interact with downstream effectors that will transmit the mating signal to the nucleus and mark the site on the membrane where polarized growth will occur. Interaction of Gβ with the PAK1 homologue Ste20 and the scaffold protein Ste5 initiates signaling to the nucleus (Feng et al., 1998; Leeuw et al., 1998). Signal transmission occurs via a mitogen activated protein kinase (MAPK) cascade involving the MEKK Ste11, the MEK Ste7, and the MAPK Fus3 (Chen and Thorner, 2007). Ultimately, this results in Fus3 activation via phosphorylation and release of the MAPK from the scaffold (Errede et al., 1993; Gartner et al., 1992). Activated Fus3 translocates to the nucleus where it phosphorylates targets, such as the cyclin-dependent kinase inhibitor Far1, and promotes transcription of mating-specific genes by relieving inhibition of the transcription factor Ste12 (Blackwell et al., 2003; Choi et al., 1999; Peter et al., 1993). Phosphorylated Far1 is thought to inhibit the cell-division kinase Cdc28, which results in cell cycle arrest at the G1 phase (Peter and Herskowitz, 1994).

Figure 2. Molecular model of the pheromone pathway.
The mating signal is mediated by a seven transmembrane receptor and its associated heterotrimeric G protein. Upon pheromone binding to the receptor, the G protein dissociates into its active GTP-bound Gα subunit and its free Gβγ dimer. The Gβ subunit is rapidly phosphorylated and initiates a MAPK signaling cascade that results in the phosphorylation and activation of the MAPK Fus3.The majority of Fus3 translocates to the nucleus to activate transcription of mating-specific genes and induce cell cycle arrest, but Fus3 is also recruited by Gα to phosphorylate substrates at the membrane. The Far1-Cdc24 complex exits the nucleus and is recruited to the membrane by free Gβγ. This marks the site for polymerization and orientation of actin cables, along which myosin motors deliver the growth cargo.

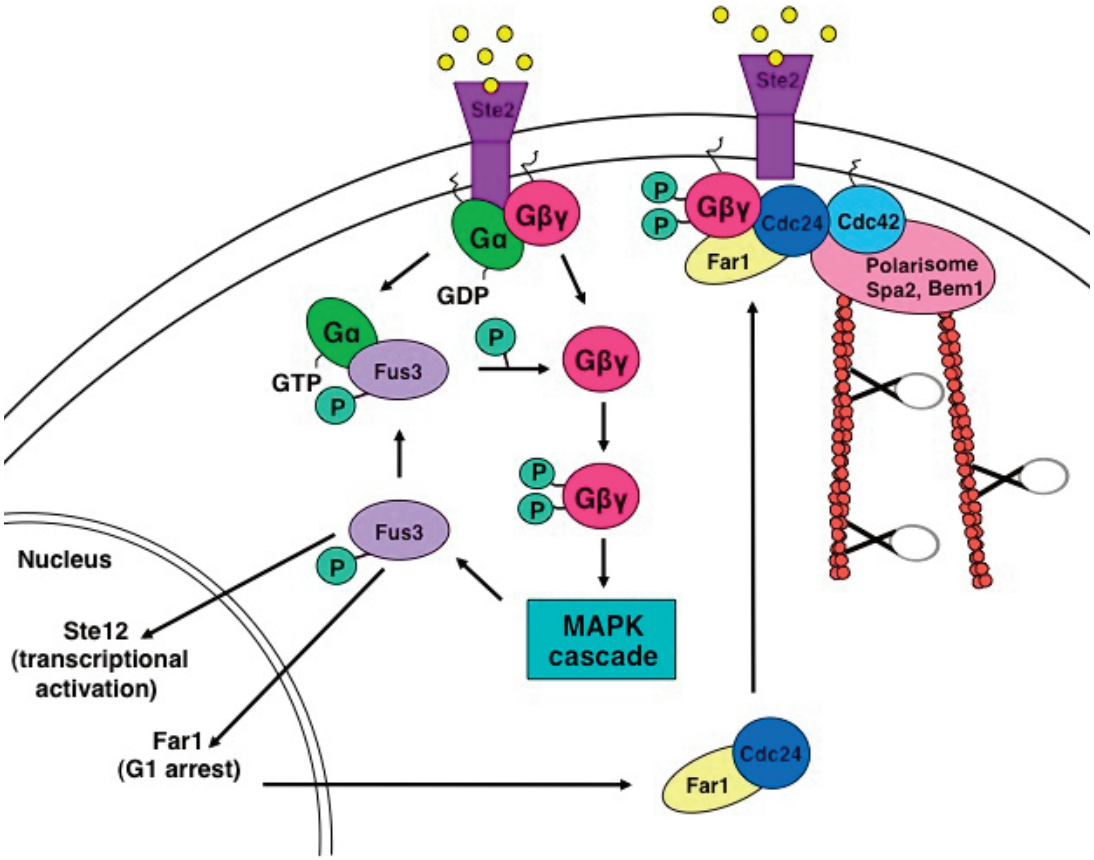
Ste2
Gβγ
Gα
GDP
Gα
GTP
Fus3
P
Gβγ
P
P
Gβγ
Fus3
P
Nucleus
Ste12
(transcriptional
activation)
Far1
(G1 arrest)
MAPK
cascade
Ste2
P
P
Gβγ
Cdc24
Cdc42
Far1
Polarisome
Spa2, Bem1
Cdc24
Far1

1.3.2 Polarization in response to pheromone

Polarized growth occurs in yeast through orientation of actin cables toward a cortical marker (Fig. 3). Upon pheromone exposure, Far1 forms a complex with Cdc24. This complex exits the nucleus and is recruited to the membrane by Gβγ (Butty et al., 1998; Nern and Arkowitz, 1999). Interaction between Gβγ and the Far1-Cdc24 complex brings Cdc24 close to its target protein and is also thought to activate Cdc24 (Wiget et al., 2004). Cdc24 is a GEF for the monomeric GTPase Cdc42. This Gβ-Far1-Cdc24 complex is referred to as the chemotropic complex, and this interaction resembles the Gβγ-PAK1-PIXα interaction required for establishment of polarity in neutrophils (Li et al., 2003). Once activated, Cdc42 recruits several proteins required for polarized growth, including Spa2 and Bem1, to the membrane to form what is known as the polarisome (Butty et al., 2002; Etienne-Manneville, 2004; Evangelista et al., 1997; Sheu et al., 1998). The polarisome complex is responsible for directing polymerization of actin cables to the site on the membrane where polarized growth will occur. Once a stable axis of polarity has been established, myosin motors carry the cargo for cell growth along the actin cables (Pruyne et al., 2004).

During vegetative growth, the Ras-related GTPase Bud1 directly interacts with Cdc24 to facilitate the activation of Cdc42 at the incipient bud site (Park et al., 1997; Shimada et al., 2004). Far1 binds Cdc24 in the nucleus until entry into the cell cycle induces Far1 degradation (Henchoz et al., 1997). Unbound Cdc24 is then free to exit the nucleus and interacts with Bud1 at the membrane. Exposure to a pheromone gradient induces cell cycle arrest and subsequently prevents Far1 degradation (Chang and Herskowitz, 1990). Far1 remains bound to Cdc24, and this complex is exported

from the nucleus by the exportin Msn5 (Blondel et al., 1999). Upon movement into the cytoplasm, Far1-Cdc24 is recruited to interact with Gβγ at the membrane, and this interaction dictates the new site for polarized growth in the direction of the closest mating partner (chemotropic shmooing), which overrides the signal to polarize growth at the previously determined bud site (Butty et al., 1998; Nern and Arkowitz, 1999; Wiget et al., 2004). However, it has been shown that cells exposed to uniform concentrations of pheromone form their mating projections at the pre-determined bud site (default shmooing) (Dorer et al., 1995; Madden and Snyder, 1992; Nern and Arkowitz, 1999).

Figure 3. Establishment of polarized growth in yeast.
Polarized growth occurs in yeast via one of two pathways. During vegetative growth (budding), the cortical marker Bud1 acts as a positional determinant that recruits Cdc24 to the membrane to direct actin polymerization to the site at the cell cortex where the next bud will form. In the absence of a pheromone gradient, the cell will form its mating projection at this pre-determined bud site (default shmooing). In the presence of a pheromone gradient, Gβγ interacts with Far1-Cdc24 to form the chemotropic complex, which marks the new site for polarized growth of a mating projection (chemotropic shmooing).

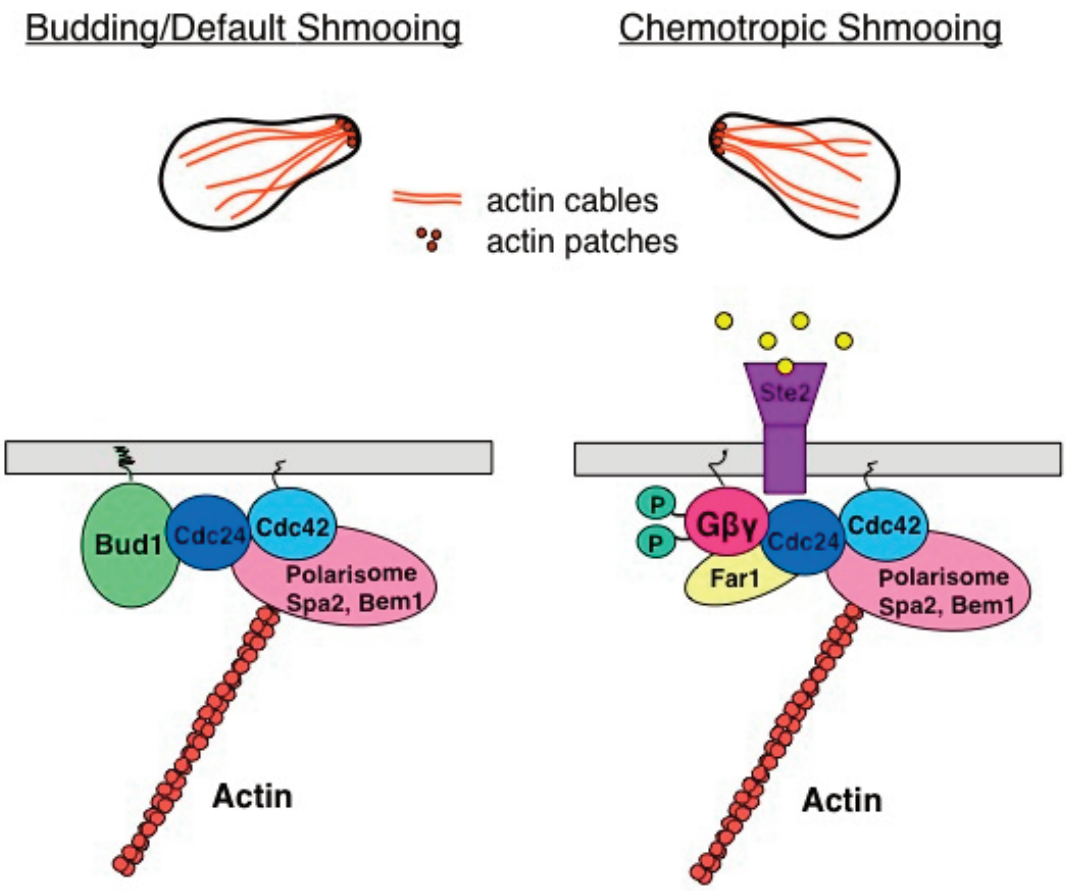
Budding/Default Shmooing
Chemotropic Shmooing
actin cables
actin patches
Bud1
Cdc24
Cdc42
Polarisome
Spa2, Bem1
Actin
Ste2
P
P
Gβγ
Cdc24
Cdc42
Far1
Polarisome
Spa2, Bem1
Actin

1.3.3 Requirements for chemotropic growth

1.3.3.1 The pheromone receptor and G protein

Although much is known about intrinsically-regulated polarized growth in yeast (*e.g.* budding and default shmooing), a mechanistic understanding of how chemotropic growth occurs is lacking. However, some of the basic requirements have been identified. In order to induce chemotropic growth, yeast cells must be able to interpret a gradient of mating pheromone. *MAT***a** cells express the GPCR Ste2, which binds the α-factor pheromone secreted by *MAT*α cells, uniformly on their cell surface resulting in approximately 10,000 ligand-binding sites (Jenness et al., 1986; Stefan et al., 1998). Upon binding of pheromone to the receptor, Ste2 is globally internalized before reappearing as a crescent on the side of the cell facing the pheromone source where directed growth will occur, suggesting it is an early mediator of chemotropic growth (Ayscough and Drubin, 1998; Jackson et al., 1991; Jenness and Spatrick, 1986; Stefan et al., 1998; Suchkov et al., 2010). Ste2 associates with its heterotrimeric G protein via its cytoplasmic carboxy terminal domain, and upon ligand binding, the activated receptor acts as a GEF to activate the Gα subunit (Celic et al., 2003; Dosil et al., 2000; Hirsch et al., 1991). The carboxy terminal domain of Ste2 is also required for receptor internalization upon exposure to pheromone (Terrell et al., 1998), proper gradient tracking (Vallier et al., 2002), and stable chemotropic growth (Konopka et al., 1988).

Active Gα-GTP dissociates from Gβγ, and it is thought that both Gα and Gβγ promote activation of downstream effectors to establish a site for polarized growth at the membrane (Arkowitz, 2009). Gα-GTP remains in this active signaling state until its GTPase accelerating protein (GAP), Sst2, promotes GTP hydrolysis (Apanovitch et al.,

1998). Gα-GDP is then available to bind free Gβγ; thus, Gα has historically been thought of as a negative regulator of the mating response. However, studies from the last decade have provided evidence that Gα may play a positive role by promoting signal activation (Metodiev et al., 2002; Slessareva et al., 2006). Gβγ has been implicated as a positive mediator of the mating response due to its numerous interactions with proteins that upregulate pheromone-induced signaling (Arkowitz, 2009).

Like the pheromone receptor, the G protein is predominately localized to the plasma membrane prior to pheromone exposure (Nern and Arkowitz, 2000; Suchkov et al., 2010). The Gα and Gγ subunits carry lipid modifications that allow their stable membrane association, and Gβ membrane association occurs via its interaction with Gγ (Hirschman and Jenness, 1999; Song and Dohlman, 1996; Stone et al., 1991). Following pheromone exposure, Gα and Gβ, like Ste2, appear as crescents on the membrane prior to morphogenesis, and all three of the subunits localize to the tips of mating projections in shmooing cells (Nern and Arkowitz, 2000; Suchkov et al., 2010). Based on their upstream position in the signaling pathway and their early localization at the future chemotropic growth site, it is likely that Ste2, Gα, and Gβ are important for amplification of the intracellular signal at the site on the membrane where directed growth will occur.

1.3.3.2 Assays of directional growth

The rate of growth of yeast cells is slow relatively to the movement of chemotaxing cells. Therefore, it is likely that yeast employ a spatial detection mechanism to distinguish the gradient concentrations on one side of the cell versus the

other. However, as the pheromone gradients yeast cells experience are extremely shallow (Moore et al., 2008; Segall, 1993), cells likely employ amplifications mechanisms to generate an intracellular gradient steeper than the extracellular gradient. Experiments assaying the ability of cells to accurately interpret pheromone gradients have implicated the receptor, the G protein, and several downstream effectors of the G protein in this process (Arkowitz, 2009).

It has been shown that *MAT***a** and *MAT*α cells are able to distinguish between several potential mating partners and choose to orient their growth toward the mating partner that secretes the highest amount of pheromone (Jackson and Hartwell, 1990a; 1990b). These studied were carried out using two different assays, each presenting a cell with two genotypically different mating partners from which to choose. In the competition assay, a responder cell is presented with WT target cells and challenger cells carrying various mutations. The effect of a mutation carried by a challenger cell is assessed by the ability of the challenger cell to compete against target cells to find a responder cell mating partner. The discrimination assay assesses the ability of a responder cell carrying various mutations to distinguish between a pheromone-secreting mating partner and a mating partner carrying a mutation that blocks pheromone secretion (non-secretor). In this assay, the effect of a mutation is determined by the responder cell's ability to seek out and mate with a pheromone-secreting cell among an excess of non-secreting cells. Other studies used confusion assays, which involve addition of exogenous pheromone to mating mixtures, to determine the importance of a pheromone gradient during chemotropism (Dorer et al., 1995; Valtz et al., 1995). These studies revealed that WT cells had severely impaired mating ability once the pheromone

gradient had been disrupted. Through use of these assays, several components required for chemotropic growth have been identified, including Ste2, the G protein, Sst2, Far1, and Cdc24 (Dorer et al., 1995; Jackson and Hartwell, 1990a; Jackson et al., 1991; Nern and Arkowitz, 1998; Schrick et al., 1997; Valtz et al., 1995).

These assays also revealed that mutations in Ste2 and Gα confer defects in partner discrimination (Jackson and Hartwell, 1990a; Metodiev et al., 2002), while mutations in Gβ, which disrupt its interaction with Ste2 and Gα (*ste4*^{K126E} and *ste4*^{L11R}), confer defects in gradient sensing (Strickfaden and Pryciak, 2008). The *ste2*^{T326} mutant lacks the carboxy terminal tail of receptor, and its defect in partner discrimination is attributed to the increased pheromone sensitivity exhibited by these cells (Jackson and Hartwell, 1990a). Gα^{DSD} is a mutant form of Gα that is specifically defective in binding the Fus3 MAPK (Metodiev et al., 2002). The partner discrimination defect observed in Gα^{DSD} cells suggests that the Gα-Fus3 interaction is important for chemotropism and supports the possibility that Gα recruits Fus3 to phosphorylate proteins involved in chemotropism. Mating-specific mutations in Far1 (*far1-H7 and far1-D1*) and Cdc24 (*cdc24-m1* and *cdc24-m3*) that disrupt interactions between Gβ, Far1, and Cdc24 conferred defects in the confusion assay and mating projection orientation in a pheromone gradient (Nern and Arkowitz, 1998; Valtz et al., 1995). Rather than orienting their mating projections toward the gradient of pheromone, these mutants form mating projections at the default site adjacent to last bud scar. These results indicate that mating projection formation can occur at sites determined by an external pheromone gradient (chemotropic shmooing) or at sites marked intrinsically by proteins that regulate bud positioning (default shmooing).

1.3.3.3 Establishing an axis of polarity

As mentioned previously, pheromone induces activation of the receptor and its G protein, which leads to dissociation of Gα-GTP from Gβγ. Gα and Gβγ are then available to interact with downstream effectors and likely recruit proteins required for the establishment of a chemotropic growth site. It is likely that Gα recruits Fus3 as it has been shown previously to interact with the activated form of this MAPK (Metodiev et al., 2002). Localization of Fus3 to phosphorylate targets at the growth site, such as the formin Bni1, is important for initiating polarized growth, and mutations that disrupt the Gα-Fus3 interaction confer defects in orientation (Matheos et al., 2004; Metodiev et al., 2002; Strickfaden and Pryciak, 2008). Fus3 is required for localization of Cdc24 and Bni1 to the membrane in cells responding to pheromone (Matheos et al., 2004; Yu et al., 2008), and Bni1 activates the small G protein Rho1 (Dong et al., 2003). It is possible that the Gα-Fus3-Bni-Rho1 interactions serve to nucleate actin cables at the growth site.

Gβγ interacts with the Far1-Cdc24 complex, and these interactions are critical for polarity establishment and proper orientation in a gradient (Butty et al., 1998; Nern and Arkowitz, 1998; 1999). As mentioned above, cells are able to form mating projections via one of two pathways: default shmooing vs. chemotropic shmooing. During default shmooing, Bud1 is the cortical marker that determines the position on the membrane where polarized growth will occur. In the presence of a gradient, it is the interaction of Gβγ with the Far1-Cdc24 complex that marks this site. It has been shown that by deleting *BUD1*, the default pathway is disabled, and cells are only able to utilize the chemotropic pathway, even in the absence of a gradient (Nern and Arkowitz, 1999).

Therefore, components required for chemotropic growth can be uncovered because mutants confer a defect in chemotropism when expressed in a *bud1*Δ background. By using this assay, it has been reported that mutations disrupting the Gβγ-Far1-Cdc24 complex confer defects in chemotropic growth (Nern and Arkowitz, 2000). Under these conditions, actin cables can be visualized, but their orientation cannot be stabilized. The axis of polarity moves rapidly along the cell cortex, preventing the unidirectional growth necessary to form a mating projection. This suggests a role for the Gβγ-Far1-Cdc24-Cdc42 interactions in localizing the position of actin cables. Considering all of the Gα and Gβγ interactions together, we can imagine a mechanism where free Gα recruits proteins responsible for nucleating actin cables at the site on the membrane where polarized growth will occur, and free Gβγ recruits proteins responsible for restricting this polarized growth to a discrete spot on the membrane.

1.4 Goal of this study

The mechanisms underlying how polarized growth occurs in yeast are well understood, but how cells are able to recognize the pheromone source and choose to orient their growth toward it remains unclear. The field is still lacking an understanding of the amplification mechanisms that convert slight asymmetries in receptor activation into a robust intracellular signaling response. Once a chemotropic growth site has been chosen, which mechanisms are employed to restrict actin polymerization to the selected site? As a dynamic gradient shifts, how are cells able to update the signal and reorient their growth in a new direction? Several key results led to the proposal and testing of a model that supports the existence of a positive-feedback loop at the level of the receptor

and G protein. Although pheromone exposure induces dissociation of Gα-GTP and Gβγ, it has been reported that both default and chemotropic shmooing require Gα-GTP hydrolysis and reassociation of the G protein with the receptor. This suggests that constant receptor-G protein communication is critical for pheromone-induced polarized growth (Strickfaden and Pryciak, 2008). As mentioned above, both the Gα-Fus3 and the Gβγ-Far1-Cdc24 interactions are required for chemotropic growth. Previous findings showed that disruption of the Gα-Fus3 interaction results in reduced levels and hypo-phosphorylation of Gβ, suggesting that there is a role for Gβ phosphorylation during chemotropism (Metodiev et al., 2002). Considering these results together, a positive feedback model in which the Gα-Fus3 interaction promotes phosphorylation of Gβ at the site of most activated receptors was proposed. Phosphorylation of Gβ enhances its ability to interact with Ste5, which leads to increased activation of Fus3 (Feng et al., 1998). This would generate a positive-feedback loop leading to a gradient of phosphorylated Gβ that would mimic the pheromone gradient and would serve as a link between the two pathways (Gα-mediated and Gβγ-mediated) responsible for stably polarizing actin-mediated growth to a single spot on the membrane. It is possible that Gβ phosphorylation also enhances its ability to communicate the position of activated receptors to its downstream effectors. This would create a complete positive feedback loop connecting the receptor and G protein. In this study, the role of Gβ phosphorylation during yeast chemotropism was examined, and new tools to study reorientation were developed.

Table I. Yeast strains used in this study

Strain	Genotype	Source
DSY257	*MAT***a** *bar1*Δ *ade1 his2 leu2-3, 112 trp1-1a ura3*Δ	Stone lab
RDY114	*MAT***a** *ste4*$^{T320A\ S335A}$ *bar1*Δ *ade1 his2 leu2-3, 112 trp1-1a ura3*Δ	Stone lab
RDY103	*MAT***a** *bud1*Δ::*KAN bar1*Δ *ade1 his2 leu2-3, 112 trp1-1a ura3*Δ	Stone lab
RDY120	*MAT***a** *ste4*$^{T320A\ S335A}$ *bud1*Δ::*KAN bar1*Δ *ade1 his2 leu2-3, 112 trp1-1a ura3*Δ	Stone lab
MMY110	*MAT***a** *gpa1*::*URA3 bud1*Δ::*KAN bar1*Δ *ade1 his2 leu2-3, 112 trp1-1a ura3*Δ + YCplac22/*gpa1*$^{K21E\ R22E}$	Stone lab
MMY111	*MAT***a** *gpa1*::*URA3 bud1*Δ::*KAN bar1*Δ *ade1 his2 leu2-3, 112 trp1-1a ura3*Δ + YCplac22/*GPA1*	Stone lab
RDY130	*MAT***a** *ste4*::*URA3 GFP-STE4::ura3 bud1*Δ::*KAN bar1*Δ *ade1 his2 leu2-3, 112 trp1 ura3*Δ	Stone lab
RDY132	*MAT***a** *ste4*::*URA3 GFP- ste4*$^{T320A\ S335A}$*::ura3 bud1*Δ::*KAN bar1*Δ *ade1 his2 leu2-3, 112 trp1 ura3*Δ	Stone lab
DSY246	*MAT*α *bar1*Δ *ade1 his2 leu2-3, 112 trp1-1a ura3*Δ	Stone lab
RDY217	*MAT*α *ste4*$^{T320A\ S335A}$ *bar1*Δ *ade1 his2 leu2-3, 112 trp1-1a ura3*Δ	Stone lab

Table II. Plasmids used in this study

Plasmid	Protein expressed	Marker/Type	Source
YCplac22	Gpa1	TRP1/CEN	Metodiev et al., 2002
YCplac22	gpa1$^{K21E\ R22E}$	TRP1/CEN	Metodiev et al., 2002
YCplac33	ste4$^{T320A\ S335A}$	URA3/CEN	Li et al., 1998
pRS316	GFP-Ste4	URA3/CEN	Kim et al., 2000
pRS316	GFP-ste4$^{T320A\ S335A}$	URA3/CEN	Stone lab
pRS406	Spa2-GFP	URA3/INT	Arkowitz and Lowe, 1997
pRS305	Bem1-GFP-Snc2	LEU2/INT	Howell et al., 2009
YCplac111	GAL1-Ste4	LEU2/CEN	Cismowski et al., 2001
YCplac111	GAL1-ste4$^{T320A\ S335A}$	LEU2/CEN	Stone lab
pESC	GAL1-FLAG-Far1	URA3/2μm	Stone lab
pRS426	GFP-Cdc42	URA3/2μm	Barale et al., 2006
pRS304	ste2$^{7XR\ GPAAD}$	TRP1/INT	Lew lab, DLB3217

2. MANUSCRIPT: Gβ PHOSPHORYLATION IS CRITICAL FOR EFFICIENT CHEMOTROPISM IN YEAST

Reagan DeFlorio[*,†], Elizabeta Apollinari[*], Marie-Elena Brett[#], Metodi Metodiev[*], Oleksii Dubrovskyi[*], David Eddington[#], Robert A. Arkowitz[†] and David E. Stone[*]

[*]Laboratory for Molecular Biology, Department of Biological Sciences, University of Illinois at Chicago, Chicago, IL 60607, USA

[#]Department of Bioengineering, University of Illinois at Chicago, Chicago, IL 60607

[†]Institute of Biology Valrose, University of Nice-Sophia Antipolis, Nice, France 06108

Author contributions to this work:

Reagan DeFlorio: Figures 4A-C, 5A-B, 6A-B, 7B-C, 8A-B, 9A-B; Tables III and IV

Elizabeta Apollinari: Figures 5C, 9C-D

Marie-Elena Brett: Developed microfluidic device used in Figures 9A-B

Metodi Metodiev: Preliminary observation of phenotypes observed in Figure 4A

Oleksii Dubrovskyi: Figure 7A

2.1 Introduction

In metazoans, directed cell movement in response to a chemical gradient (chemotaxis), plays a vital role in embryogenesis, postnatal development and homeostasis, and immunity. Moreover, the survival of many single celled organisms depends on their ability to detect and move in response to chemical stimuli. The related phenomenon, directed cell growth in response to a chemical gradient (chemotropism), is also essential in many species. For example, in mammals, chemotropism is integral to axon guidance (Hong and Nishiyama, 2010; Tojima et al., 2011) and angiogenesis (Basile et al., 2004; English et al., 2001). Pollen tube guidance is also a chemotropic process (Kim et al., 2004; Palanivelu and Preuss, 2000), and there is an increasing appreciation for the role of chemotropism in the life cycles of fungal species, including plant and human pathogens (Daniels et al., 2006; Snetselaar et al., 1996).

To direct movement or growth up a chemical gradient, chemotactic and chemotropic cells must solve a set of common challenges. They must be able to detect the presence of the extracellular signaling molecule and determine the direction of its source. Many chemosensing cells express GPCRs for this purpose (Weiner, 2002). Using the spatial information encoded in the distribution of activated receptors, the cell must establish a site or landmark for polarization. Actin and/or microtubule cytoskeletal elements are then assembled at, or recruited to, this site to promote directional movement or growth. Finally, the cell must be able to stabilize the axis of polarity over time, while retaining the plasticity to change its orientation in response to changes in the direction of the gradient.

Because physiological gradients of chemoattractant are typically very shallow, 1-10% across the cell's length (Lohef et al., 1992; Mato et al., 1975; Segall, 1993; Tranquillo et al., 1988; Zigmond, 1977), establishment of the polarity site requires the conversion of small differences in receptor occupancy into a substantially steeper intracellular signaling gradient. This is thought to depend on feedback loops such as those first discovered in *Dictyostelium* and neutrophils. Exposure of these cells to chemoattractant gradients leads to a gradient of receptor occupancy such that slightly more receptors are activated on the surface of the cell closest to the signaling source (Hoeller and Kay, 2007). This results in a similar gradient of activated heterotrimeric G protein subunits, Gα-GTP and free Gβγ (Jin et al., 2000). Gβγ then recruits and activates the lipid kinase, PI3K, which phosphorylates PIP_2 to PIP_3. In addition, Gβγ activates the Rho GTPases, Rac and Cdc42, and Rac-GTP enhances PIP_3 accumulation (Takeda et al., 2007). PIP_3, in turn, promotes further Rac activation. Together, these actions generate a “local excitation” that enhances signaling at the cell’s leading edge. Key to generating the steep gradient of PIP_3 is a second pathway that causes a graded inhibition of PIP_3 accumulation across the cell. This depends on the localization of the PIP_3 phosphatase, PTEN, to the lagging edge. Although other signaling pathways are now known to be essential for chemotaxis (Chen et al., 2007; Kamimura et al., 2008; Veltman et al., 2008), feedback loops that generate and couple local excitation with global inhibition (LEGI) have emerged as a generally accepted mechanism underlying directional sensing (Devreotes and Janetopoulos, 2003; Iijima et al., 2002; Weiner, 2002).

In comparison to chemotactic models, the amplification mechanisms that underlie directional sensing in chemotropic systems are less well understood. To date, the best characterized example of eukaryotic chemotropism occurs during the mating response of the budding yeast, *S. cerevisiae*. In the haploid phase of its life cycle, budding yeast exist as two mating types, *MAT***a** and *MAT*α. Each mating type constitutively secretes a specific peptide mating pheromone that binds to GPCRs on cells of the opposite type. When occupied by ligand, the pheromone receptors activate the mating-specific Gα protein, Gpa1, *via* guanine nucleotide exchange and the subsequent dissociation of Gα-GTP from the Gβγ dimer, Ste4/Ste18. The signal is then transmitted by Gβγ via the Fus3 MAPK cascade that ultimately induces arrest in the G1 phase of the cell cycle, broad changes in gene expression, and morphogenesis (Arkowitz, 2009; Jones and Bennett, 2011). Cells polarize their growth and form pear-shaped cells called shmoos, in response to both uniform (isotropic) pheromone and pheromone gradients. In mating mixtures, cells find and then contact the closest potential mating partner by determining the direction of the most potent pheromone source and growing toward it (Jackson and Hartwell, 1990a; 1990b).

Polarized growth in *S. cerevisiae*, like that in higher eukaryotes, requires the marking of a growth site at the cell cortex and alignment of the actin cytoskeleton towards it. Cargo bound for the polarized structures is transported by myosin motors along the actin cables (Pruyne and Bretscher, 2000a; 2000b). Actin polarization depends on Cdc42, which is thought to activate the formin protein Bni1 that nucleates and tethers actin cables to the polarization site (Evangelista et al., 2002; Sagot et al., 2002). Bni1 is part of the polarisome complex, together with Spa2, Bem1, Bud6, and

Pea2 (Pruyne and Bretscher, 2000b). Cdc42 is activated by the guanine nucleotide exchange factor, Cdc24, which itself undergoes localized activation by positional cues during both vegetative budding and mating. In vegetative cells, cortical tags promote localized activation of the Ras-related GTPase, Bud1, which binds directly to Cdc24 (Park et al., 1997) and Cdc42 (Kang et al., 2010). In cells exposed to pheromone, Gβγ interacts with the Far1-Cdc24 complex (Butty et al., 1998; Nern and Arkowitz, 1998; 1999). Interaction of Gβγ with Far1 is thought to activate Cdc24 (Wiget et al., 2004), leading to localized GTP-loading of Cdc42, recruitment of Bni1, nucleation of actin cables, and polarized growth to form the mating projection. Under physiological conditions, the Gβγ-Far1-Cdc24 complex is presumed to assemble in the region of the cell surface that experiences the highest concentration of pheromone, and to mark this area for growth in preference to the predetermined bud site (*i.e.* formation of the Gβγ-Far1-Cdc24 chemotropic complex competitively inhibits formation of the Bud1-Cdc24 budding complex) (Nern and Arkowitz, 2000). In this way, the cell is thought to orient its growth toward the source of pheromone, although a mechanistic understanding of the feedback loops that amplify the directional signal is lacking. When cells are unable to sense a gradient of pheromone, they form a mating projection at the site that would have been used for the next bud, which is the site marked by Bud1 (Dorer et al., 1995; Nern and Arkowitz, 1999). This is called the default mating projection site.

Like chemotaxing cells, yeast exhibit a remarkable ability to interpret chemical gradients. It has been estimated that a 1% difference in receptor occupancy across the 5μm length of a yeast cell in a pheromone gradient is sufficient to elicit robust orientation toward the pheromone source (Segall, 1993), and recent microfluidic studies

suggest an even greater acuity (Moore et al., 2008). How is this very slight asymmetry in activated receptor and G protein amplified internally to establish a unique shmoo site, and how is this positional information continually communicated to the polarisome to ensure properly oriented growth over time?

Since it was first reported that pheromone induces the phosphorylation of Gβ on multiple sites (Cole and Reed, 1991), the function of this modification has been elusive. In the initial attempt to assess the pheromone response of cells unable to phosphorylate Gβ, a deletion allele of *STE4* lacking 40 codons was used. The resulting defect in adaptation to pheromone was most likely due to the internal Gβ deletion rather than to a lack of phosphorylation because, subsequently, a double point mutant form of Gβ that cannot be phosphorylated was found to have no measurable effect on signal transmission to the nucleus, adaptation, or diploid formation (Li et al., 1998). More recently, we discovered that the activated forms of the mating-specific Gα protein and the Fus3 MAPK interact directly. A mutant form of Gα that is severely defective in binding Fus3, $G\alpha^{DSD}$, confers a defect in partner discrimination, indicating a problem in directional sensing and/or directed growth (Metodiev et al., 2002; Strickfaden and Pryciak, 2008; Yu et al., 2008). $G\alpha^{DSD}$ also results in hypo-phosphorylation and reduced levels of Gβ, as does *fus3*Δ. These observations raised the possibility that the phosphorylation of Gβ plays a role in chemotropism. Here we show that Gβ phosphorylation is critical for this process. Specifically, this modification of Gβ appears to promote communication between activated receptors and downstream components essential for polarized growth. Cells unable to phosphorylate Gβ exhibit specific defects in pheromone-induced morphogenesis, orientation towards mating partners, and the

ability to reorient in response to a vectorial change in the gradient. We propose a model in which Gβ phosphorylation provides a means to amplify the spatial signal and the Gβ phosphorylation/dephosphorylation cycle constitutes an updating mechanism that conveys the status of the receptor to the chemotropic complex and downstream cell polarity proteins.

2.2 Materials and methods

Molecular and microbiological techniques.

Standard methods were used for microbial and molecular manipulation (Ausubel et al., 1994; Guthrie and Fink, eds 1991; Sherman, 1986). The yeast strains used in this study, listed in Table I, were all derived from strain 15Dau *bar1*Δ (*MAT***a** *ade1 his2 leu2-3*, *-112 trp1 ura3*D), which is congenic with strain BF264-15D (Reed et al., 1985). RDY114 was generated by *in situ* transplacement of *ste4*::*URA3* in strain ELY104 (Li et al., 1998) with *ste4*$^{T320A\ S335A}$, excised as an *Eco*RI-*Sph*I fragment from the plasmid YCplac33/*ste4*$^{T320A\ S335A}$ (Li et al., 1998). Recombinants were selected on 5´FOA and confirmed by sequencing. The *BUD1/RSR1* locus was deleted in strains 15Dau *bar1*Δ and RDY114 to create strains RDY103 and RDY120, respectively, using a *bud1*Δ*::KANMX4* cassette which was PCR-amplified from pFA6a-Kan (Wach et al., 1994) using the oligomers 5´- GCGCATTCATCCTCGACATTCTCAAACGCGAAATATC GTCGAACGTACGCTGCA GGTCGACGG - 3´ and 5´- GTTGTGAAGTAGCGCTAATTC CTGTCCTGTTGCTAGAAC CAGATATCGATGAATTCGAGCTCG - 3´. GFP-tagging was performed *in situ* by transplacement of an excised *Eco*RI-*Sma*I fragment from

pRS316/*STE4*p-*GFP*-*STE4* (Hirsch lab, BLT49) or pRS316/*STE4*p-*GFP*-*ste4*$^{T320A\ S335A}$ (RDB122, see construction below) into strain ELY104 to create strains RDY126 and RDY139, respectively. The *BUD1* locus was deleted as described above in strains RDY126 and RDY139 to create strains RDY130 and RDY132, respectively. RDY114 was transformed with p*GAL*-*HO* and the mating type was switched to generate RDY217 as described (Guthrie and Fink, eds 1991). Strains EAY100 and EAY101 were created by transforming pRS304/*ste2*$^{7XR/GPAAD}$ (Lew Lab, DLB3217) cut with *Bsm*I into strains RDY103 and RDY120, respectively.

Plasmid construction.

The plasmids used in this study are listed in Table II. RDB122 was created by sequential site-directed mutagenesis of pRS316/*STE4p*-*GFP*-*STE4* (Hirsch lab, BLT49), and YCplac111/*GAL1*- *STE4*$^{T320A\ S335A}$ was created by sequential site-directed mutagenesis of YCplac111/*GAL1*- *STE4*, using QuikChange II XL kit (Qiagen) The oligomers used to create the T320A mutation were 5´- CGAGGTTATGAAGAACGTACC CCTGCCCCTACTTATATGGCAGC - 3´and 5´- GCTGCCATATAAGTAGGGGCAGGG GTACGTTCTTCATAACCTCG - 3´. The oligomers used to create the sequential S335A mutation were 5´- GGAGTACAATACCGCGCAAGCGCCACAAACTT TAAAATCAAC - 3´and 5´-GTTGATTTTAAAGTTTGTGGCGCTTGCGCGGTATTGTACT CC - 3´. To create pEB15.1 (pESC/*GAL10*-FLAG-*FAR1*), *FAR1* was PCR-amplified from strain 15Dau genomic DNA and the product was cloned into pESC/*URA* as a *Pac*I-*Bgl*II fragment, thereby placing *FAR1* under *GAL10* promoter control. The priming

oligonucleotides were: 5´- CCTTAATTAAGCGTAGTATAGACGTGGAG - 3´ and 5´- GAAGATCTTGAAGACACCAACAAGAGTTTCG - 3´.

Spa2-GFP time-lapse fluorescent microscopy in mating mixtures.

Wild type BF264-15D *MAT*α cells were stained with 10µg/ml ConA-Alexa Fluor 594 (Molecular Probes, Eugene, Oregon) for 1hr and then washed 3X with water prior to mixing with strains RDY246 and RDY247 (*MAT***a** *bud1*Δ Gβ or $G\beta^{P-}$ cells expressing *SPA2-GFP*). Mating mixtures were incubated at 30°C on agar pads, and images were acquired 25min after mixing and at 15min intervals thereafter. Six fields were imaged at each time point with 6 DIC and 6 GFP Z-stacks collected in 0.5µm slices using a DeltaVision deconvolution microscopy system (Applied Precision, Issaquah, Washington) on an Olympus IX-70 microscope with an NA 1.4 X 60 objective. The images were then deconvolved, sum projected (GFP) or average projected (DIC), and converted into 8-bit TIF files using Huygens Deconvolution Software (Scientific Volume Imaging, Hilversum, The Netherlands). Tracking analysis was performed using Fiji (NIH).

GFP-Gβ time-lapse fluorescent microscopy in isotropic conditions.

Strains RDY130 (*MAT***a** *bud1*Δ GFP-Gβ) and RDY132 (*MAT***a** *bud1*Δ GFP-$G\beta^{P-}$) were incubated at 30°C on agar pads containing 150nM α-factor. Cells were first imaged 15min after exposure to pheromone and at 15min intervals thereafter. Six fields were imaged at each time point with 15 DIC and 15 GFP Z-stacks collected in 0.3µm slices using an ANDOR Revolution XD spinning disk laser confocal microscopy system comprised of a fully motorized Olympus IX-81 inverted microscope, a Yokogawa CSU-

X1 confocal spinning disk unit, motorized XYZ control (piezo) and two DU-897D-iXonEM+ EMCCD cameras all controlled by Andor iQ2 software. A UplanSApo NA 1.4 X 100 objective was used with 488nm laser excitation. An Oxolab chamber was used to maintain cells at 30ºC. The images were then sum projected and converted into 8-bit TIF files using Fiji (NIH). Data analysis was carried out using a MatLab program, BudPolarity, developed by PRISM engineer Dr. Schaub at the Université de Nice-Sophia Antipolis. BudPolarity has an intuitive interface dedicated for the analyses of the intensity profile along the major axis of yeast cells and its variations along time. 3D images are converted into 2D images by sum projection. Yeast morphology is defined by user-defined intensity threshold, and the straight axis is defined by the major axis of the ellipse fitting the morphology of the yeast. To compare profiles during cell growth, the axis length has been normalized. Fluorescence intensity is integrated on this axis to follow concentration along this axis. Signal polarization was defined by a concentration peak intensity 2x higher than the background signal.

GFP-Gβ time-lapse fluorescent microscopy in mating mixtures.

Wild type BF264-15D *MAT*α cells were stained with 10µg/ml ConA-Alexa Fluor 594 (Molecular Probes, Eugene, Oregon) for 1h and then washed 3X with water prior to mixing with strains RDY130 (*MAT***a** *bud1*Δ GFP-Gβ) or RDY132 (*MAT***a** *bud1*Δ GFP-$G\beta^{P-}$). Mating mixtures were incubated at 30°C on agar pads and images were acquired 15min after mixing and at 15min intervals thereafter. Six fields were imaged at each time point with 15 DIC and 15 GFP Z-stacks collected in 0.3µm slices using an ANDOR Revolution XD spinning disk laser confocal microscopy system comprised of a

fully motorized Olympus IX-81 inverted microscope, a Yokogawa CSU-X1 confocal spinning disk unit, motorized XYZ control (piezo) and two DU-897D-iXonEM+ EMCCD cameras all controlled by Andor iQ2 software. A UplanSApo NA 1.4 X 100 objective was used with 488nm laser excitation. An Oxolab chamber was used to maintain cells at 30ºC. The images were then sum projected and converted into 8-bit TIF files using Fiji (NIH). Data analysis was carried out using the MatLab program, BudPolarity, developed by PRISM engineer Dr. Schaub at the Université de Nice-Sophia Antipolis described above. Signal polarization was defined by a concentration peak intensity 1.5x higher than the background signal.

Far1 and Gβ co-overexpression genetic assay.

15Dau *bar1*Δ cultures cotransformed with pESC/*GAL1-FAR1* and either YCplac111/*GAL1-STE4* or YCplac111/*GAL1- STE4*$^{T320A\ S335A}$ were grown to mid-log phase in selective sucrose medium. 10-fold serial dilutions from 10^5 to 1 were then set up in micro-titer dishes and frogged to both selective galactose and selective glucose medium. Plates were incubated at 30°C for 48hr prior to imaging.

FRAP analysis of Spa2-GFP.

*MAT***a** *bud1*Δ Gβ or Gβ^{P-} cells expressing *SPA2-GFP* (RDY246 and RDY247) were grown to mid-log phase at 30°C in rich media containing 10x adenine and exposed to 30nM α-factor at 30°C for 1.5hr at OD_{600} = 10^7 cells/ml. Fluorescence recovery after photo-bleaching (FRAP) analysis was performed using a Zeiss LSM 510 META confocal on an Axiovert 200M microscope using an NA 1.4 X 63 Plan-Apo objective and 488nm LASER excitation. Images were captured every 1s at 2–5% maximum laser

intensity and 10 x 0.5ms photo-bleaching scans at 100% laser intensity were performed on a circular area of 1 μ m^2 at the shmoo tip. Data analysis was carried out essentially as described (Bassilana and Arkowitz, 2006). The average intensity of the bleached or unbleached area was normalized for photo-bleaching during image acquisition, using the average intensity of the cell with MatLab. Regression analysis to determine the FRAP $t_{1/2}$ was done using a one-phase exponential association function in MatLab, as follows:

Y = bottom + (top - bottom)(1 - exp[-kt]) where k is the rate constant and $t_{½}$ is 0.69/k.

iFRAP analysis of GFP-Cdc42.

*MAT***a** *bud1*Δ Gβ or $G\beta^{P-}$ cells expressing *GFP-CDC42* (RDY259 and RDY260) were grown to mid-log phase at 30°C in rich media containing 10x adenine and exposed to 30nM α-factor at 30°C for 1.5hr at OD_{600} = 10^7 cells/ml. Inverse fluorescence recovery after photo-bleaching (iFRAP) analysis was performed using a Zeiss LSM 510 META confocal on an Axiovert 200M microscope using an NA 1.4 X 63 Plan-Apo objective and 488nm LASER excitation. Images were captured every 1s at 2–5% maximum laser intensity and 10 x 0.5ms photo-bleaching scans at 100% laser intensity were performed on the entire cell except the area of reporter polarization at the shmoo tip. The average intensity of the bleached or unbleached area was normalized for photo-bleaching during image acquisition, using the average intensity of the cell with MatLab. Loss of fluorescence intensity was then fitted to an exponential curve.

Mating projection assays.

To study mating projection formation and maintenance under isotropic pheromone conditions, cells were grown to mid-log phase at 30°C in rich liquid medium. Diluted cultures OD_{600} = 10^7 cells/ml were exposed to α-factor at the concentrations and times indicated. To study mating projection formation and maintenance in physiological pheromone gradients, cultures were grown to mid-log phase at 30°C in rich medium. Dilute bilateral Gβ and $G\beta^{P-}$ mating mixtures containing 10^7 *MAT*α cells and 10^7 *MAT***a** cells were then spread on rich medium plates and incubated at 30°C. Time points were taken at 60min intervals for 5hr and fixed with 4% formaldehyde. Percentages in each shmoo class were scored using a haemocytometer. DIC images for both experiments were acquired using a Zeiss Axioskop 2 microscope fitted with a 63X oil immersion objective and a Zeiss AxioCam digital camera. Images were processed with Zeiss AxioVision software.

Orientation assays.

To measure the ability of cells to orient their growth in physiological pheromone gradients, cultures were grown to mid-log phase at 30°C in rich medium. Dilute bilateral Gβ and $G\beta^{P-}$ mating mixtures containing $5x10^6$ *MAT*α cells and $5x10^6$ *MAT***a** cells were then incubated at 30°C for 3hr on filters (0.45 μm Millipore) placed on rich medium. Matings were between either wild type *MAT*α (DSY246) and wild type *MAT***a** (DSY257) cells or *MAT*α $G\beta^{P-}$ (RDY217) and *MAT***a** $G\beta^{P-}$ (RDY114) cells. Filters were washed in 1ml sterile water to harvest cells. DIC images of zygotes were collected using a Zeiss Axioskop 2 microscope fitted with a 63X oil immersion objective and a Zeiss AxioCam

digital camera. Images were processed with Zeiss AxioVision software. Zygote angles were measured using ImageJ (NIH). The response of cells to artificial pheromone gradients was assayed using a microfluidic device (Dave Eddington, UIC collaboration).

Reorientation assays.

Cells were grown to mid-log phase at 30°C in rich medium. Liquid cultures containing 10^7 *MAT*α cells and 10^7 *MAT***a** cells for each cross were shaken together vigorously at 30°C for 3hr to induce shmooing prior to mating. Cultures of either wild type *MAT*α (DSY246) and wild type *MAT***a** (DSY257) cells or *MAT*α $G\beta^{P-}$ (RDY217) and *MAT***a** $G\beta^{P-}$ (RDY114) cells were then spread onto rich media plates and incubated at 30°C for 3hr. Images of zygotes were collected using an Olympus digital camera attached to an Olympus BH-2 inverted microscope and a 63X objective. Reorientation angles of zygotes were measured using ImageJ (NIH).

2.3 Results

2.3.1 Gα plays an essential role in the chemotropic shmoo pathway

The findings that $G\alpha^{DSD}$ confers partial defects in partner discrimination and mating efficiency (Metodiev et al., 2002), as well as in shmooing and actin polarization (Matheos et al., 2004), suggest that the Gα-Fus3 interaction plays a role in chemotropism. Moreover, Gα has been implicated in chemotropism by two other studies (Strickfaden and Pryciak, 2008; Yu et al., 2008). To further test this possibility, we asked whether $G\alpha^{DSD}$ *bud1*Δ cells can shmoo. It has been established that cells can form mating projections if either the default or chemotropic shmoo pathways are inactivated, but are unable to polarize their growth in response to pheromone if neither pathway is

functional (Nern and Arkowitz, 2000). In essence, components required for chemotropic growth can be uncovered by examining mutations in a *bud1*Δ background. For example, the inability of *cdc24-m1 bud1*Δ and *far1-H7 bud1*Δ cells to shmoo (Nern and Arkowitz, 2000) is expected, as Cdc24 and Far1 are essential chemotropic elements (Nern and Arkowitz, 1998; Valtz et al., 1995). As shown in Figure 4A, $G\alpha^{DSD}$ *bud1*Δ cells were unable to form mating projections. Whereas the Gα *bud1*Δ control cells formed normally shaped shmoos, the $G\alpha^{DSD}$ *bud1*Δ cells either enlarged uniformly, or exhibited highly aberrant morphologies (Fig. 4A), consistent with the idea that the Gα-Fus3 interaction is required for chemotropic growth.

2.3.2 $G\beta^{P-}$ *bud1*Δ cells exhibit a range of defects in pheromone-induced polarized growth

Gβ phosphorylation and level are greatly reduced in pheromone-treated $G\alpha^{DSD}$ and *fus3*Δ cells, raising the possibility that Gβ is a target of Gα-Fus3. Because $G\alpha^{DSD}$ also confers defects in partner discrimination and in the genetic assay for chemotropic shmooing described above (Fig. 4A), we wondered whether the phosphorylation of Gβ plays a role in the chemotropic response. As a first test of this idea, we again used the genetic assay of chemotropic shmooing. The T320A S335A allele of *STE4* encodes a mutant form of Gβ that is not phosphorylated *in vivo* (Li et al., 1998). Strains were created in which the native *STE4* was replaced with $ste4^{T320A\ S335A}$ (henceforth $G\beta^{P-}$) in *BUD1* and *bud1*Δ backgrounds. The $G\beta^{P-}$ *bud1*Δ, Gβ *bud1*Δ, $G\beta^{P-}$ *BUD1*, and Gβ *BUD1* (henceforth WT, for wild type) cells were treated with a range of pheromone concentrations in liquid medium and examined at 60min intervals for 5 hours. When

stimulated with isotropic pheromone, the morphological response of Gβ^{P-} *BUD1* cells was indistinguishable from that of WT cells. In contrast, although almost all of the Gβ^{P-} *bud1*Δ cells were capable of pheromone-induced polarized growth, they exhibited a variety of shmoo abnormalities at all doses and time points, with a significant fraction apparently unable to sustain unidirectional growth long enough to form a projection even after 5 hours of treatment (Fig. 4B). The percentages of such cells ± SEM were 16.2 ± 1.4 and 4.0 ± 0.5 for the Gβ^{P-} *bud1*Δ and Gβ *bud1*Δ cultures, respectively; $n \geq 200$; $p < 0.0001$.

A high proportion of the Gβ^{P-} *bud1*Δ shmoos were significantly shorter and broader than those formed by the Gβ *bud1*Δ control cells, as if their growth was less well focused. Their mean lengths were 0.89 and 0.84 that of the Gβ *bud1*Δ cells 4 and 5 hours after treatment, respectively ($n = 300$; $p < 0.0001$ for each time point), and most were abnormally shaped. Instead of narrowing smoothly to a pointed tip, Gβ^{P-} *bud1*Δ mating projections often extended almost straight out from the cell body and terminated in a bulbous curve, forming a shape reminiscent of a light bulb. Although aberrant shmoo morphologies were also seen in the Gβ *bud1*Δ culture, likely due to the absence of Bud1, their occurrence was greatly increased by Gβ^{P-} (80.7% as compared to 16.7%; $n \geq 260$; $p < 0.0001$).

It has been shown that WT yeast cells treated with high mating pheromone concentrations form successive mating projections with regular periodicity (Bidlingmaier and Snyder, 2004). Under isotropic pheromone conditions, the second growth site is usually established far from the first one, so that the two projections ultimately form a wide angle (distal projections). Another striking phenotype of the Gβ^{P-} *bud1*Δ cells was

their tendency to form second and third mating projections earlier than the control and in abnormal positions (Fig. 4C). In the *bud1*Δ strain, we observed a small fraction of cells with two or more projections adjacent to one another (proximal projections). However, the occurrence of such cells was dramatically increased in the $G\beta^{P-}$ *bud1*Δ strain, with the ratio of proximal to distal shmoos more than 10-fold greater in $G\beta^{P-}$ as compared to control cells. Similar results were observed at all pheromone concentrations and incubation times.

Although none of the $G\beta^{P-}$ *bud1*Δ cells were completely incapable of polarized growth in isotropic pheromone, as are $G\alpha^{DSD}$ *bud1*Δ and *cdc24-m*1 *bud1*Δ cells, a small but significant fraction was dramatically impaired in this regard. Such cells were usually quite small and formed multiple protrusions that, on the basis of morphological criteria, could not be considered true mating projections. In Figure 4C, these cells are counted in the "proximal" category, and we refer to them as small multiple protrusion (SMP) cells. Together, the results presented in Figure 4 suggest that in cells unable to shmoo *via* the Bud1-dependent default pathway, phosphorylation of Gβ is critical for the stabilization of the axis of polarity and hence the focused growth of mating projections.

Figure 4. Effect of $G\alpha^{DSD}$ and $G\beta^{P-}$ on the chemotropic shmoo pathway. (A) $G\alpha^{DSD}$ *bud1*Δ cells are unable to form mating projections. *MAT***a** *gpa1*Δ *bud1*Δ cells transformed with centromeric plasmids containing either Gα or $G\alpha^{DSD}$ were exposed to 150nM pheromone for 3hr. Bar, 5μm. (B) $G\beta^{P-}$ *bud1*Δ cells exhibit a variety of mating projection abnormalities. *MAT***a** Gβ *bud1*Δ, $G\beta^{P-}$ *bud1*Δ, Gβ *BUD1*, and $G\beta^{P-}$ *BUD1* cells were exposed to 50nM pheromone for 3hr. Representative images are shown. Lower right is a composite. White arrowheads indicate cells scored as bulbous shmoos, white arrows indicate proximal double shmoos, and white asterisks mark examples of SMP cells. Bar, 5μm. (C) $G\beta^{P-}$ *bud1*Δ cells form projections proximal to the initial growth site. *MAT***a** Gβ *bud1*Δ and $G\beta^{P-}$ *bud1*Δ cells were exposed to 30nM pheromone for the indicated times. At each time point, the percentages of cells with a single projection, multiple distal projections, and multiple proximal projections were determined. $n \geq 200$ for each strain and time point. The data represent the average of three independent experiments ± SEM. $^*p < 0.0001$ for comparing the higher to lower percentage of a given projection type.

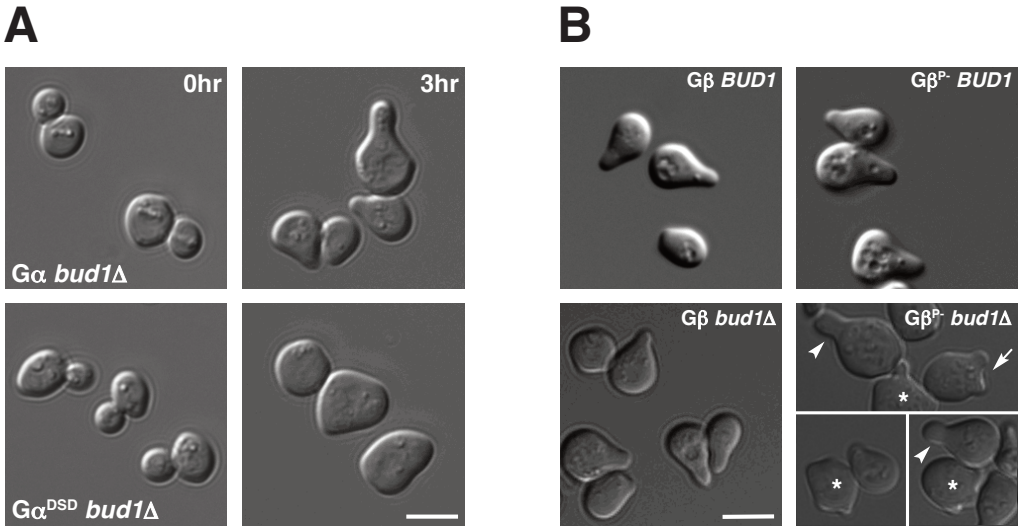
A
0hr
3hr
Gα bud1Δ
Gα^DSD bud1Δ
B
Gβ BUD1
Gβ^P- BUD1
Gβ bud1Δ
Gβ^P- bud1Δ

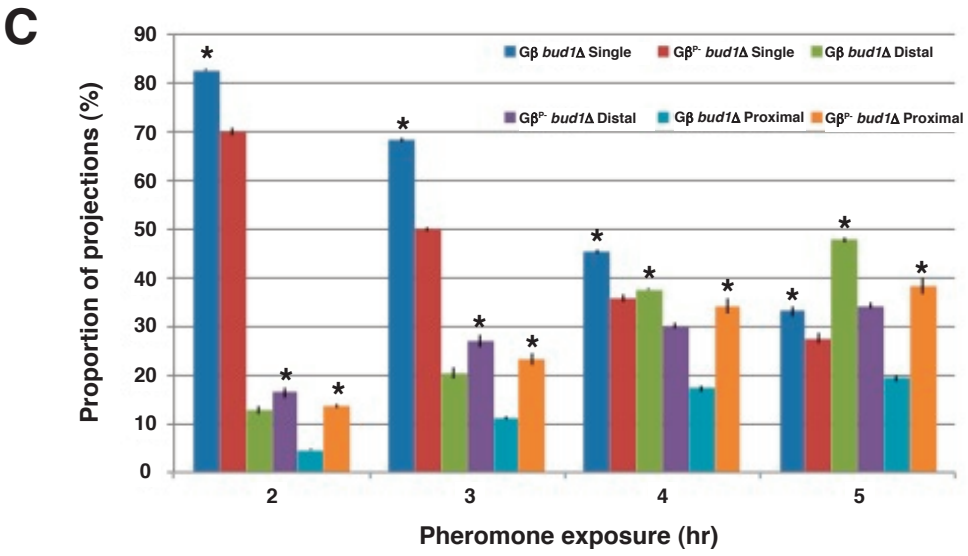
C
Gβ bud1Δ Single
Gβ^P- bud1Δ Single
Gβ bud1Δ Distal
Gβ^P- bud1Δ Distal
Gβ bud1Δ Proximal
Gβ^P- bud1Δ Proximal
Proportion of projections (%)
0
10
20
30
40
50
60
70
80
90
2
3
4
5
Pheromone exposure (hr)

2.3.3 The growth site of pheromone-treated Gβ^{P-} *bud1*Δ cells wanders where the receptor is concentrated

As discussed above, cells in which both the default and chemotropic pathways have been inactivated are unable to form mating projections. Surprisingly, this phenotype arises not from a failure to establish polarity, but from an inability to maintain it. This was first demonstrated by Nern and Arkowitz, who found that in pheromone-treated *cdc24-m1 bud1*Δ cells, the Cdc42 GEF, Cdc24, and the polarisome component Spa2 localized to discrete sites. The cell grows uniformly, however, because its axis of polarity wanders (Nern and Arkowitz, 2000). Indeed, markers for secretion, new cell wall incorporation, and the Ste2 pheromone receptor were spread out over approximately half the cell after several hours of pheromone treatment. More recently, it has been found that another polarisome marker, Bem1-GFP, wanders very rapidly around the membrane of pheromone-treated *cdc24-m1 bud1*Δ cells (Daniel Lew, personal communication). This supports the earlier conclusion that chemotropic/default shmoo pathway double mutants are unable to shmoo because they cannot stabilize their axis of polarity long enough to polarize their growth.

Could the blunt shmoo and SMP phenotypes be the result of a less severe wandering-axis phenotype as observed in *cdc24-m1 bud1*Δ cells? Perhaps the axis of polarity wanders in Gβ^{P-} *bud1*Δ cells, but the wandering is confined to a smaller region. To test this possibility, we mixed *MAT***a** Gβ^{P-} *bud1*Δ and *MAT***a** Gβ *bud1*Δ cells expressing Spa2-GFP with WT *MAT*α cells and assayed the localization of the reporter over time (Fig. 5A). In the Gβ *bud1*Δ control cells, Spa2-GFP typically localized tightly and invariantly to the tip of the growing mating projection, moving steadily outward along the axis of polarity. In the Gβ^{P-} *bud1*Δ cells, Spa2-GFP moved more than twice

as fast and twice as far, even though the mutant shmoos did not elongate more than the control cells. Rather, the increased mobility of Spa2-GFP correlated with a significantly increased tendency to change direction (Table III). Multiple Spa2-GFP spots were also commonly observed in the mutant, but rarely in control cells. Thus, the axis of polarity exhibited confined wandering within the broad mating projections formed by Gβ^{P-} *bud1*Δ cells during mating.

It is well established that essential regulators of actin cable polymerization (*e.g.* Cdc24, Cdc42, Bem1, and Spa2) cluster tightly in a patch at the tips of shmooing cells. A recent study concluded that in pheromone-treated WT cells, this "polarity patch" wanders along the cell cortex before stabilizing at the incipient growth site (Daniel Lew, personal communication). Polarity patch movement, which is driven primarily by actin-dependent vesicle fusion tangential to the center of Cdc42 activity, is thought to be retarded by free Gβγ. Hence, in this model, the position of the polarized growth site is ultimately determined by the local density of activated receptor. A supporting observation is that the role of the receptor and Gβγ in stabilizing the polarity patch can be bypassed by a chimeric protein consisting of Bem1 and the transmembrane domain of the v-SNARE, Snc2. Expression of Bem1-GFP-Snc2 dramatically slowed movement of the polarity patch, focusing the growth of WT cells and restoring the ability of *cdc24-m1 bud1*Δ cells to shmoo (Daniel Lew, personal communication). If the shmoo morphology and maintenance defects displayed by Gβ^{P-} *bud1*Δ cells are also due to a wandering axis of polarity stemming from a weakened link between the receptor and polarity patch, we would expect these phenotypes to be suppressed by Bem1-GFP-Snc2 as well. This proved to be the case; the shmoos formed by Gβ *bud1*Δ and Gβ^{P-}

*bud1*Δ cells transformed with the Bem1-GFP-Snc2 construct were indistinguishable (Fig. 5B).

One explanation for the results shown in Figure 5A-B is that the axis of polarity wanders in Gβ^{P-} *bud1*Δ cells, and that it does so due to a weakening of the interaction between the polarisome and the Ste2 pheromone receptor. Like the Bem1-GFP-Snc2 chimera, the receptor is a slowly diffusing, integral membrane protein. Moreover, the receptor is the primary determinant of chemotropic growth. In cells responding to pheromone, the receptor polarizes to the mating projection (Suchkov et al., 2010), and this is the same area within which the growth site wanders in pheromone-treated Gβ^{P-} *bud1*Δ cells. This confined wandering might underlie the formation of proximal projections. To determine whether receptor polarity influences the ability of Gβ^{P-} *bud1*Δ cells to form proximal mating projections, we constructed Gβ^{P-} *bud1*Δ and Gβ *bud1*Δ strains expressing the Ste2^{7XR} mutant form of the receptor. The Ste2^{7XR} receptor cannot be internalized upon ligand binding. Therefore, this mutant form of the receptor does not polarize in response to pheromone and instead, remains uniformly distributed on the plasma membrane (Terrell et al., 1998). Consistent with our hypothesis, preventing internalization and polarization of the receptor completely suppressed the tendency of Gβ^{P-} *bud1*Δ cells to form proximal projections (Fig. 5C).

Together, the data shown in Figure 5 indicate that, although there is a tendency for the axis of polarity to wander in Gβ^{P-} *bud1*Δ cells, the movement of the growth site is limited to the region of highest receptor density. This implies that phosphorylation of Gβ helps to link the position of the polarity patch to that of the receptor.

Figure 5. The growth site of pheromone-treated Gβ^{P-} *bud1*Δ cells wanders where the receptor is concentrated.
(A) Time-lapse images of Spa2-GFP in mating cells. *MAT***a** Gβ *bud1*Δ or Gβ^{P-} *bud1*Δ cells transformed with an integrative vector carrying *SPA2-GFP* were mixed with congenic *MAT*α cells, incubated on agar pads at 30°C, and imaged every 15min for 3hr. The movement of Spa2-GFP between each 15min step was tracked using the Manual Tracking plugin (developed by Fabrice Cordelières, Institut Curie, Orsay FR) in ImageJ. Final images show an overlay of the track from 60-180min. Bar, 5μm. (B) Bem1-GFP-Snc2 rescues the Gβ^{P-} *bud1*Δ shmoo abnormalities. *MAT***a** Gβ *bud1*Δ or Gβ^{P-} *bud1*Δ cells transformed with an integrative vector carrying a *BEM1-GFP-SNC2* fusion were exposed to 30nM pheromone for 3hr. Representative images are shown. Bar, 5μm. (C) Gβ^{P-} *bud1*Δ cells don't form proximal projections when receptor internalization is blocked. *MAT***a** Gβ *bud1*Δ, Gβ *bud1*Δ Ste2^{7XR}, Gβ^{P-} *bud1*Δ, and Gβ^{P-} *bud1*Δ Ste2^{7XR} cells were exposed to 25nM pheromone for 4hr. The percentages of cells with a single projection, multiple distal projections, and multiple proximal projections were determined. The bar graphs represent the mean of three independent experiments ± SEM, with n = 300 for each strain and trial. *$p < 0.0001$ for the comparisons Gβ^{P-} *bud1*Δ vs. Gβ *bud1*Δ and Gβ^{P-} *bud1*Δ Ste2^{7XR} single-projection cells; **$p < 0.0001$ for the comparisons Gβ^{P-} *bud1*Δ vs. Gβ *bud1*Δ and Gβ^{P-} *bud1*Δ Ste2^{7XR} proximal-projection cells.

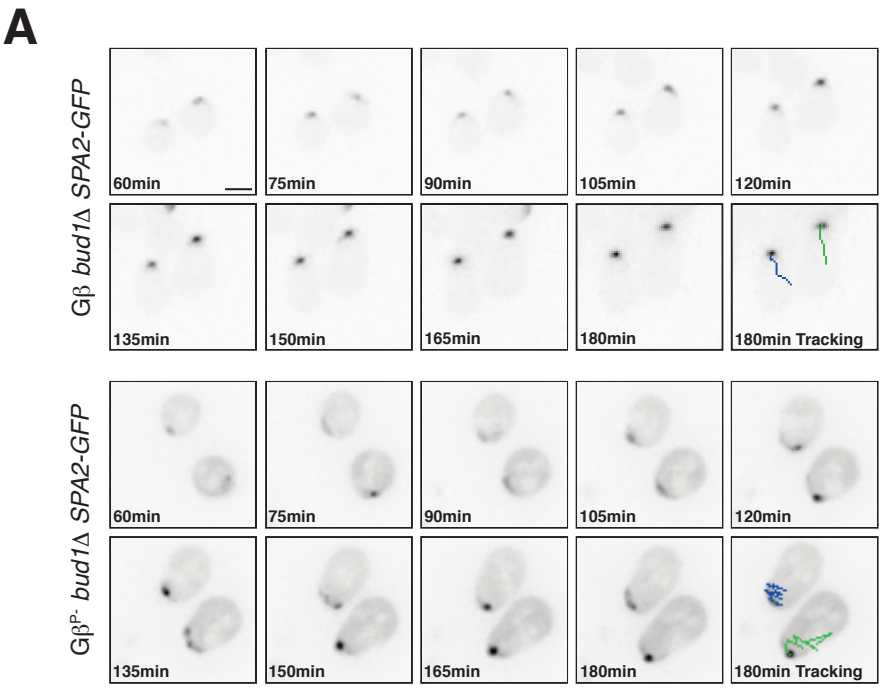
A
Gβ bud1Δ SPA2-GFP
60min
75min
90min
105min
120min
135min
150min
165min
180min
180min Tracking
Gβ^P- bud1Δ SPA2-GFP
60min
75min
90min
105min
120min
135min
150min
165min
180min
180min Tracking

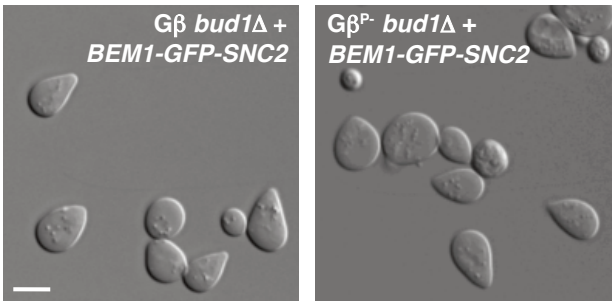
B
Gβ bud1Δ +
BEM1-GFP-SNC2
Gβ^P- bud1Δ +
BEM1-GFP-SNC2

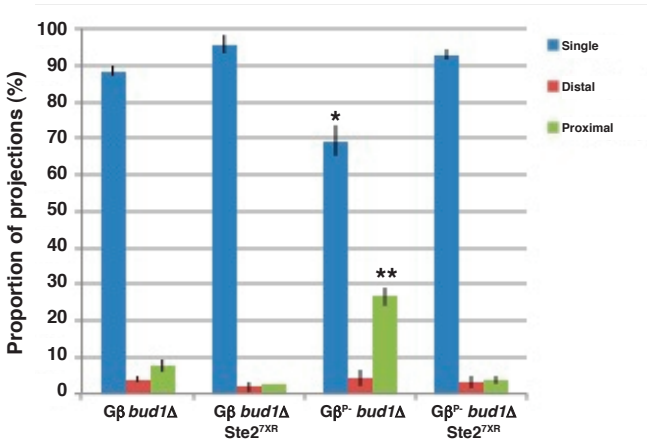
C
Proportion of projections (%)
100
90
80
70
60
50
40
30
20
10
0
*
**
Single
Distal
Proximal
Gβ bud1Δ
Gβ bud1Δ Ste2^7XR
Gβ^P- bud1Δ
Gβ^P- bud1Δ Ste2^7XR

Table III. Spa2-GFP Mobility

Strain	Movement/step (μm)	Velocity (μm/hr)	Δ Direction (%)[a]	Final length (μm)	≥ 2 spots	*n*
$G\beta^{WT}$ *bud1*Δ	0.54 ± 0.15	2.15 ± 0.61	19± 13	8.07 ± 0.97	1	89
$G\beta^{P-}$ *bud1*Δ	1.13 ± 0.24	4.51 ± 0.96	52± 15	7.39 ± 1.10	18	38

[a] ΔDirection (%) was calculated by dividing the number of direction changes by the number of steps observed for each cell.

2.3.4 The effect of Gβ phosphorylation on Gβ localization

One way that the cell's inability to phosphorylate Gβ could result in the phenotypes we observe in $G\beta^{P-}$ *bud1*Δ cells is if the mutant form of Gβ is not properly localized. To test this possibility, we tagged the N-termini of WT Gβ and $G\beta^{P-}$ with GFP *in situ*. In cells subjected to isotropic pheromone treatment, the WT Gβ reporter polarized to the incipient shmoo site significantly earlier than did GFP-$G\beta^{P-}$ (Table IV; Fig. 6A). Moreover, GFP-$G\beta^{P-}$ failed to stably polarize in a significantly higher proportion of cells. Similar but more pronounced defects were observed in mating mixtures (Table IV; Fig. 6B). Notably, a substantial fraction of mating GFP-Gβ cells clearly switched from one polarization site to another, perhaps due to orientation away from the default site or to changes in the direction of the strongest ambient gradient. In contrast, mating GFP-$G\beta^{P-}$ cells were significantly defective in site switching, as well as in consolidating the reporter in a single region of the membrane. These data suggest that Gβ phosphorylation plays an important role in the pheromone-induced redistribution of Gβ, particularly in gradient-stimulated cells.

Figure 6. GFP-Gβ^{P-} polarizes later and less stably than GFP-Gβ in both isotropic and gradient conditions.

(A) Isotropic treatment. *MAT***a** GFP-Gβ *bud1*Δ and GFP-Gβ^{P-} *bud1*Δ cells were exposed to 150nM pheromone on agar pads at 30°C, and imaged every 10min for 90min. Bar, 5µm. (B) Mating mixtures. *MAT***a** GFP-Gβ *bud1*Δ and GFP-Gβ^{P-} *bud1*Δ cells were mixed with congenic *MAT*α cells, incubated on agar pads at 30°C, and imaged every 15min for 3hr. Bar, 5µm. For A and B, black arrowheads mark morphogenesis and white arrowheads mark reporter polarity. Reporter polarity was quantified using the MatLab program BudPolarity as described in the Materials and Methods and is represented in the charts below each image. Fluorescent images were false-colored using Fiji software. For B, white arrows mark spots and the white asterisk marks non-consolidated polarization (see Table IV).

A

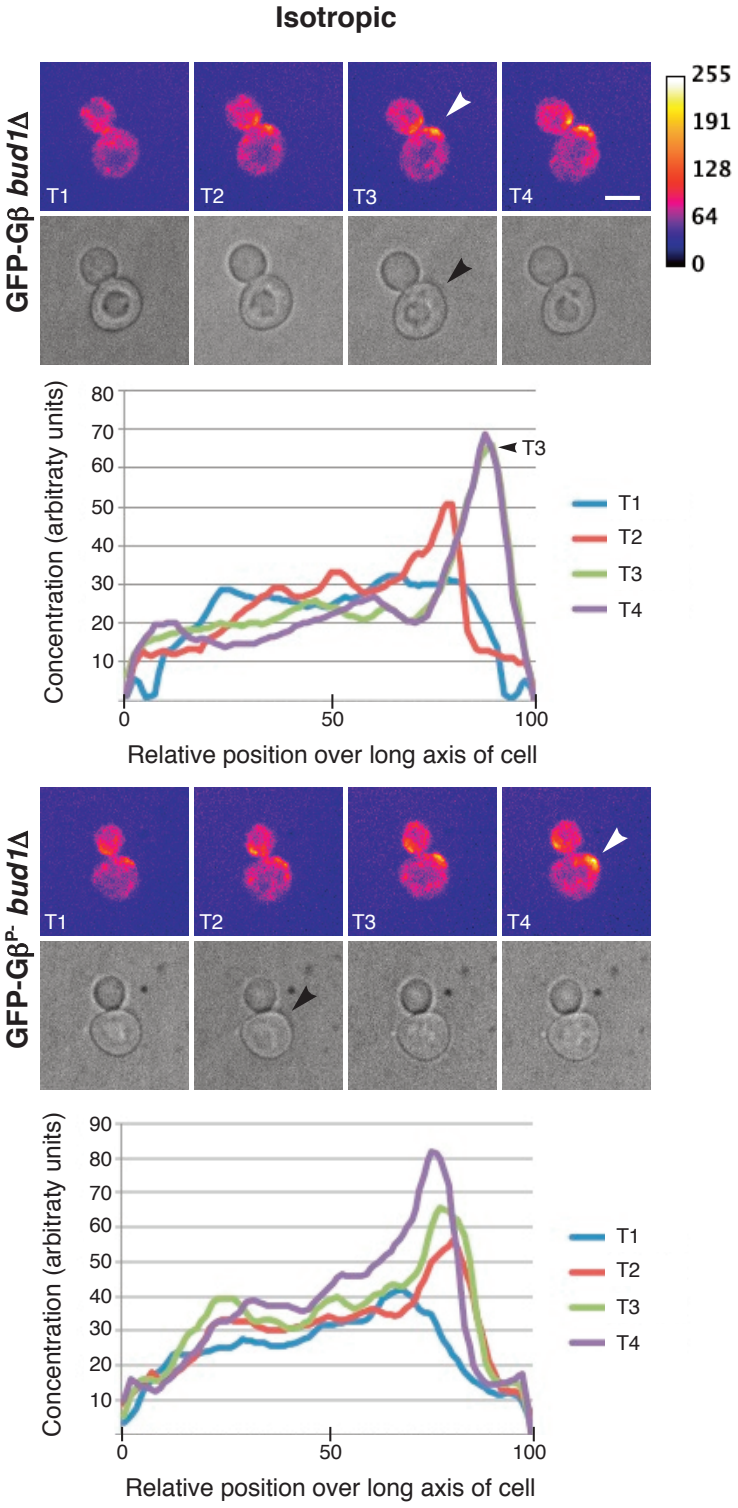
Isotropic
GFP-Gβ bud1Δ
T1
T2
T3
T4
255
191
128
64
0
Concentration (arbitraty units)
80
70
60
50
40
30
20
10
0
50
100
Relative position over long axis of cell
T1
T2
T3
T4
GFP-Gβ^P- bud1Δ
T1
T2
T3
T4
Concentration (arbitraty units)
90
80
70
60
50
40
30
20
10
0
50
100
Relative position over long axis of cell
T1
T2
T3
T4

B

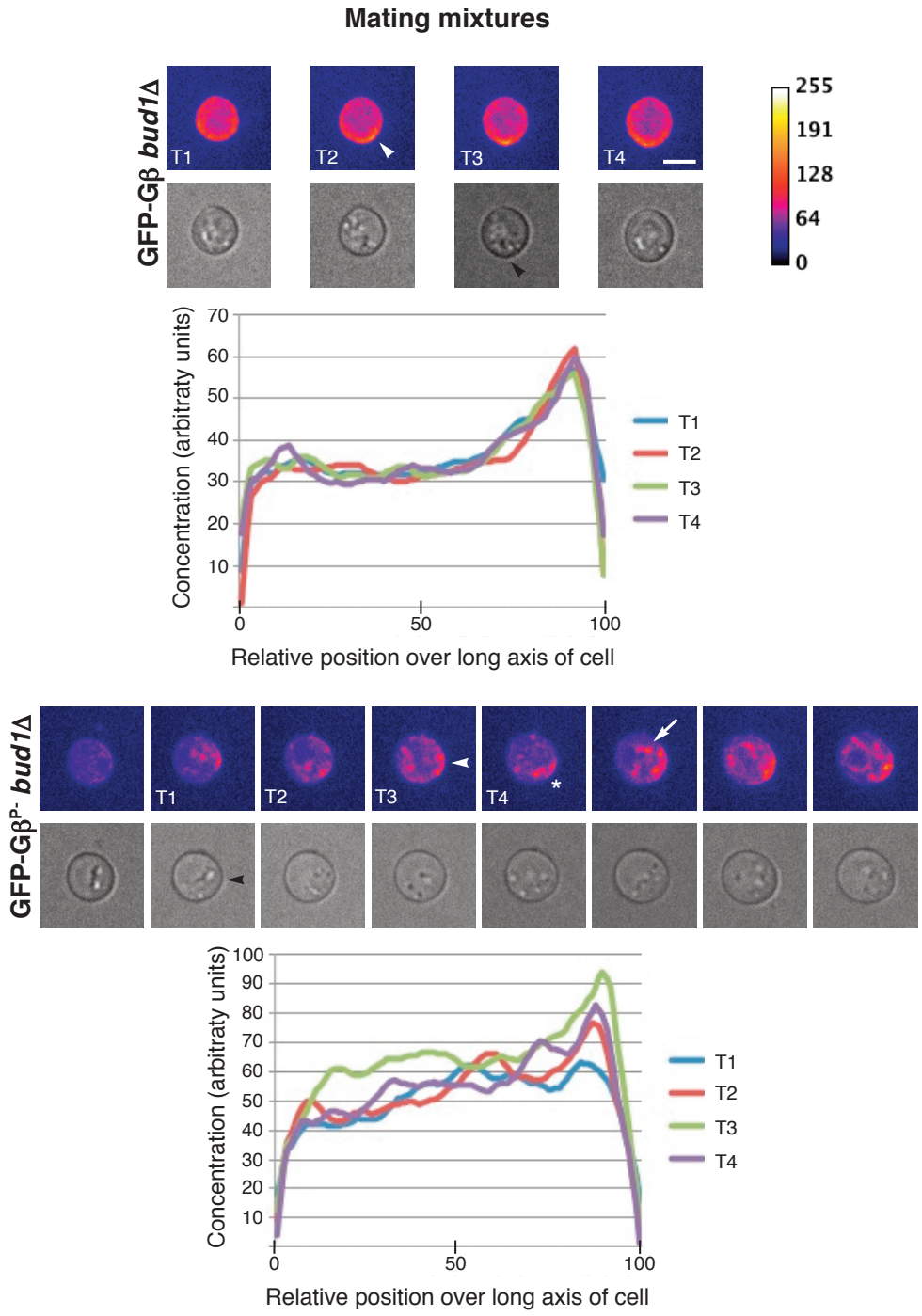
Mating mixtures
GFP-Gβ bud1Δ
T1
T2
T3
T4
255
191
128
64
0
Concentration (arbitraty units)
70
60
50
40
30
20
10
0
50
100
Relative position over long axis of cell
T1
T2
T3
T4
GFP-Gβ^P- bud1Δ
T1
T2
T3
T4
*
Concentration (arbitraty units)
100
90
80
70
60
50
40
30
20
10
0
50
100
Relative position over long axis of cell
T1
T2
T3
T4

Table IV. Pheromone-induced polarization of Gβ

	Isotropic			*Mating*		
	GFP-Gβ	GFP-Gβ^{P-}	*p* value	GFP-Gβ	GFP-Gβ^{P-}	*p* value
Total *n*/Polarized *n*	49/47	52/39		36/33	43/25	
% Polarized[a]	95.9	75	< 0.0001	91.7	58.1	< 0.0001
Mean time of polarization (min)[b]	1. 8 ± 0.4	17.3 ± 1.73	< 0.0001	-8.8 ± 2.4	16.8 ± 4.2	< 0.0001
% Polarized pre-morphogenesis[c]	55.3	38.4	0.034	84.8	28.0	< 0.0001
% Switch[d]	NA	NA		39.4	12.0	0.005
% Wandering[e]	ND	ND		9.1	36.0	< 0.0001
% Not consolidated[f]	ND	ND		34.4	92.0	< 0.0001
% Spots[g]	ND	ND		21.2	72.0	< 0.0001

[a] Cells were scored as polarized or unable to polarize according to the criteria described the legend to Fig. 6

[b] For cells that polarized Gβ, mean times of polarization ± SEM relative to the onset of morphogenesis are indicated

[c] Percentage of Gβ-polarized cells in which polarization occurred at or before morphogenesis

[d] Percentage of Gβ-polarized cells that clearly switched polarization sites during the time-course

[e] Percentage of Gβ-polarized cells in which the region of concentrated Gβ appeared to wander

[f] Percentage of Gβ-polarized cells in which the region of concentrated Gβ was composed of two or more spots

[g] Percentage of Gβ-polarized cells in which high-intensity spots were observed far from the region of concentrated Gβ

2.3.5 The effect of Gβ^{P-} on Gβ-Far1 interaction and Spa2 and Cdc42 dynamics

Another way that inability to phosphorylate Gβ could impact the cell is if the phosphorylation of Gβ affects the strength of its interactions. There is evidence, for example, that Ste5 interacts preferentially with the phosphorylated form of Gβ in yeast (Feng et al., 1998) and that phosphorylation affects the activity of a mammalian Gβ (Chakrabarti and Gintzler, 2003). Given the phenotypes conferred by Gβ^{P-}, the interaction of Gβ with the Far1-Cdc24 chemotropic complex is a good candidate to be regulated by Gβ phosphorylation. To test of this possibility, we used a well-established genetic assay to ask whether Far1 can discriminate between Gβ and Gβ^{P-}. The assay is based on the observation that by triggering the pheromone-responsive MAPK pathway, overexpression of Gβ blocks cell cycle progression and therefore, cell proliferation. Co-overexpression of a protein that binds Gβ can prevent pathway induction and thereby rescue the vegetative growth of cells expressing excess Gβ. At the level of transcriptional induction, cell cycle arrest, and shmooing, Gβ and Gβ^{P-} appear to be equally potent (Li et al., 1998; Fig. 4B). Nevertheless, overexpression of Far1 specifically rescued the cell growth defect due to the overexpression of Gβ^{P-}, and not that of Gβ (Fig. 7A), suggesting that Far1 has a greater affinity for the unphosphorylated form of Gβ.

To further investigate the possibility that the phosphorylation of Gβ affects the dynamic interactions of the chemotropic complex, we used *in vivo* fluorescence photo-bleaching approaches. First, we compared recovery times of the Spa2-GFP signal after photo-bleaching the shmoo tips of Gβ^{P-} *bud1*Δ and Gβ *bud1*Δ cells. We chose to study

Spa2 because, as a component of the polarisome, its positional stability is likely linked to that of the chemotropic complex. In FRAP analysis, the recovery time is a function of the reporter protein's dynamics (*i.e.* the slower the exchange into and out of a complex, the longer the signal will take to recover). As shown in Figure 7B, the signal recovered in bleached Gβ *bud1*Δ shmoo tips significantly faster and to a greater degree than in bleached $G\beta^{P-}$ *bud1*Δ shmoo tips. This suggests that the duration of Spa2 interactions at the shmoo tip is increased when Gβ cannot be phosphorylated.

To assess the effect of $G\beta^{P-}$ on the stability of the chemotropic complex itself, we performed iFRAP analysis of GFP-Cdc42 at the shmoo tips of $G\beta^{P-}$ *bud1*Δ and Gβ *bud1*Δ cells. In this technique, the area that serves as a source of reporter molecules bound for the complex of interest is photo-bleached, and the rate at which the signal intensity decays at the site of complex formation is measured. The rate of signal decay is inversely related to the stability of the complex. In our experiment, the back two thirds of cells were bleached, and the rate of GFP-Cdc42 signal decay at the shmoo tip was determined. As shown in Figure 7C, the Cdc42-GFP signal decayed faster in Gβ *bud1*Δ shmoo tips than in the $G\beta^{P-}$ *bud1*Δ shmoo tips. Consistent with the Spa2-GFP FRAP results, this suggests that the duration of Cdc42 interactions at the shmoo tip are increased when Gβ cannot be phosphorylated. Together, these data suggest that the unphosphorylated form of Gβ binds more tightly than the phosphorylated form to components of the chemotropic complex and polarisome. In other words, Gβ phosphorylation may negatively affect the stability of the chemotropic complex and polarisome.

Figure 7. The effect of $G\beta^{P-}$ on Gβ-Far1 interaction and positional stability of Spa2 and Cdc42.

(A) Far1 overexpression rescues overexpression of $G\beta^{P-}$ but not of Gβ. Strains transformed with the indicated plasmids were spotted on galactose-containing medium to induce the overexpression of Far1 and Gβ or Far1 and $G\beta^{P-}$. Ten transformants of each type were tested, and representative results for two strains of each type are shown. All transformants spotted on glucose-containing medium grew normally (not shown). (B) FRAP analysis of Spa2-GFP. *MAT***a** Gβ *bud1*Δ and $G\beta^{P-}$ *bud1*Δ cells transformed with an integrative vector carrying *SPA2-GFP* were exposed to 60nM pheromone for 1hr prior to bleaching. The data represent the means of two independent experiments ± SEM. The FRAP $t_{1/2}$ in seconds and % recovery were 9.7 +/- 1.87 and 40.3, respectively, in Gβ *bud1*Δ cells (*n* = 18), as compared to 19.3 +/- 2.32 (*p* = 0.003) and 24.6 (*p* = 0.0002) in Gβ *bud1*Δ cells (*n* = 20). (C) iFRAP analysis of GFP-Cdc42. *MAT***a** Gβ *bud1*Δ and $G\beta^{P-}$ *bud1*Δ cells transformed with a 2μm vector carrying *GFP-CDC42* were exposed to 60nM pheromone for 1hr prior to bleaching. Representative scatter plots of fluorescence loss and corresponding trend lines are shown. The iFRAP $t_{1/2}$ in seconds ± SEM and % loss from three independent experiments were 41.9 +/- 3.25 and 22.9, respectively, in Gβ *bud1*Δ cells (*n* = 27), as compared to 54.3 +/- 3.55 (*p* = 0.01) and 21.1 in $G\beta^{P-}$ *bud1*Δ cells (*n* = 28).

A

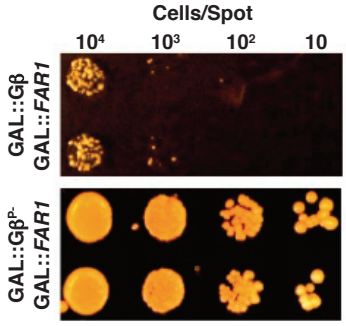
Cells/Spot
10⁴
10³
10²
10
GAL::Gβ
GAL::FAR1
GAL::Gβ^P-
GAL::FAR1

B

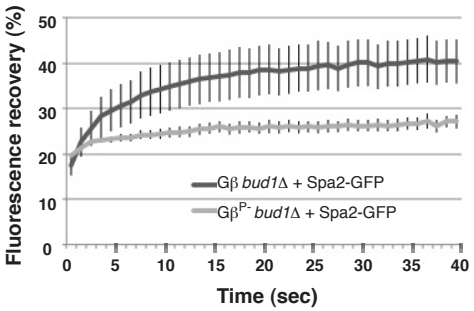
Fluorescence recovery (%)
50
40
30
20
10
0
0 5 10 15 20 25 30 35 40
Time (sec)
Gβ bud1Δ + Spa2-GFP
Gβ^P- bud1Δ + Spa2-GFP

C

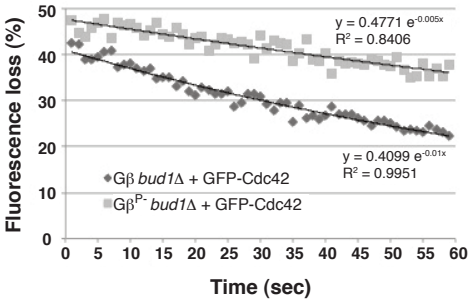
Fluorescence loss (%)
50
40
30
20
10
0
0 5 10 15 20 25 30 35 40 45 50 55 60
Time (sec)
y = 0.4771 e^-0.005x
R² = 0.8406
y = 0.4099 e^-0.01x
R² = 0.9951
Gβ bud1Δ + GFP-Cdc42
Gβ^P- bud1Δ + GFP-Cdc42

2.3.6 Gβ^{P-} confers defects in directional sensing and chemotropic growth

In cells lacking Bud1, mating projection formation in isotropic pheromone is thought to depend on chemotropic components (Nern and Arkowitz, 2000). Therefore, the observation that Gβ^{P-} *bud1*Δ cells but not Gβ^{P-} *BUD1* cells shmoo aberrantly in isotropic pheromone implicates Gβ phosphorylation in chemotropism. To determine whether Gβ phosphorylation plays a role in actual gradient sensing, we set up dilute bilateral mating mixtures, in which the cells best able to form stable, chemotropic mating projections were most likely to find and fuse with a partner, and analyzed images of newly formed zygotes (Fig. 8A). How precisely a cell orients towards a potential mating partner (*i.e.* the accuracy of its gradient sensing) can be inferred by measuring the angle created when two cells fuse. When gradient sensing is optimal, the two cells of a mating pair grow directly toward one another, and consequently, their angle of fusion is ~ 0°. In contrast, large fusion angles are indicative of poor gradient sensing. In the zygote formation assay Gβ^{P-} cells exhibited a clear orientation defect, forming significantly greater fusion angles (the mean ± SEM was 15.4 ± 0.3° in the WT crosses and 27.1.9 ± 0.5° in the Gβ^{P-} crosses; total $n > 200$ for each strain in 3 trials; $p < 0.0001$).

In addition to their well studied ability to orient growth toward a pheromone source, budding yeast are also adept at changing the direction of their growth in response to a vectorial change in the gradient (Moore et al., 2008; Segall, 1993). Cells respond to a change in the direction of a pheromone gradient in one of two ways. They either initiate a second projection oriented toward the new source, or the existing projection bends in the direction of the new source (Moore et al., 2008). These

phenomena are collectively referred to as *reorientation*. Although there are, as yet, no published insights into how cells reorient, the mechanisms underlying this process are likely to overlap and/or interact with those involved in initial orientation and maintenance. As our data suggest a role for Gβ phosphorylation in initial orientation and stable chemotropic growth, we asked whether it is involved in reorientation as well. WT and $G\beta^{P-}$ bilateral mating mixtures were shaken vigorously to induce non-directional (default) shmooing while preventing cell fusion, then allowed to produce and respond to pheromone gradients on solid medium. As shown in Figure 8B, $G\beta^{P-}$ conferred a clear reorientation defect. Whereas pre-stimulated WT cells often bent dramatically to contact a mating partner, $G\beta^{P-}$ cells formed zygotes that were predominantly the result of "collision matings" where two shmoos appeared to have simply grown into one another without having significantly changed their direction of growth. The mean angles of reorientation ± SEM were 35.7 ± 4.8° for WT vs. 10.2 ± 3.1° for $G\beta^{P-}$ (n = 58 for both strains; $p < 0.0001$).

Figure 8. $G\beta^{P-}$ confers a defect in directional sensing.
(A) Representative straight and angled zygotes from the orientation assays. Zygotes were analyzed from WT and $G\beta^{P-}$ bilateral matings. The angle of orientation was measured by drawing a line from the base of each shmooing cell (white) to the zone of fusion (black). Bar, 5μm. (B) Representative zygotes from the reorientation assays. Pre-stimulated *MAT***a** and *MAT*α cells were allowed to mate on solid media and scored for their ability to reorient growth of an existing mating projection. Zygotes were analyzed from WT and *MAT***a** $G\beta^{P-}$ bilateral matings. Reorientation was defined as a change in direction in a line drawn from the base of a shmoo to the zone of fusion. The angle of reorientation for a given shmoo was measured by drawing a line from the original axis of polarity (white) to the zone of fusion (black). Bar, 5μm.

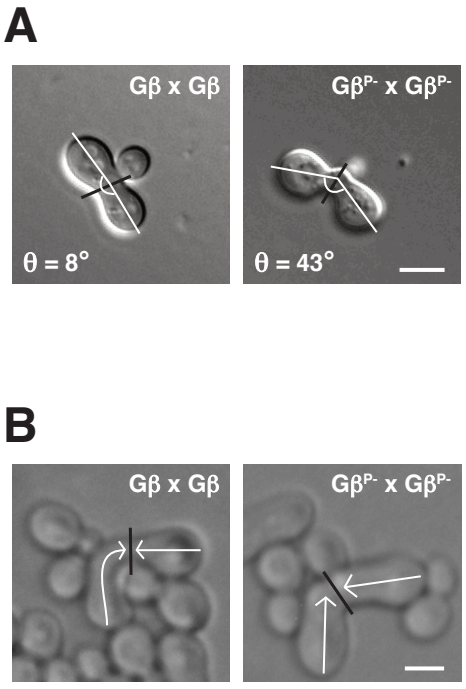
A
Gβ x Gβ
θ = 8°
Gβ^P- x Gβ^P-
θ = 43°
B
Gβ x Gβ
Gβ^P- x Gβ^P-

One explanation for the results of the orientation and reorientation assays is that Gβ^{P-} confers a defect in directional sensing and/or chemotropic shmooing. However, it is also possible that Gβ^{P-} cells signal their positions less effectively than WT cells because their pheromone secretion is less focused. To distinguish these possibilities, we compared the ability of Gβ and Gβ^{P-} cells to grow toward a source of pheromone *in vitro*, using a microfluidic device (Dave Eddington, UIC collaboration). As previously reported, the Gβ control cells formed normal mating projections in the artificial gradient (Fig. 9A) and oriented toward its source with an accuracy similar to that observed in other published microfluidic experiments (Moore et al., 2008; Paliwal et al., 2007; Dave Eddington, UIC collaboration). Surprisingly, the Gβ^{P-} cells were unable to sustain growth in a single direction. Rather, they formed multiple small protrusions, often without growing much in overall size very much like the SMP cells found in Gβ^{P-} *bud1*Δ cultures treated with isotropic pheromone (Fig. 4B). Moreover, the first protrusions formed by the gradient-stimulated Gβ^{P-} cells were directed randomly, virtually without detectable orientation toward the pheromone. In contrast, Gβ^{P-} cells formed normal mating projections when treated with isotropic pheromone in the microfluidic device (Fig. 9B), as they did in liquid medium (Fig. 4B). These data strongly support the idea that Gβ phosphorylation plays a role in the positioning and maintenance of the chemotropic growth site. Under isotropic conditions, Gβ^{P-} cells form normal mating projections at the presumptive default site, apparently unaffected by their inability to phosphorylate Gβ. When subjected to directional stimulation, however, the mutant cells appear to recognize that they are in a gradient, repeatedly trying and failing to stably

grow towards the source. Remarkably, Gβ^{P-} cells exposed to an artificial pheromone gradient were unable to stabilize their growth at the default shmoo site.

The inability of Gβ^{P-} cells to maintain a single axis of polarity in an artificial gradient combined with their ability to form normal mating projections in isotropic pheromone provides the first example, to our knowledge, of a gradient-specific shmoo phenotype. We therefore wished to confirm this observation using natural gradients. To look for gradient-dependent destabilization of polarized growth under physiological conditions, we compared WT and Gβ^{P-} shmoos formed in liquid culture (isotropic treatment) with those formed in bilateral crosses. Although the Gβ^{P-} cells in mating mixtures were not as severely handicapped in chemotropic shmooing as the Gβ^{P-} cells in the microfluidic device, they exhibited a number of obvious shmoo defects (Fig. 9C-D). In fact, the response of Gβ^{P-} *BUD1* cells exposed to natural pheromone gradients was essentially the same as that of Gβ^{P-} *bud1*Δ cells exposed to isotropic pheromone. Gβ^{P-} mating mixtures accumulated fewer shmoos, shorter shmoos (their mean length was 0.852 of the control cells after 5 hours of mating; $n \geq 105$; $p < 0.0001$), and a significantly higher proportion of aberrant shmoos (compare Fig. 9D to Fig. 4C). In contrast, the Gβ^{P-} and WT shmoos induced by isotropic treatment were indistinguishable at all concentrations and time points (Fig. 4B). These data suggest that the phosphorylation of Gβ plays a critical role in chemotropic, but not default, shmooing.

Figure 9. $G\beta^{P-}$ confers chemotropic growth defects in both artificial and natural pheromone gradients.

(A) $G\beta^{P-}$ *BUD1* cells cannot properly orient and stabilize polarized growth in an artificial pheromone gradient. Representative time-lapse images of gradient-stimulated WT and $G\beta^{P-}$ cells in a microfluidic device are shown. Black arrows indicate the direction of the gradient. The mean orientation angle ± SEM for the first protrusions formed by $G\beta^{P-}$ cells was 89.9 ± 4.2° (*n* = 314), as compared to 56.9 ± 4.6° (*n* = 83) for WT shmoos, where 90° indicates random orientation. Bar, 5μm. (B) $G\beta^{P-}$ *BUD1* cells form normal mating projections when stimulated with isotropic pheromone in the microfluidic device. Representative time-lapse images of shmooing $G\beta^{P-}$ *BUD1* cells are shown. Bar, 5μm. (C) $G\beta^{P-}$ *BUD1* cells in mating mixtures exhibit shmoo defects similar to $G\beta^{P-}$ *bud1*Δ cells exposed to isotropic pheromone. Representative images of cells removed from bilateral Gβ *BUD1* and $G\beta^{P-}$ *BUD1* mating mixtures after 5hr. Black arrowheads indicate cells scored as single shmoos, white arrowheads indicate distal double projections, and black arrows indicate proximal double projections. Small squares are examples of SMP cells. Bar, 5μm. (D) Quantification of the shmoo types found in the WT and $G\beta^{P-}$ bilateral mating mixtures. The percentages of shmooed cells in each class are shown in the bar graph. *n* = 300 for both strains; **p* < 0.0001 for the comparison Gβ vs. $G\beta^{P-}$ in each class. Similar results were obtained in each of 3 trials.

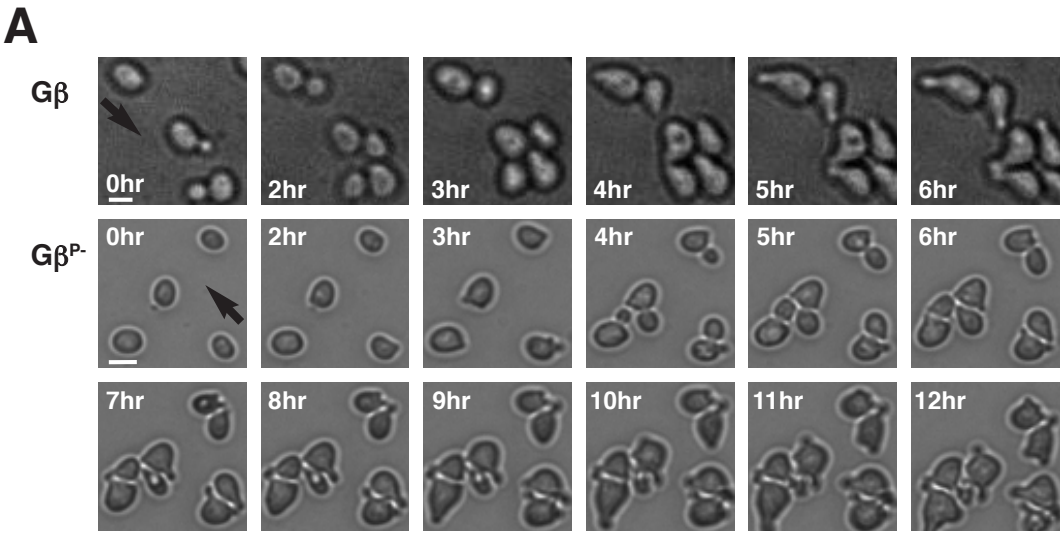
A
Gβ
0hr
2hr
3hr
4hr
5hr
6hr
Gβ^P-
0hr
2hr
3hr
4hr
5hr
6hr
7hr
8hr
9hr
10hr
11hr
12hr

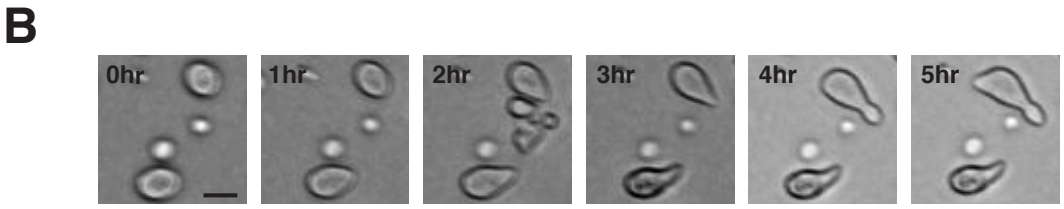
B
0hr
1hr
2hr
3hr
4hr
5hr

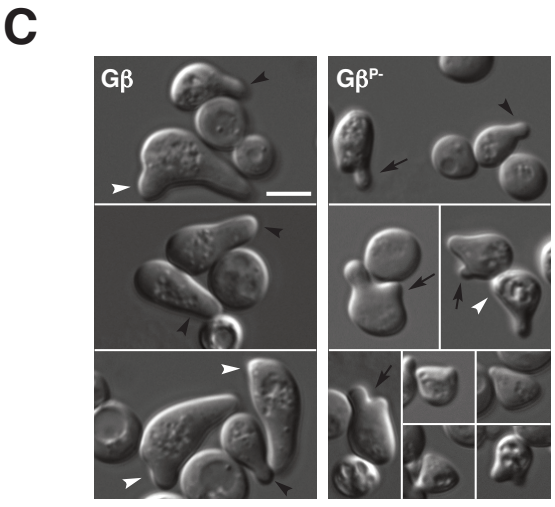
C
Gβ
Gβ^P-

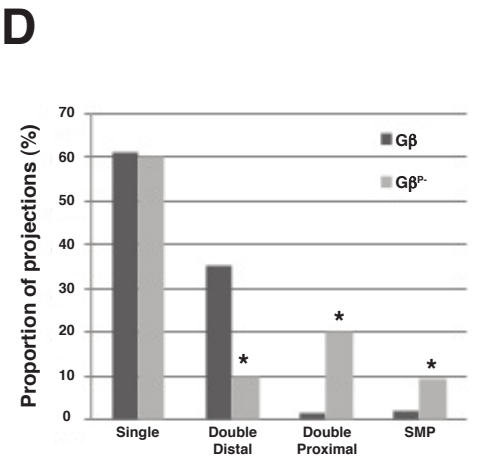
D
Proportion of projections (%)
70
60
50
40
30
20
10
0
Gβ
Gβ^P-
*
*
*
Single
Double Distal
Double Proximal
SMP

2.4 Discussion

The rapid phosphorylation of Gβ in yeast cells responding to mating pheromone was observed over 20 years ago (Cole and Reed, 1991), and yet, its function has remained enigmatic. Two early studies failed to elucidate its role (Cole and Reed, 1991; Li et al., 1998). We were compelled to revisit this issue by the discovery that the activated forms of Gα and Fus3 interact, and that a double mutation that uncouples them, $G\alpha^{DSD}$, conferred defects in mating and partner discrimination (Metodiev et al., 2002). Indeed, we show here that $G\alpha^{DSD}$ *bud1*Δ cells cannot form mating projections, which identifies $G\alpha^{DSD}$ as a chemotropic-defective allele (Fig. 4A), in the same class as *cdc24-m1* and *far1-H7* (Nern and Arkowitz, 1999). This suggests that the Gα-Fus3 interaction, like the Cdc24-Far1 interaction, is critical for chemotropism. Because $G\alpha^{DSD}$ also results in reduced Gβ phosphorylation and protein levels in stimulated cells, we hypothesized that Gβ phosphorylation plays a role in chemotropism. Our results demonstrate that this is the case.

2.4.1 Aberrant shmoo morphology and proximal projections: confined wandering determined by receptor density

When combined with mutations that inactivate the default shmoo pathway (*e.g.* *bud1*Δ), mutations that inactivate the chemotropic shmoo pathway result in the inability to form mating projections (Dorer et al., 1995; Nern and Arkowitz, 1999). We therefore examined the morphological response of $G\beta^{P-}$ *bud1*Δ cells in isotropic pheromone conditions. Although not completely defective for mating projection formation, $G\beta^{P-}$ *bud1*Δ cells exhibited a variety of shmoo morphologies (Fig. 4B-C), including short and

blunt shmoos, cells that formed multiple projections proximal to the first, and very small cells with multiple protrusions (SMP cells). Time-lapse imaging of Spa2-GFP in these cells indicated that the axis of polarity wandered, albeit in a confined area (Fig. 5A). This broader region of Spa2 movement correlated with the generation of proximal projections that, as noted above, were formed in the region in which receptor density is expected to be highest. It is therefore of significance that preventing receptor polarization in $G\beta^{P-}$ *bud1*Δ cells dramatically suppressed the proximal-projection phenotype and that expression of Bem1-GFP-Snc2, which slows polarity site wandering by a mechanism independent of the receptor and G protein, restored their ability to shmoo normally (Fig. 5B-C). Together, these observations suggest that although the axis of polarity is destabilized in pheromone-treated $G\beta^{P-}$ *bud1*Δ cells, its wandering is limited by the high concentration of receptor (Suchkov et al., 2010) in the nascent mating projection. This confined wandering likely underlies the formation of short, blunt shmoos, and is responsible for the emergence of multiple projections proximal to the first site of growth.

2.4.2 The role of Gβ phosphorylation in receptor communication to actin cables

What causes confined wandering? In essence, chemotropism is the translation of an extracellular pheromone gradient into a gradient of activated receptors across the cell surface, and the communication of this spatial information to the actin cytoskeleton. The receptor does not communicate with actin directly, but rather via its Gβγ, which recruits Far1-Cdc24. Along with the polarisome, Cdc42, and Bem1, the Gβγ-Far1-Cdc24 chemotropic complex ultimately nucleates actin cables at the incipient mating

projection site. In *cdc24-m1* and *far1-H1* cells, the link between the receptor and chemotropic complex is completely severed. According to our proposed model, polarization sites are established in such cells, but lacking the constraint provided by interaction with a slowly diffusing integral membrane protein, their position is not sufficiently stable to sustain polarized growth. $G\beta^{P-}$ *bud1*Δ cells exhibit a similar, although less severe, phenotype. Instead of global wandering and uniform growth, wandering is confined to the area of most concentrated receptor. This implies that the link between the receptor and chemotropic complex is weakened, but not broken.

We explored the effect of Gβ phosphorylation on the stability of the chemotropic complex and polarisome. Surprisingly, the results of a genetic assay suggested that phosphorylation of Gβ reduces its affinity for Far1 (Fig. 7A). This conclusion was supported by the results of the Spa2-GFP FRAP and GFP-Cdc42 iFRAP analyses (Fig. 7B-C). Both the Spa2 and Cdc42 reporters exhibited substantially decreased mobility in $G\beta^{P-}$ cells as compared to Gβ cells, consistent with longer-lived associations at the shmoo tips. This suggests that the phosphorylation of Gβ decreases its affinity for the chemotropic complex and destabilizes the association of Spa2 with the polarisome. Considering our results along with our proposed model, we can explain the confined wandering observed in $G\beta^{P-}$ *bud1*Δ cells as follows.

Immediately after exposure to pheromone, the activated receptor and G protein are distributed almost uniformly on the plasma membrane, as are the first chemotropic and polarisome complexes to be assembled. As the receptor polarizes, however, so do Gα and Gβγ, leading to the eventual concentration of the signaling proteins at the incipient shmoo site. The high density of free Gβγ in this area biases the recruitment of

Far1-Cdc24, and thus the localized formation of the chemotropic complex. Moreover, as chemotropic complexes dissociate, they are much more likely to reassemble where free Gβγ is concentrated. The half-life of the chemotropic complex is critical. If it is too short, the cell will not be able to initiate polarized growth. If it is too long, the complex will wander out of the region of high-density receptor and G protein before the axis of polarity is established. In WT cells, phosphorylation of Gβ decreases the half-life of the complex, thereby limiting the distance it can travel before dissociating. This increases the chance that the complex components will reassemble within the active growth area, where receptor and G protein concentration are highest. In $G\beta^{P-}$ cells, on the other hand, the half-life of the complex is longer, which allows it to move across the entire region of high-density receptor and G protein. Additionally, the zone of Gβ appears to be less well consolidated in $G\beta^{P-}$ cells (Table IV; Fig. 6). A key aspect in this scenario is the recycling of the G protein (*i.e.* the re-association of the heterotrimer with the receptor). Gβγ cannot report the position of active receptor until it releases from the chemotropic complex and binds inactive Gα. Conversely, the chemotropic complexes are free to move away from the growth site, blind to local Gβγ density, as long as they remain intact. Interestingly, mutations that disrupt the interaction of Gβ with the N-terminal interface of Gα (Strickfaden and Pryciak, 2008), and mutations that slow or prevent inactivation of Gα, *sst2*Δ and $G\alpha^{Q323L}$, have been reported to be defective in chemotropism (Strickfaden and Pryciak, 2008; Daniel Lew, personal communication). We infer that by increasing the rate at which the position of the activated receptor is reported, the Gα-GDP/GTP and the Gβ-phosphorylation/dephosphorylation cycles

strengthen the indirect link between the receptor and the chemotropic complex and consequently, influence the position of the polarisome.

2.4.3 Polarization of Gβ

The results shown in Table IV and Figure 6 suggest that Gβ phosphorylation is critical for pheromone-induced Gβ polarization. Although the GFP-Gβ^{P-} polarization defect could result simply from the drifting axis of polarity discussed above, a number of observations raise a more interesting possibility. Gβ phosphorylation could play a key role in the genesis of pheromone-induced intracellular signaling gradients. Given that full pheromone-induced phosphorylation of Gβ depends on Fus3 and on the Gα-Fus3 interaction (Metodiev et al., 2002) and that gradients of active Fus3 emanate from the tips of shmooing cells (Blackwell et al., 2003; Choi et al., 1999), we propose that Gα recruits Fus3 to phosphorylate Gβ at the incipient shmoo site. As it is also known that pheromone-induced polarization of Gα and Gβ requires their co-internalization with the receptor (Suchkov et al., 2010), it will be interesting to determine whether unphosphorylated Gβ is preferentially internalized along with Gα and the receptor while phosphorylated Gβ is left on the membrane. A synergistic combination of these two mechanisms — localized Gβ phosphorylation at the shmoo site and preferential internalization of unphosphorylated Gβ at the back of the cell — would be expected to rapidly generate a steep gradient of phosphorylated Gβ via what is essentially a LEGI mechanism. An intracellular gradient of phosphorylated Gβ, central to yeast chemotropism, would provide an interesting analogy to the intracellular gradient of the

phosphorylated lipid, PIP_3, found in numerous chemotactic systems (Comer and Parent, 2002; Jin et al., 2000; Servant et al., 2000).

2.4.4 The role of Gβ phosphorylation in chemotropism

If Gβ phosphorylation contributes to chemotropic growth, and not just to the growth of stable mating projections, we would expect $G\beta^{P-}$ to compromise oriented growth towards a pheromone source. To test this, we examined how the inability to phosphorylate Gβ affects chemotropism in both natural and artificial pheromone gradients. These experiments were performed with *BUD1* strains, as we wished to determine how well the chemotropic shmoo pathway would override the default shmoo pathway to orient and sustain growth up a gradient. In mating mixtures, $G\beta^{P-}$ conferred significant defects in initial orientation (Fig. 8A) and polarized growth (Fig. 9C). Similar but more pronounced defects were observed in artificial pheromone gradients (Fig. 9A). Remarkably, the polarized growth phenotypes were gradient-specific. $G\beta^{P-}$ cells formed normal shmoos when treated with isotropic pheromone, whether in liquid media or the microfluidic device but could not maintain polarized growth in either artificial or natural gradients generated by mating partners. It is noteworthy that the types and proportions of aberrant shmoos formed by $G\beta^{P-}$ (*BUD1*) cells in mating mixtures were very similar to those formed by $G\beta^{P-}$ *bud1*Δ cells in isotropic pheromone (compare Fig. 9C-D and 4B-C). In both cases, the cells were forced to use the chemotropic pathway without being able to phosphorylate Gβ. The resulting defects reveal that the cells attempt to shmoo chemotropically but cannot maintain a stable axis of polarity. These data

strongly suggest that Gβ phosphorylation is critical for the initial positioning and maintenance of the chemotropic growth site.

In addition to mechanisms that establish and stabilize directional growth, chemotroping yeast cells must have a means to alter their direction and track what are presumed to be dynamic pheromone gradients in mating mixtures. To successfully fuse with the shmoo tip of a partner, a cell must not only determine the direction of the strongest source of pheromone and orient its growth accordingly, it must continually reassess the position of the target cell while ignoring weaker signals. The shape of the gradient and concentration of pheromone most likely change as the two cells grow toward each other. The directional signals may also change as zygotes form and pheromone secretion decreases. Although the mechanisms underlying reorientation are unknown, it is easy to appreciate that the establishment of a chemotropic growth site and ongoing adjustments to its position pose distinct challenges. To date, only one mutation that specifically affects reorientation has been reported, *ste2*^{T236} (Vallier et al., 2002). It is therefore of considerable interest that Gβ^{P-} confers a dramatic defect in reorientation. This suggests that Gβ phosphorylation plays a critical role in gradient tracking. In summary, we propose that the phosphorylation of Gβ contributes to chemotropism in two ways: (1) to rapidly generate a signaling gradient in which phosphorylated Gβ is concentrated at the incipient shmoo site, facilitating the amplification of other intracellular signaling gradients (2) decreasing Gβ affinity for Far1 and other chemotropic components, thereby shortening the cycle time between the receptor and polarisome. More frequent updating of receptor status increases sensitivity to changes in the pheromone gradient.

3. REORIENTATION OF GROWTH IN DYNAMIC GRADIENTS

3.1 Introduction

As it is a fundamental process in development, much research has been focused on understanding how cells interpret chemical gradients and initially orient their growth in the proper direction. However, the chemical gradients to which cells are exposed are constantly changing, yet cells are still able to grow accurately toward their targets. Thus, cells must employ mechanisms to reorient their growth away from the initial site of polarization in a dynamic gradient. During initial orientation, cells select a specific site for growth based on the direction of the gradient, and it is likely that these cells employ mechanisms to facilitate growth exclusively at this chosen site while simultaneously inhibiting growth at other sites (Arkowitz, 2009; Berzat and Hall, 2010; Raper and Mason, 2010; Wang et al., 2011; Williams et al., 2011). As the gradient shifts, a new growth site will be chosen, and if this site is in the area of the cell where growth was being inhibited prior to the gradient shift, then cells must employ mechanisms to relieve this inhibition and facilitate growth in the new direction of the gradient. Despite its importance, the phenomenon of cell reorientation in response to a changing gradient has not been well studied. Although the ability to change direction is essential to both chemotroping and chemotaxing cells, very little is known about it. There is little to no information regarding reorientation in *S. cerevisiae*, let alone in higher eukaryotes, despite the obvious importance of this process in all chemotropic systems.

3.1.1 Changes in direction during axon pathfinding

A chemotroping axon must interpret both attractive and repulsive external cues that change the cell's trajectory as it is guided to its final destination (Raper and Mason, 2010). This process is highly regulated by differential expression of guidance receptors and external molecular cues that transmit spatial and temporal signals to mediate axon chemotropism (Lowery and Van Vactor, 2009; Raper and Mason, 2010). Most of our knowledge of how axons interpret opposing guidance cues at the molecular level comes from studies of the vertebrate and invertebrate midlines (Dickson and Zou, 2010).

Growing commissural axons in the developing vertebrate nervous system are initially guided to the midline by the attractant, Netrin and later are directed away from the midline by the repellant, Slit (Raper and Mason, 2010). During their growth toward the midline, the responsiveness of axons to Slit is thought to be repressed by expression of Robo-3/Rig-1, which is a receptor that decreases Slit sensitivity by preventing premature binding of Slit to its target receptor Robo1 (Chen et al., 2008; Sabatier et al., 2004). Upon arrival at the midline, interaction between Netrin and its receptor DCC is inhibited by Slit binding to Robo1, as activated Robo1 interacts with the intracellular domain of DCC (Moore et al., 2007; Stein and Tessier-Lavigne, 2001). This loss of axon sensitivity to Netrin attraction allows Slit to repel growth toward the midline. Studies in *Drosophila melanogaster* have revealed that axons guidance toward the invertebrate ventral midline is mediated through downregulation of Robo by the activated Netrin receptor frazzled/DCC (Yang et al., 2009). Internalization of the Robo receptor enhances Netrin attraction by reducing the amount of Slit binding sites

(Keleman et al., 2002). These examples highlight the complex regulation that underlies axon guidance.

Once a signal is induced by the appropriate guidance cue, the growing axon must generate a cytoskeletal response. In general, repulsive guidance cues activate Rho and ROCK to induce growth cone collapse, while attractive cues activate Rac and Cdc42 to promote forward protrusion (Hall and Lalli, 2010). In rat commissural neurons, Netrin induces Rac and Cdc42 activation (Shekarabi and Kennedy, 2002). Rac and Cdc42 are then linked to DCC via the adaptor protein Nck, which binds Rac and a PAK/Cdc42 complex (Li et al., 2002a; Shekarabi et al., 2005). It is worth noting that downregulation of Rho or ROCK can also induce DCC-mediated axon growth (Li et al., 2002b). In the *Drosophila* embryo, Slit stimulation also leads to Rac activation and recruitment of PAK to the Robo receptor via the Nck adaptor protein (Fan et al., 2003). Even though Slit is a repulsive cue, it is not clear if Rho and ROCK are activated in response to Slit signaling, which is a testament of the complex regulation underlying axon guidance.

One key difference between guidance decisions made during axon growth and other chemosensing processes is that axons rely on several different receptors and external molecular cues to induce directional changes in growth. How do cells expressing only one type of receptor or responding to only one molecular cue interpret a spatial change in a gradient? This type of cell reorientation has been observed in a few model systems, but to date there have only been descriptive studies of this phenomenon. A mechanistic understanding of how cells reorient in a gradient that has shifted is lacking in both chemotactic and chemotropic model systems.

3.1.2 Gradient tracking in granulocytes and yeast

Reorientation of granulocytes has been observed in micropipette-generated gradients (Gerisch and Keller, 1981). In this descriptive study, it was shown that granulocytes are able to form lamellipodia from any side of the cell, and the first lamellipodia formed was usually in the direction of the gradient. Once a cell began migrating up the gradient, the gradient was switch by 180°. Cells responded to the change in direction in one of two ways. Either they maintained polarity of the already extended lamellipodia, turned, and migrated toward the new source, or they ceased growth of the initial lamellipodia and extended growth of a second one in the new direction.

Reorientation of yeast cells had not previously been examined under conditions where the cells were exposed to a directional change in the pheromone gradient prior to the work discussed here. However, several studies have examined the ability of yeast cells to track the same gradient over time. Cells exposed to a micropipette-generated pheromone gradient that exhibited imperfect initial orientation were accessed for their ability to improve orientation over time (Vallier et al., 2002). Wild type cells oriented their mating projections toward the gradient with an angle ≈ 33°. Additionally, cells with imperfect orientation (± 45° away from the source at 0hr) were scored for their ability to improve directionality over time. After 4 hours, 92% of these cells had reoriented toward the pheromone source with an angle ≈ 40°. This was the first study to show that yeast cells can improve orientation in a gradient over time. By examining cells expressing a mutant form of the pheromone receptor that cannot be internalized upon ligand binding, *ste2*^{T326}, this study revealed that this mutation affects cell reorientation. Although these

cells exhibited similar initial orientation to that of WT cells, they could not maintain this directionality over time and often turned away from the gradient. This was the first example of a reorientation-specific mutation in yeast.

More recently, the development of microfluidic chambers has allowed the examination of yeast cells in gradients that can be controlled more precisely than those generated by a micropipette. Using tubular, Y-shaped microfluidic chambers, cells are positioned so that all cells experience the same gradient direction, but groups of cells are exposed to varying pheromone concentrations and gradient steepness (Hao et al., 2008; Moore et al., 2008; Paliwal et al., 2007). From these studies, it was observed that mating projections formed predominantly in the direction of the gradient with angles ≈ 37-53°. Cells sensed the gradient most accurately when exposed to low concentrations of pheromone, but the most influential component was the steepness of the gradient; the steeper the gradient, the more accurately cells could track it (angle ≈ 0°). As in the study using a micropipette-generated gradient, it was observed in the microfluidic gradients that cells improve their orientation in a gradient over time. Interestingly, depending on the pheromone concentration, cells exhibited reorientation behaviors similar to those observed in granulocytes exposed to a 180° change in gradient direction (Gerisch and Keller, 1981; Moore et al., 2008). Cells with imperfect initial orientation exposed to lower concentrations of pheromone (5-40nM) bent their mating projections toward the pheromone source over time. At higher pheromone concentrations (≥ 50nM), cells that formed randomly positioned initial mating projections extended second projections accurately aligned with the gradient. Taken together, these studies of yeast reorientation confirm that cells are continually updating the location of

the gradient and promoting growth toward it, but the mechanisms underlying gradient tracking remain unclear.

3.2 Materials and methods

Time-lapse fluorescent microscopy of Spa2-GFP reorientation.

Strain RDY246 (*MAT***a** *bud1*Δ Gβ *SPA2-GFP*) was grown to mid-log phase and exposed to 50nM αxposed in rich media at 30°C for 3hr. Cells were washed 3X with water prior to mixing with the WT strain BF264-15D *MAT*α. Mating mixtures were incubated at 30°C on agar pads, and images were acquired 15min after mixing and at 10min intervals for 3hr. Six fields were imaged at each time point with 6 DIC and 6 GFP Z-stacks collected in 0.5μm slices using a DeltaVision deconvolution microscopy system (Applied Precision, Issaquah, Washington) on an Olympus IX-70 microscope with an NA 1.4 X 60 objective. The images were then deconvolved, sum projected (GFP) or average projected (DIC), and converted into 8-bit TIF files using Huygens Deconvolution Software (Scientific Volume Imaging, Hilversum, The Netherlands). Fluorescent images (green) and DIC images (red) were merged in ImageJ (NIH).

GFP-Gβ^{P-} time-lapse fluorescent microscopy in isotropic conditions.

Strain RDY132 (*MAT***a** *bud1*Δ GFP-Gβ^{P-}) was grown to mid-log phase in rich media and incubated at 30°C on an agar pad containing 50nM 0ntaining t 30g phase in rich med 15min after exposure to pheromone and at 15min intervals for 4hr. Six fields were imaged at each time point with 6 DIC and 6 GFP Z-stacks collected in 0.5μm slices using a DeltaVision deconvolution microscopy system (Applied Precision, Issaquah, Washington) on an Olympus IX-70 microscope with an NA 1.4 X 60 objective. The

images were then deconvolved, sum projected (GFP) or average projected (DIC), and converted into 8-bit TIF files using Huygens Deconvolution Software (Scientific Volume Imaging, Hilversum, The Netherlands).

Spa2-GFP time-lapse fluorescent microscopy in isotropic conditions.

Strains RDY246 (*MAT***a** *bud1*Δ GFP-Gβ *SPA2-GFP*) and RDY247 (*MAT***a** *bud1*Δ GFP-$G\beta^{P-}$ *SPA2-GFP*) were grown to mid-log phase in rich media and incubated at 30°C on agar pads containing 100nM 00taining t 30g phase in rich med 15min after exposure to pheromone and at 15min intervals for 3hr. Six fields were imaged at each time point with 6 DIC and 6 GFP Z-stacks collected in 0.5μm slices using a DeltaVision deconvolution microscopy system (Applied Precision, Issaquah, Washington) on an Olympus IX-70 microscope with an NA 1.4 X 60 objective. The images were then deconvolved, sum projected (GFP) or average projected (DIC), and converted into 8-bit TIF files using Huygens Deconvolution Software (Scientific Volume Imaging, Hilversum, The Netherlands). Fluorescent images (green) and DIC images (gray) were merged in ImageJ (NIH).

3.3 Results

3.3.1 Spa2-GFP relocates to the new site before the initiation of polarized growth in the new direction

As a first attempt to gain mechanistic insight into how a polarized cell is able to update the signal and change its direction of growth in response to a dynamic gradient, I examined the localization of Spa2-GFP in WT cells that were challenged to reorient their growth. *MAT***a** *SPA2-GFP* cells were exposed to isotropic pheromone until they

had fully formed mating projections. These cells were then mixed with wild type *MAT*α cells on agar pads and imaged for up to 3 hours. The images collected showed that Spa2-GFP was redistributed from its initial site of concentration at the tip of the mating projection toward a new site of polarized growth near the closest potential mating partner (Fig. 10). Although this experiment did not provide evidence that the same Spa2-GFP molecules traveled from the initial growth site to the new growth site, it did show that this polarity marker disappeared from the initial growth site, appeared to migrate along the cell cortex, and ultimately localized at the chemotropic growth site prior to polarized growth of the cell toward its mating partner. These data suggest that Spa2 is an early indicator of where polarized growth will occur during reorientation, as it localizes to the membrane at the chemotropic growth site prior to morphogenesis.

Figure 10. Spa2-GFP is redistributed to the new site of polarized growth in reorienting cells.

Time-lapse images of Spa2-GFP in reorienting cells. *MAT***a** Gβ *bud1*Δ cells transformed with an integrative vector carrying *SPA2-GFP* (labeled 'a') were exposed to isotropic pheromone and allowed to form mating projections before being placed in mating mixtures with wild type *MAT*α cells (labeled α). Mating mixtures were incubated on agar pads at 30°C, and imaged every 10min for 3hr. Fluorescent images are deconvolved maximum projections. DIC (red) and fluorescent Spa2-GFP (green) images were merged in ImageJ. White arrowheads indicate reporter redistribution prior to morphogenesis. Bar, 5µm.

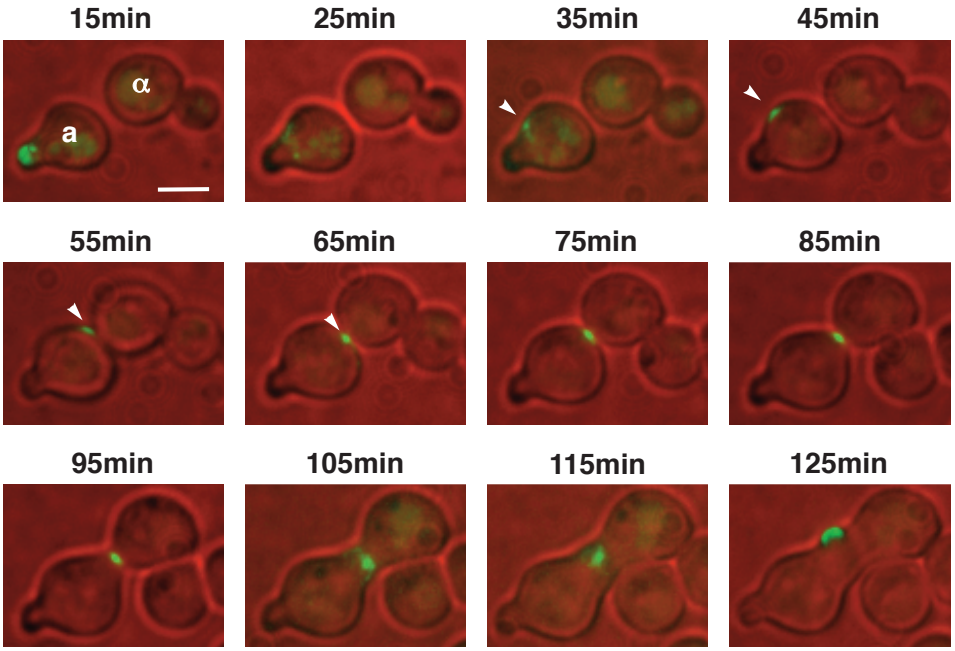
15min
25min
35min
45min
α
a
55min
65min
75min
85min
95min
105min
115min
125min

3.3.2 GFP-Gβ^{P-} wanders toward the new site before polarized growth occurs

As discussed in Chapter 2, Gβ phosphorylation is required for proper initial orientation and stabilized growth of a mating projection. Interestingly, cells unable to phosphorylate Gβ also exhibited a marked defect in their ability to change direction and grow toward a new pheromone source. This suggested that Gβ phosphorylation is involved in the reorientation process. During pheromone exposure, Gβ^{P-} *bud1*Δ cells initiate a second axis of polarity earlier and more frequently than Gβ *bud1*Δ cells (Fig. 4C). In a microfluidic chamber, these additional projections formed randomly with regard to the gradient direction (Fig. 9A) and likely result from the inability of Gβ^{P-} *bud1*Δ cells to stabilize the axis of polarity. Often the second projection formed by Gβ^{P-} *bud1*Δ cells is adjacent to the first projection as opposed to second projections formed by Gβ *bud1*Δ cells, which generally form on the side of the cell opposite the first projection (Fig. 4C). While tracking GFP-Gβ^{P-} *bud1*Δ cells responding to isotropic pheromone, a redistribution of reporter polarity from the initial site of polarization to the second site, adjacent to the first, can be observed prior to morphogenesis (Fig. 11). This result is consistent with my findings, which suggest Gβ mediates localization of the machinery required for polarized growth during the pheromone response and that phosphorylation of Gβ is required to stabilize polarized growth exclusively at the initially selected site on the membrane. Examination of WT GFP-Gβ in reorienting cells will provide a better understanding of Gβ's role during this process.

Figure 11. GFP-Gβ^{P-} wanders to the second site of polarized growth prior to morphogenesis.
Time-lapse GFP (top) and DIC (bottom) images of GFP-Gβ^{P-}. *MAT***a** GFP-Gβ^{P-} *bud1*Δ cells were exposed to pheromone on an agar pads at 30°C and imaged every 15min for 4hr. Fluorescent images are deconvolved maximum projections. White arrowheads indicate reporter redistribution prior to morphogenesis. Bar, 5μm.

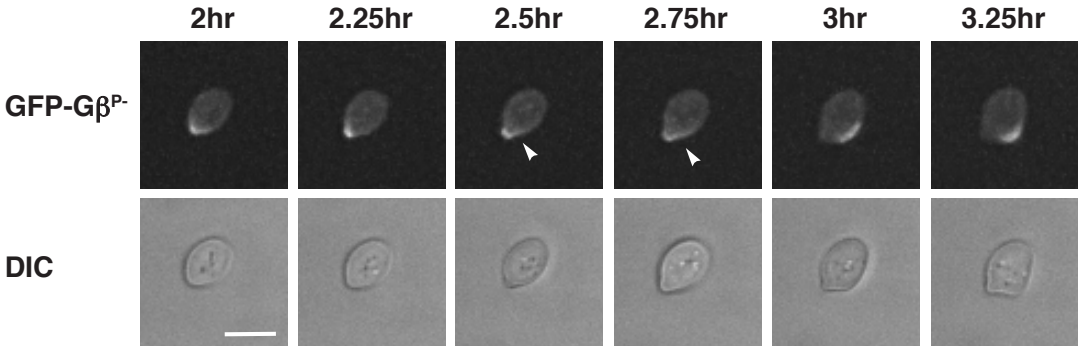
2hr
2.25hr
2.5hr
2.75hr
3hr
3.25hr
GFP-Gβ^{P-}
DIC

3.3.3 Spa2-GFP localizes to multiple growth sites in Gβ^{P-} cells

When exposed to high doses of pheromone for an extended period of time, WT cells eventually change their direction of polarized growth and extend a second mating projection. It has been shown previously that growth of the first mating projection is terminated before growth of the second projection is initiated in 90% of WT cells (Bidlingmaier and Snyder, 2004). Since Gβ^{P-} *bud1*Δ cells establish a second axis of polarity earlier and more frequently than do Gβ *bud1*Δ cells, I investigated this process more closely by examining Spa2-GFP localization in Gβ *bud1*Δ cells and Gβ^{P-} *bud1*Δ cells that formed more than one mating projection. Cells were exposed to a high dose of isotropic pheromone on agar pads and imaged for up to 3 hours. Of the Gβ *bud1*Δ cells that extended a second mating projection, 73% localized Spa2-GFP to the second projection only (n = 11). The decrease from the 90% observed by Bidlingmaier and Snyder is likely due to the absence of Bud1 in these cells. Of the Gβ^{P-} *bud1*Δ cells that formed more than one mating projection, 82% localized Spa2-GFP to both mating projections simultaneously (n = 17; $p < 0.0001$ compared to WT) (Fig. 12). These results suggest that phosphorylated Gβ regulates the localization of the polarity protein, Spa2, which is an early marker of new growth sites during reorientation (Fig. 10). Further examination of these cells will reveal whether actin-dependent polarized growth is occurring within both projections at the same time or whether growth at the initial site is terminated normally but the mechanisms that disassemble polarity complexes in the initial projection are disrupted.

Figure 12. Spa2-GFP localizes to multiple mating projections in Gβ^{P-} cells. Time-lapse images of Spa2-GFP in cells exposed to isotropic pheromone. *MAT***a** Gβ *bud1*Δ (top) or Gβ^{P-} *bud1*Δ (bottom) cells transformed with an integrative vector carrying *SPA2-GFP* were exposed to pheromone on agar pads at 30°C and imaged every 15min for 3hr. Fluorescent images are deconvolved maximum projections. DIC (gray) and fluorescent Spa2-GFP (green) images were merged in ImageJ. White arrowheads indicate reporter localization within multiple mating projections. Bar, 5μm.

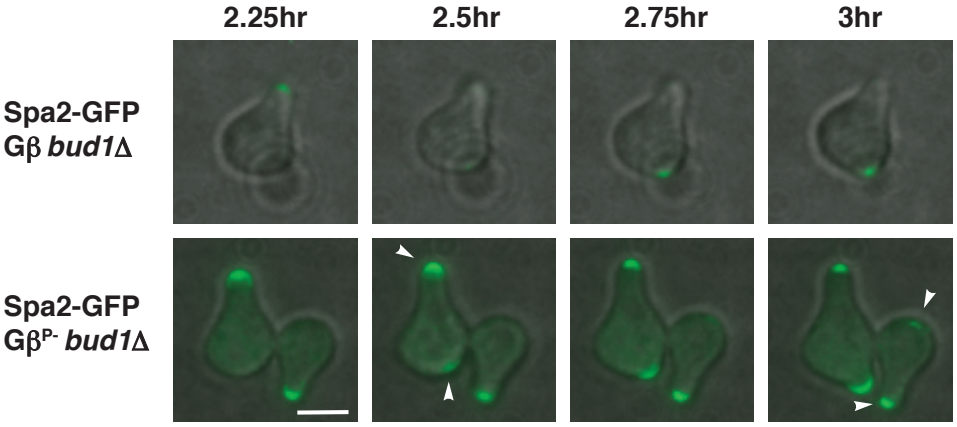
2.25hr
2.5hr
2.75hr
3hr
Spa2-GFP
Gβ bud1Δ
Spa2-GFP
Gβ^P- bud1Δ

3.3.4 Development of a genetic screen to identify genes involved in reorientation

Although the protein complexes that position the shmoo site and catalyze directed growth when a cell first establishes its axis of polarity are likely the same as those that perform these functions when the cell changes directions, it is not known how the growth site is moved. To identify proteins that regulate this transition, I developed and validated a simple yet powerful method to screen for defects in both orientation and reorientation. The screen is based on the partner discrimination assay (Jackson and Hartwell, 1990a) and takes advantage of the fact that *ade1* cells form red colonies. This screen will be used in the future by the Stone lab to further study the reorientation process.

The details are as follows: A *MAT***a** *ade1* strain of yeast is mutagenized with UV or transformed with a yeast *GAL1*-cDNA overexpression library. About 40,000 mutagenized or transformed cells are spread onto 40 plates. Once these cells have grown into medium-sized colonies, the plates are replicated to medium ± pheromone. After the stimulated cells have begun to shmoo, the colonies are replicated to plates spread with a mixture of *MAT*α *ade1* pheromone-secreting cells and *MAT*α *ADE1* cells carrying a mutation that prevents pheromone secretion (non-secretors). The cells are then allowed to mate before being replicated to diploid-selection medium. Once the diploid colonies have grown up, they are scored for color. The pre-stimulated shmooing *MAT***a** cells that are able to reorient and grow in the direction of the nearest pheromone source will mate almost exclusively with the *ade1* partner, and therefore will yield red diploid colonies on the final plate. In contrast, *MAT***a** cells that are unable to reorient efficiently will mate with both the *ade1*/pheromone secreting and the *ADE1*/non-secreting cells, and will therefore yield a red/white mixture of diploid colonies on the final plate.

The one published allele that specifically confers a defect in reorientation is *ste2*^{T236} (Vallier et al., 2002), and its phenotype is easily detectable in this screen (Fig. 13). To my knowledge, this is the only method yet developed to isolate chemotropic mutants. Note that the colorimetric screen described here, which illustrates the resolving power of this method, can be easily modified to create an even more powerful genetic selection. By using tester strains with complimentary auxotrophic markers, one can select directly for the growth of diploids that result from matings with the non-secretors and against the growth of diploids from matings with secretors.

In addition to identifying mutant and overexpression phenotypes, this protocol could be used to screen the entire yeast deletion library or to evaluate the effects of deleting candidate genes. *A priori*, one imagines that reorientation is accomplished by the movement of a continually active growth site or by the inactivation of the first site followed by initiation at the second. Some evidence in support of the latter possibility has been reported, although the experiment was performed under uniform pheromone conditions so the results may not be relevant to reorientation in a gradient (Bidlingmaier and Snyder, 2004). In either case, it would be worthwhile to analyze negative regulators of the signaling proteins in a directed approach. Candidates that are essential genes could be subjected to saturation mutagenesis and screening. As a collection of mutations that impair reorientation is built, this method could also be used to identify suppressors of reorientation defects.

Figure 13. Genetic screen proof of principle experiment.
WT and *ste2*^{T326} colonies were tested in the screen described in 3.3.4. Diploid selection plates are shown. Pre-stimulated WT *MAT***a** cells were able to discriminate between pheromone-secreting and non-secreting cells and therefore, formed exclusively red colonies. Pre-stimulated *MAT***a** cells carrying the *ste2*^{T326} mutation mated with both pheromone-secreting and non-secreting cells, which resulted in the formation of mixed red and white colonies.

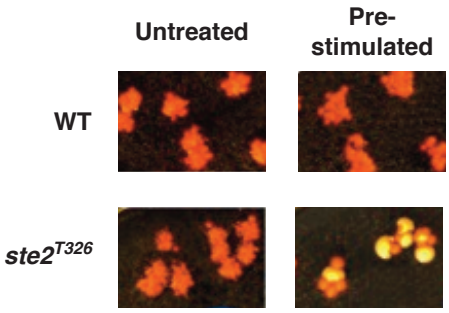
Untreated
Pre-
stimulated
WT
ste2T326

3.4 Discussion

Since a mechanistic understanding of how chemotropic cells reorient their growth in dynamic gradients is lacking, I began to study this phenomenon at the molecular level. My preliminary data suggest that Gβ and Spa2 are early mediators of this process and that Gβ phosphorylation is important for regulating the change in growth direction. Spa2-GFP was observed migrating from the initial site of polarized growth toward the new gradient source prior to visible morphogenesis at the new site. This implicates Spa2 in the reorientation process. Spa2 is a polarity marker that localizes to sites of Cdc42 activity. Therefore, it is likely there are proteins acting upstream of Spa2 that redistribute active Cdc42 from the original growth site to the future growth site during reorientation. These results provide a basis for future studies of the mechanisms underlying reorientation during the mating response. Future work will be focused on determining whether the same molecules migrate from the first site to the second site and whether the axis of polarity moves as an intact module or undergoes a series of breakdown/reestablishment events. Spa2 localization should also be examined in reorienting cells carrying mutations in Cdc42 and known Cdc42 regulators to determine the temporal level of Spa2 regulation.

GFP-Gβ polarizes on the membrane where the initial mating projection will form prior to morphogenesis, and phosphorylated Gβ functions to stabilize polarized growth specifically to this chosen site (Chapter 2). The observation that GFP-$G\beta^{P-}$ wanders from the initial site of polarized growth and localizes to the second site prior to the occurrence of new growth suggests that misregulated Gβ can induce unwanted growth. Therefore, one can imagine that Gβ normally functions as a mediator that directs where

polarized growth will occur initially and during reorientation. This hypothesis is further supported by the observance of Spa2-GFP at multiple growth sites in cells unable to phosphorylate Gβ. There exists a normal periodicity to projection growth during mating. Growth of the initial projection is terminated prior to growth of a second projection (Bidlingmaier and Snyder, 2004). In $G\beta^{P-}$ cells, this periodicity appears to be lost as these cells polarize Spa2-GFP to multiple projections simultaneously, suggesting phosphorylated Gβ regulates the localization of polarity proteins at initial and subsequent growth sites.

If Gβ regulates where polarized growth will occur during reorientation, then one would expect to GFP-Gβ to localize at a distal chemotropic growth site prior to morphogenesis. Based on the localization of Spa-GFP in reorienting cells (Fig. 10), one would also expect GFP-Gβ to migrate along the cell cortex toward the new growth site. During initial orientation, it is likely that the activated receptor first marks the site for polarized growth, and phosphorylated Gβ is then required to stabilize the axis of polarity at this site. However, once a mating projection has formed, delivery of newly synthesized receptors will occur at the site on the membrane where the axis of polarity is stabilized. This leads to the interesting possibility that Gβ could become the most upstream component during reorientation. Dual-labeling studies examining the localization of both the activated receptor and Gβ in reorienting cells could provide some insight into which of these proteins localizes to new sites of growth first.

Taken together, these data have begun to provide some insight into which molecular players are involved in cell reorientation, but additional work is required to understand this process at a mechanistic level. To further this investigation, I've

developed a powerful genetic screen to identify genes specifically involved in the reorientation process. Any candidates identified in this screen will be analyzed using the newly developed zygotic reorientation (Chapter 2) and microfluidic assays (Dave Eddington, UIC collaboration). Together these novel tools will allow future examination of molecular markers under true gradient reorientation conditions both *in vivo* and *in vitro*, and these analyses will surely provide a better mechanistic understanding of this poorly studied phenomenon.

4. FUTURE DIRECTIONS

Chemotaxis and chemotropism are processes required throughout eukaryotic development. Understanding how cells interpret external signaling gradients and direct their movement or growth in response to these gradients is a fundamental question in cell biology. This study has shown that Gβ phosphorylation is critical for proper communication between the pheromone receptor and proteins that mediate chemotropic growth during the mating response of *S. cerevisiae*. As Gβ phosphorylation was also shown to be important for cell reorientation, a previously unstudied phenomenon, I developed tools and assays to begin to uncover the mechanisms guiding this process. Although this work has advanced our understanding of directional sensing during yeast mating, there remain several outstanding questions. By carrying out the proposed experiments, our understanding of initial orientation and reorientation during yeast chemotropism will be greatly advanced.

Using FRAP and iFRAP analysis, I demonstrated that Gβ phosphorylation affects the dynamics of the chemotropic complex within mating projections (Fig. 7), and my analysis of GFP-tagged Gβ and $G\beta^{P-}$ revealed that phosphorylation promotes localization of the reporter to the growth site prior to morphogenesis (Fig. 6). Does the phosphorylation state of Gβ also influence the localization of polarity proteins during initial orientation before polarized growth is observed? Examination of cells expressing functional GFP-tagged polarity markers in mating mixtures could provide some insight. By tracking the movement of these markers from the abscission of a daughter cell to the formation of a chemotropic mating projection, one could determine which polarity

proteins polarize at the membrane prior to morphogenesis and if their polarity is affected by Gβ phosphorylation.

I observed that Gβ accumulates at the site on the membrane where polarized growth will occur (Fig. 6). In WT cells, in which Gβ can be phosphorylated, there likely exist both the phosphorylated and unphosphorylated forms of Gβ. Could phosphorylation of Gβ be a mechanism to reinforce initial selection of a growth site? One can imagine that Gβ phosphorylation leads to increased local concentration of Gβγ at the incipient shmoo site by enhancing its interactions with Ste5 (Feng et al., 1998), which would lead to increased Fus3 activation and increased Gβ phosphorylation. A key tenet of this model is that Gβ is phosphorylated by Fus3. It has been shown that both Gβ phosphorylation and Gβ levels are reduced in cells lacking Fus3 (Metodiev et al., 2002). By mapping the phosphorylation sites in Gβ and using an *in vitro* kinase assay, one could determine if Fus3 directly phosphorylates Gβ. If such a feedback mechanism exists to enrich phosphorylated Gβ at the incipient shmoo site, it is possible that there also exists a mechanism to exclude phosphorylated Gβ from the back of the cell. In *D. Discoideum*, PTEN actively dephosphorylates PIP_3 at the rear of the cell to enhance the gradient of PIP_3 at the leading edge of the cell (Funamoto et al., 2002). Is there such a phosphatase present in yeast that acts to prevent accumulation of phosphorylated Gβ at the rear of the cell? In a directed screen, the level of Gβ phosphorylation could be determined in cells deleted for the known yeast phosphatases. The localization of phosphorylated versus unphosphorylated Gβ could also be determined by examining cells expressing equal levels of GFP-Gβ and mCherry-$G\beta^{P-}$. If, upon pheromone

exposure, the two reporters segregate to the front and back of the cell, respectively, it would support the existence of such a phosphatase.

My finding that Gβ phosphorylation is important for reorientation and my examination of Spa2-GFP in reorienting cells has provided some insight as to how this process might be regulated. However, the mechanisms underlying reorientation are still largely unknown. Some basic questions include: How do known polarity markers localize during reorientation? Is the new growth site established by the movement of protein complexes from the previous growth site or by delivery of nascent proteins? Is actin required for targeting of proteins to the new growth site?

Analysis of protein localization during reorientation could be carried out using the microfluidic chamber capable of delivering a linear pheromone gradient in one direction and allowing a switch in the direction of the gradient in 90° increments. Using this device, the localization of fluorescently tagged proteins can be followed as the gradient changes. Some proteins to be examined initially would be markers of actin patches (Abp1, Cap1), actin cables (Abp140), sites of endocytosis (Snc1, Snc2) and exocytosis (Sec3), activated Cdc42 (Gic2), and the polarisome (Bem1, Spa2). Using Volocity software, the speed, displacement distance, and trajectory of these markers could be tracked as the cell reorients its growth. These experiments would identify which cellular processes are involved in reorientation and the temporal order in which they operate.

To determine whether molecules localized at the original growth site relocate to the new site or if delivery of newly synthesized or recruited chimeras establishes this site, FLIP experiments could be performed on cells in the microfluidic chamber. By repetitively bleaching of the initial growth site just before and continuously after

changing the direction of the gradient, proteins at the initial growth site would become photo-bleached. If the new growth site is composed predominantly of molecules that migrate from the initial growth site, we should observe a decrease in fluorescence at the new site after the direction of the gradient has been switched. Similar experiments could also be carried out with the green-to-red photo-switchable fluorescent protein Dendra2 (Onischenko et al., 2009). Upon photo-conversion of Dendra2 at the initial growth site to red and subsequent switching of the gradient, it could be determined whether the new growth site is red (originated from old site) or green (newly synthesized or recruited proteins).

The role of actin cables and patches in establishing the new growth site could be determined by expressing fluorescently labeled polarity markers in a temperature-sensitive *act1* mutant strain that grows normally at 23°C but undergoes rapid loss of actin cables and delocalization of actin patches when shifted to 37°C (Chen and Rubenstein, 1995). Using a microscope with a temperature-controlled chamber, probes could be imaged at 23°C in cells exposed to a linear gradient and continually tracked as the temperature is increased and the direction of the gradient is switched. If actin is not required, one would expect to see probes localized to the side of the cell facing the new direction of the gradient even if the cell is unable to polarize its growth. If actin cables or patches are required for localization of proteins at the new growth site, one would expect to see little or no localization of probes on the side of the cell facing the new source. As an independent means of examining actin cytoskeleton requirements, LatA could be added at the time of the gradient switch.

Although there may be considerable overlap between proteins that determine the site of initial orientation and catalyze polarized growth in this direction and those that perform these functions when the cell changes direction, there are likely proteins that are specific to one process or the other. In addition to defining the role of various known polarity markers, the novel genetic screen I developed will allow identification and characterization of new genes previously unknown to be involved in reorientation. This screen was designed to distinguish between defects in orientation and reorientation, and any genes identified in this screen could be further characterized to determine their specific role in reorientation by carrying out *in vivo* mating assays, *in vitro* microfluidic assays, and the analyses of known polarity markers described above. Each gene would be fluorescently tagged with GFP to determine the protein localization, and genes would either be cloned into 2μm overexpression plasmids or deleted to examine gain-of-function and loss-of-function phenotypes, respectively. If an identified gene product has known interactors, potential binding sites could be mutated to disrupt these interactions, and the effects on reorientation could be observed.

CITED LITERATURE

Apanovitch DM, Slep KC, Sigler PB, Dohlman HG (1998) Sst2 is a GTPase-activating protein for Gpa1: Purification and characterization of a cognate RGS-Galpha protein pair in yeast. *Biochemistry* **37**: 4815-4822

Arkowitz RA, Lowe N (1997) A small conserved domain in the yeast Spa2p is necessary and sufficient for its polarized localization. *J Cell Biol* **138**: 17-36

Arkowitz RA (2009) Chemical gradients and chemotropism in yeast. *Cold Spring Harb Perspect Biol* **1**: a001958

Ausubel FM, Brent R, Kingston RE, Moore DD, Seidman JG, Smith JA, Struhl K (1994) Current Protocols in Molecular Biology. John Wiley & Sons, New York, NY

Ayscough KR, Drubin DG (1998) A role for the yeast actin cytoskeleton in pheromone receptor clustering and signalling. *Curr Biol* **8**: 927-930

Barale S, McCusker D, Arkowitz RA (2006) Cdc42p GDP/GTP cycling is necessary for efficient cell fusion during yeast mating. *Mol Biol Cell* **17**: 2824-2838

Basile JR, Barac A, Zhu T, Guan KL, Gutkind JS (2004) Class IV semaphorins promote angiogenesis by stimulating Rho-initiated pathways through plexin-B. *Cancer Res* **64**: 5212-5224

Bassilana M, Arkowitz RA (2006) Rac1 and Cdc42 have different roles in *Candida albicans* development. *Eukaryot Cell* **2**: 321-329

Berzat A, Hall A (2010) Cellular responses to extracellular guidance cues. *EMBO J* **29**: 2734-2745

Bidlingmaier S, Snyder M (2004) Regulation of polarized growth initiation and termination cycles by the polarisome and Cdc42 regulators. *J Cell Biol* **164**: 207-218

Blackwell E, Halatek IM, Kim HJ, Ellicott AT, Obukhov AA, Stone DE (2003) Effect of the pheromone-responsive Gα and phosphatase proteins of *Saccharomyces cerevisiae* on the subcellular localization of the Fus3 mitogen-activated protein kinase. *Mol Cell Biol* **23**: 1135-1150

Blondel M, Alepuz PM, Huang LS, Shaham S, Ammerer G, Peter M (1999) Nuclear export of Far1p in response to pheromones requires the export receptor Msn5p/ Ste21p. *Genes Dev* **13**: 2284-2300

Blumer KJ, Thorner J (1990) Beta and gamma subunits of a yeast guanine nucleotide-binding protein are not essential for membrane association of the alpha subunit but are required for receptor coupling. *Proc Natl Acad Sci USA* **87**: 4363-4367

Bouzigues C, Morel M, Triller A, Dahan M (2007) Asymmetric redistribution of GABA receptors during GABA gradient sensing by nerve growth cones analyzed by single quantum dot imaging. *Proc Natl Acad Sci USA* **104**: 11251-11256

Butty AC, Perrinjaquet N, Petit A, Jaquenoud M, Segall JE, Hofmann K, Zwahlen C, Peter M (2002) A positive feedback loop stabilizes the guanine-nucleotide exchange factor Cdc24 at sites of polarization. *EMBO J* **21**: 1565-1576

Butty AC, Pryciak PM, Huang LS, Herskowitz I, Peter M (1998) The role of Far1p in linking the heterotrimeric G protein to polarity establishment proteins during yeast mating. *Science* **282**: 1511-1516

Cai H, Das S, Kamimura Y, Long Y, Parent CA, Devreotes PN (2010) Ras-mediated activation of the TORC2-PKB pathway is critical for chemotaxis. *J Cell Biol* **190**: 233-245

Celic A, Martin NP, Son CD, Becker JM, Naider F, Dumont ME (2003) Sequences in the intracellular loops of the yeast pheromone receptor Ste2p required for G protein activation. *Biochemistry* **42**: 3004-3017

Chakrabarti S, Gintzler AR (2003) Phosphorylation of Gβ is augmented by chronic morphine and enhances Gβγ stimulation of adenylyl cyclase activity. *Mol Brain Res* **119**: 144-151

Chang F, Hersowirz I (1990) Identification of a gene necessary for cell cycle arrest by a negative growth factor of yeast: *FAR1* is an inhibitor of a G1 cyclin, *CLN2*. *Cell* **63**: 999-1011

Charest PG, Shen Z, Lakoduk A, Sasaki AT, Briggs SP, Firtel RA (2010) A Ras signaling complex controls the RasC-TORC2 pathway and directed cell migration. *Dev Cell* **18**: 737-749

Chen L, Iijima M, Tang M, Landree MA, Huang YE, Xiong Y, Iglesias PA, Devreotes PN (2007) PLA2 and PI3K/PTEN pathways act in parallel to mediate chemotaxis. *Dev Cell* **12**: 603-614

Chen MY, Insall RH, Devreotes PN (1996) Signaling through chemoattractant receptors in *Dictyostelium*. *Trends Genet* **12**: 52-57

Chen R, Thorner J (2007) Function and regulation in MAPK signaling pathways: Lessons learned from the yeast *Saccharomyces cerevisiae*. *Biochim Biophys Acta* **1773**: 1311-1340

Chen X, Rubenstein P (1995) A mutation in an ATP-binding loop of *Saccharomyces cerevisiae* actin causes a temperature-sensitive phenotype *in vivo* and *in vitro*. *J Biol Chem* **270**: 11406-11414

Chen Z, Gore B, Long H, Ma L, Tessier-Lavigne M (2008) Alternative splicing of the Robo3 axon guidance receptor governs the midline switch from attraction to repulsion. *Neuron* **58**: 325-332

Choi KY, Kranz JE, Mahanty SK, Park KS, Elion EA (1999) Characterization of Fus3 localization: active Fus3 localizes in complexes of varying size and specific activity. *Mol Biol Cell* **10**: 1553-1568

Cismowski MJ, Metodiev MV, Draper EM, Stone DE (2001) Biochemical analysis of yeast Gα mutants that enhance adaptation to pheromone. *Biochem Biophys Res Comm* **284**: 247-254

Cole GM, Reed SI (1991) Pheromone-induced phosphorylation of a G protein β subunit in *S. cerevisiae* is associated with an adaptive response to mating pheromone. *Cell* **64**: 703-716

Comer FI, Parent CA (2002) PI 3-kinases and PTEN: how opposites chemoattract. *Cell* **109**: 541-544

Daniels KJ, Srikantha T, Lockhart SR, Pujol C, Soll DR (2006) Opaque cells signal white cells to form biofilms in *Candida albicans*. *EMBO J* **25**: 2240-2252

Daub H, Gevaert K, Vandekerckhove J, Sobel A, Hall A (2001) Rac/Cdc42 and p65PAK regulate the microtubule-destabilizing protein stathmin through phosphorylation at serine 16. *J Biol Chem* **276**: 1677-1680

de Anda FC, Pollarolo G, Da Silva JS, Camoletto PG, Feiguin F, Dotti CG (2005) Centrosome localization determines neuronal polarity. *Nature* **436**: 704-708

Devreotes P, Janetopoulos C (2003) Eukaryotic chemotaxis: distinctions between directional sensing and polarization. *J Biol Chem* **278**: 20445-20448

Dickson BJ, Zou Y (2010) Navigating intermediate targets: the nervous system midline. *Cold Spring Harb Perspect Biol* **2**: a002055

Dong X, Mitchell DA, Lobo S, Zhao L, Bartels DJ, Deschenes RJ (2003) Palmitoylation and plasma membrane localization of Ras2p by a nonclassical trafficking pathway in *Saccharomyces cerevisiae*. *Mol Cell Biol* **23**: 6574-6584

Dorer RP, Pryciak P, Hartwell LH (1995) *Saccharomyces cerevisiae* cells execute a default pathway to select a mate in the absence of pheromone gradients. *J Cell Biol* **131**: 854-861

Dosil M, Schandel KA, Gupta E, Jenness DD, Konopka JB (2000) The C terminus of the *Saccharomyces cerevisiae* alpha-factor receptor contributes to the formation of pre-activation complexes with its cognate G protein. *Mol Cell Biol* **20**: 5321-5329

Dottie CG, Sullivan CA, Banker GA (1988) The establishment of polarity by hippocampal neurons in culture. *J Neurosci* **8**: 1454-1468

English DJ, Garcia G, Brindley DN (2001) Platelet-released phospholipids link haemostasis and angiogenesis. *Cardiovasc Res* **49**: 588-599

Errede B, Gartner A, Zhou Z, Nasmyth K, Ammerer G (1993) MAP kinase-related Fus3 from *S. cerevisiae* is activated by Ste7 *in vitro*. *Nature* **362**: 261-264

Etienne-Manneville S (2004) Cdc42-the centre of polarity. *J Cell Sci* **117** (Pt 8): 1291-1300

Evangelista M, Blundell K, Longtine MS, Chow CJ, Adames N, Pringle JR, Peter M, Boone C (1997) Bni1p, a yeast formin linking Cdc42p and the actin cytoskeleton during polarized morphogenesis. *Science* **276**: 118-122

Evangelista M, Pruyne D, Amberg C, Boone C, Bretscher A (2002) Formins direct Arp2/3-independent actin filament assembly to polarize cell growth in yeast. *Nat Cell Biol* **4**: 260-269

Fan X, Labrador JP, Hing H, Bashaw GJ (2003) Slit stimulation recruits Dock and Pak to the roundabout receptor and increases Rac activity to regulate axon repulsion at the CNS midline. *Neuron* **40**: 113-127

Feng Y, Song LY, Kincaid E, Mahanty SK, Elion EA (1998) Functional binding between Gβ and the LIM domain of Ste5 is required to activate the MEKK Ste11. *Curr Biol* **8**: 267-278

Fisher PR, Merkl R, Gerisch G (1989) Quantitative analysis of cell motility and chemotaxis in *Dictyostelium discoideum* by using an image processing system and a novel chemotaxis chamber providing stationary chemical gradients. *J Cell Biol* **108**: 973-984

Fivaz M, Bandara S, Inoue T, Meyer T (2008) Robust neuronal symmetry breaking by Ras-triggered local positive feedback. *Curr Biol* **18**: 44-50

Franca-Koh J, Willard SS, Devreotes PN (2009) G protein signaling in chemotaxis. *Handbook of Cell Signaling* 2ed Oxford: Academic Press 1705-1712

Funamoto S, Meili R, Lee S, Parry L, Firtel RA (2002) Spatial and temporal regulation of 3-phosphoinositides by PI3-kinase and PTEN mediates chemotaxis. *Cell* **109**: 611-623

Gamba A, de Candia A, Di Talia S, Coniglio A, Bussolino F, Serini G (2005) Diffusion-limited phase separation in eukaryotic chemotaxis. *Proc Natl Acad Sci USA* **102**: 16927-16932

Gartner A, Nasmyth K, Ammerer G (1992) Signal transduction in *Saccharomyces cerevisiae* requires tyrosine and threonine phosphorylation of Fus3 and Kss1. *Genes Dev* **6**: 1280-1292

Gerisch G, Keller HU (1981) Chemotactic reorientation of granulocytes stimulated with micropipettes containing fMet-Leu-Phe. *J Cell Sci* **52**: 1-10

Goldberg JM, Bosgraaf L, Van Haastert PJ, Smith JL (2002) Identification of four candidate cGMP targets in *Dictyostelium*. *Proc Natl Acad Sci USA* **99**: 6749-6754

Guthrie C, Fink G Eds (1991) Guide to yeast genetics and molecular biology. *Methods Enzymol* **194**, Academic Press

Hall A, Lalli G (2010) Rho and Ras GTPases in axon growth, guidance, and branching. *Cold Spring Harb Perspect Biol* **2**: a001818

Hao N, Nayak S, Behar M, Shanks RH, Nagiec MJ, Errede B, Hasty J, Elston TC, Dohlman HG (2008) Regulation of cell signaling dynamics by the protein kinase-scaffold Ste5. *Mol Cell* **30**: 649-656

Henchoz S, Chi Y, Catarin B, Herskowitz I, Deshaies RJ, Peter M (1997) Phosphorylation- and ubiquitin-dependent degradation of the cyclin-dependent kinase inhibitor Far1p in budding yeast. *Genes Dev* **11**: 3046-3060

Hirsch JP, Dietzel C, Kurjan J (1991) The carboxyl terminus of Scg1, the G alpha subunit involved in yeast mating, is implicated in interactions with the pheromone receptors. *Genes Dev* **5**: 467-474

Hirschman JE, Jenness DD (1999) Dual lipid modification of the yeast Ggamma subunit Ste18p determines membrane localization of Gbetagamma. *Mol Cell Biol* **19**: 7705-7711

Hoeller O, Kay RR (2007) Chemotaxis in the absence of PIP_3 gradients. *Curr Biol* **17**: 813–817

Hong K, Nishiyama M (2010) From guidance signals to movement: signaling molecules governing growth cone turning. *Neuroscientist* **16**: 65-78

Howell AS, Savage NS, Johnson SA, Bose I, Wagner AW, Zyla TR, Nijhout HF, Reed MC, Goryachev AB, Lew DJ (2009) Singularity in polarization: rewiring yeast cells to make two buds. *Cell* **139**: 731-743

Iglesias PA, Devreotes PN (2008) Navigating through models of chemotaxis. *Curr Opin Cell Biol* **20**: 35-40

Iijima M, Devreotes P (2002) Tumor suppressor PTEN mediates sensing of chemoattractant gradients. *Cell* **109**: 599-610

Iijima M, Huang YE, Devreotes P (2002) Temporal and spatial regulation of chemotaxis. *Dev Cell* **3**: 469-478

Iijima M, Huang YE, Luo HR, Vazquez F, Devreotes PN (2004) Novel mechanism of PTEN regulation by its phosphatidylinositol 4,5-bisphosphate binding motif is critical for chemotaxis. *J Biol Chem* **279**: 16606-16613

Jackson C, Hartwell L (1990a) Courtship in *S. cerevisiae*: Both cell types choose mating partners by responding to the strongest pheromone signal. *Cell* **63**: 1039-1051

Jackson C, Hartwell L (1990b) Courtship in *Saccharomyces cerevisiae*: an early cell-cell interaction during mating. *Mol Cell Biol* **10**: 2202-2213

Jackson CL, Konopka JB, Hartwell LH (1991) *S. cerevisiae* alpha pheromone receptors activate a novel signal transduction pathway for mating partner discrimination. *Cell* **67**: 389-402

Janetopoulos C, Ma L, Devreotes PN, Iglesias PA (2004) Chemoattractant-induced phosphatidylinositol 3,4,5-trisphosphate accumulation is spatially amplified and adapts, independent of the actin cytoskeleton. *Proc Natl Acad Sci USA* **101**: 8951-8956

Jenness DD, Burkholder AC, Hartwell LH (1986) Binding of alpha-factor pheromone to *Saccharomyces cerevisiae* a cells: Dissociation constant and number of binding sites. *Mol Cell Biol* **6**: 318-320

Jenness DD, Spatrick P (1986) Down regulation of the alpha-factor pheromone receptor in *S. cerevisiae*. *Cell* **46**: 345-353

Jiang H, Guo W, Liang X, Rao Y (2005) Both the establishment and the maintenance of neuronal polarity require active mechanisms: critical roles of GSK-3beta and its upstream regulators. *Cell* **120**: 123-135

Jin T, Xu X, Hereld D (2008) Chemotaxis, chemokine receptors and human disease. *Cytokine* **44**: 1-8

Jin T, Zhang N, Long Y, Parent CA, Devreotes PN (2000) Localization of the G protein betagamma complex in living cells during chemotaxis. *Science* **287**: 1034-1036

Jones SK, Bennett RJ (2011) Fungal mating pheromones: Choreographing the dating game. *Fungal Genet Biol* **48**: 668-676

Kae H, Lim CJ, Spiegelman GB, Weeks G (2004) Chemoattractant-induced Ras activation during *Dictyostelium* aggregation. *EMBO Rep* **5**: 602-606

Kamimura Y, Xiong Y, Iglesias PA, Hoeller O, Bolourani P, Devreotes PN (2008) PIP_3-independent activation of TorC2 and PKB at the cell's leading edge mediates chemotaxis. *Curr Biol* **18:** 1034-1043

Kang PJ, Be L, Hariharan S, Park HO (2010) The Rsr1/Bud1 GTPase interacts with itself and the Cdc42 GTPase during bud-site selection and polarity establishment in budding yeast. *Mol Biol Cell* **21**: 3007-3016

Keleman K, Rajagopalan S, Cleppien D, Teis D, Paiha K, Huber LA, Technau GM, Dickson BJ (2002) Comm sorts robo to control axon guidance at the *Drosophila* midline. *Cell* **110**: 415-427

Khosla M, Spiegelman GB, Insall R, Weeks G (2000) Functional overlap of the *Dictyostelium* RasG, RasD and RasB proteins. *J Cell Sci* **113**: 1427-1434

Kim J, Bortz E, Zhong H, Leeuw T, Leberer E, Vershon AK, Hirsch JP (2000) Localization and signaling of G(beta) subunit Ste4p are controlled by a-factor receptor and the a-specific protein Asg7p. *Mol Cell Biol* **20**: 8826-8835

Kim S, Dong J, Lord EM (2004) Pollen tube guidance: the role of adhesion and chemotropic molecules. *Curr Top Dev Biol* **61**: 61-79

Klagsbrun M, Eichmann A (2005) A role for axon guidance receptors and ligands in blood vessel development and tumor angiogenesis. *Cytokine Growth F R* **16**: 535-548

Kolsch V, Charest PG, Firtel RA (2008) The regulation of cell motility and chemotaxis by phospholipid signaling. *J Cell Sci* **121**: 551-559

Konopka JB, Jenness DD, Hartwell LH (1988) The C-terminus of the *S. cerevisiae* alpha-pheromone receptor mediates an adaptive response to pheromone. *Cell* **54**: 609-620

Kortholt A, King JS, Keizer-Gunnink I, Harwood AJ, Van Haastert PJ (2007) Phospholipase C regulation of phosphatidylinositol 3,4,5-trisphosphate-mediated chemotaxis. *Mol Biol Cell* **18**: 4772-4779

Kutscher B, Devreotes P, Iglesias PA (2004) Local excitation, global inhibition mechanism for gradient sensing: an interactive applet. *Sci STKE* **2004**: PL3

Laird DJ, von Andrian UH, Wagers AJ (2008) Stem cell trafficking in tissue development, growth, and disease. *Cell* **132**: 612-630

Leeuw T, Wu C, Schrag JD, Whiteway M, Thomas DY (1998) Interaction of a G-protein β-subunit with a conserved sequence in Ste20/PAK family protein kinases. *Nature* **4**: 191-195

Levchenko A, Iglesias PA (2002) Models of eukaryotic gradient sensing: application to chemotaxis of amoebae and neutrophils. *Biophys J* **82**: 50-63

Levine H, Kessler DA, Rappel WJ (2006) Directional sensing in eukaryotic chemotaxis: a balanced inactivation model. *Proc Natl Acad Sci USA* **103**: 9761-9766

Li E, Cismowski MJ, Stone DE (1998) Phosphorylation of the pheromone responsive Gβ protein of *Saccharomyces cerevisiae* does not affect its mating-specific signaling function. *Mol Gen Genet* **258**: 608-618

Li X, Meriane M, Triki I, Shekarabi M, Kennedy TE, Larose L, Lamarche-Vane N (2002a) The adaptor protein Nck-1 couples the netrin-1 receptor DCC (deleted in colorectal cancer) to the activation of the small GTPase Rac1 through an atypical mechanism. *J Biol Chem* **277**: 37788-37797

Li X, Saint-Cyr-Proulx E, Aktories K, Lamarche-Vane N (2002b) Rac1 and Cdc42 but not RhoA or Rho kinase activities are required for neurite outgrowth induced by the Netrin-1 receptor DCC (deleted in colorectal cancer) in N1E-115 neuroblastoma cells. *J Biol Chem* **277**: 15207-15214

Li Z, Hannigan M, Mo Z, Liu B, Lu W, Wu Y, Smrcka AV, Wu G, Li L, Liu M, Huang CK, Wu D (2003) Directional sensing requires Gβγ-mediated PAK1 and PIXα-dependent activation of Cdc42. *Cell* **114**: 215-227

Lim CJ, Spiegelman GB, Weeks G (2001) RasC is required for optimal activation of adenylyl cyclase and Akt/PKB during aggregation. *EMBO J* **20**: 4490-4499

Lohof AM, Quillan M, Dan Y, Poo MM (1992) Asymmetric modulation of cytosolic cAMP activity induces growth cone turning. *J Neurosci* **12**: 1253-1261

Lowery LA, Van Vactor D (2009) The trip of the tip: understanding the growth cone machinery. *Nat Rev Mol Cell Biol* **10**: 332-343

Madden K, Snyder M (1992) Specification of sites for polarized growth in *Saccharomyces cerevisiae* and the influence of external factors on site selection. *Mol Biol Cell* **3**: 1025-1035

Matheos D, Metodiev M, Muller E, Stone D, Rose MD (2004) Pheromone-induced polarization is dependent on the Fus3p MAPK acting through the formin Bni1p. *J Cell Biol* **165**: 99-109

Mato JM, Losada A, Nanjundiah V, Konijn TM (1975) Signal input for a chemotactic response in the cellular slime mold *Dictyostelium discoideum*. *Proc Natl Acad Sci USA* **72**: 4991-4993

Meier-Schellersheim M, Xu X, Angermann B, Kunkel EJ, Jin T, Germain RN (2006) Key role of local regulation in chemosensing revealed by a new molecular interaction-based modeling method. *PLoS Comput Biol* **2**: e82

Menager C, Arimura N, Fukata Y, Kaibuchi K (2004) PIP_3 is involved in neuronal polarization and axon formation. *J Neurochem* **89**: 109-118

Metodiev MV, Matheos D, Rose MD, Stone DE (2002) Regulation of MAPK function by direct interaction with the mating-specific Gα in yeast. *Science* **296**: 1483-1486

Milne JL, Kim JY, Devreotes PN (1997) Chemoattractant receptor signaling: G protein-dependent and -independent pathways. *Adv Second Messenger Phosphoprotein Res* **31**: 83-104

Moore SW, Tessier-Lavigne M, Kennedy TE (2007) Netrins and their receptors. *Adv Exp Med Biol* **621**: 17-31

Moore TI, Chou CS, Nie Q, Jeon NL, Yi TM (2008) Robust spatial sensing of mating pheromone gradients by yeast cells. *PLoS One* **3**: e3865

Mrass P, Weninger W (2006) Immune cell migration as a means to control immune privilege: lessons from the CNS and tumors. *Immunol Rev* **213**: 195-212

Narang A (2006) Spontaneous polarization in eukaryotic gradient sensing: A mathematical model based on mutual inhibition of frontness and backness pathways. *J Theor Biol* **240**: 538-553

Narumiya S, Tanji M, Ishizaki T (2009) Rho signaling, ROCK and mDia1, in transformation, metastasis and invasion. *Cancer Metastasis Rev* **28**: 65-76

Nern A, Arkowitz RA (1999) A Cdc24p-Far1p-Gbetagamma protein complex required for yeast orientation during mating. *J Cell Biol* **144**: 1187-1202

Nern A, Arkowitz RA (1998) A GTP-exchange factor required for cell orientation. *Nature* **391**: 195-198

Nern A, Arkowitz RA (2000) G proteins mediate changes in cell shape by stabilizing the axis of polarity. *Mol Cell* **5**: 853-864

Nishikimi A, Fukuhara H, Su W, Hongu T, Takasuga S, Mihara H, Cao Q, Sanematsu F, Kanai M, Hasegawa H, Tanaka Y, Shibasaki M, Kanaho Y, Sasaki T, Frohman MA, Fukui Y (2009) Sequential regulation of DOCK2 dynamics by two phospholipids during neutrophil chemotaxis. *Science* **324**: 384-387

Nishimura T, Yamaguchi T, Kato K, Yoshizawa M, Nabeshima Y, Ohno S, Hoshino M, Kaibuchi K (2005) PAR-6-PAR-3 mediates Cdc42-induced Rac activation through the Rac GEFs STEF/Tiam1. *Nat Cell Biol* **7**: 270-277

Nishio M, Watanabe K, Sasaki J, Taya C, Takasuga S, Iizuka R, Balla T, Yamazaki M, Watanabe H, Itoh R, Kuroda S, Horie Y, Forster I, Mak TW, Yonekawa H, Penninger JM, Kanaho Y, Suzuki A, Sasaki T (2007) Control of cell polarity and motility by the PtdIns(3,4,5)P3 phosphatase SHIP1. *Nat Cell Biol* **9**: 36-44

O'Donnell M, Chance RK, Bashaw GJ (2009) Axon growth and guidance: receptor regulation and signal transduction. *Annu Rev Neurosci* **32**: 383-412

Onischenko E, Stanton L, Madrid A, Kieselbach T, Weis K (2009) Role of the Ndc1 interaction network in yeast nuclear pore complex assembly and maintenance. *J Cell Biol* **185**: 475-491

Palanivelu R, Preuss D (2000) Pollen tube targeting and axon guidance: parallels in tip growth mechanisms. *Trends Cell Biol* **10**: 517-524

Paliwal S, Iglesias PA, Campbell K, Hilioti Z, Groisman A, Levchenko A (2007) MAPK-mediated bimodal gene expression and adaptive gradient sensing in yeast. *Nature* **446**: 46-51

Parent CA, Blacklock BJ, Froehlich WM, Murphy DB, Devreotes PN (1998) G protein signaling events are activated at the leading edge of chemotactic cells. *Cell* **95**: 81-91

Parent CA, Devreotes PN (1999) A cell's sense of direction. *Science* **284**: 765-770

Park HO, Bi E, Pringle JR, Herskowitz I (1997) Two active states of the Ras-related Bud1/Rsr1 protein bind to different effectors to determine yeast cell polarity. *Proc Natl Acad Sci USA* **94**: 4463-4468

Peter M, Gartner A, Horecka J, Ammerer G, Herskowitz I (1993) *FAR1* links the signal transduction pathway to the cell cycle machinery in yeast. *Cell* **73**: 747-760

Peter M, Herskowitz I (1994) Joining the complex: cyclin-dependent kinase inhibitory proteins and the cell cycle. *Cell* **79**: 191-194

Postlethwaite AE, Snyderman R, Kang AH (1976) The chemotactic attraction of human fibroblasts to a lymphocyte-derived factor. *J Exp Med* **144**: 1188-1203

Postma M, Van Haastert PJ (2001) A diffusion-translocation model for gradient sensing by chemotactic cells. *Biophys J* **81**: 1314-1323

Pruyne D, Bretscher A (2000a) Polarization of cell growth in yeast. I. Establishment and maintenance of polarity states. *J Cell Sci* **113** (Pt 3): 365-375

Pruyne D, Bretscher A (2000b) Polarization of cell growth in yeast. *J Cell Sci* **113** (Pt 4): 571-585

Pruyne D, Legesse-Miller A, Gao L, Dong Y, Bretscher A (2004) Mechanisms of polarized growth and organelle segregation in yeast. *Annu Rev Cell Dev Biol* **20**: 559-591

Raper J, Mason C (2010) Cellular strategies of axonal pathfinding. *Cold Spring Harb Perspect Biol* **2**: a001933

Reed SI, Hadwiger JA, Lorinez AT (1985) Protein kinase activity associated with the product of the yeast cell division cycle gene *CDC28*. *Proc Natl Acad Sci USA* **82**: 4055-4059

Sabatier C, Plump AS, Le M, Brose K, Tamada A, Murakami F, Lee EY, Tessier-Lavigne M (2004) The divergent Robo family protein rig-1/Robo3 is a negative regulator of slit responsiveness required for midline crossing by commissural axons. *Cell* **117**: 157-169

Sagot I, Klee SK, Pellman D (2002) Yeast formins regulate cell polarity by controlling the assembly of actin cables. *Nat Cell Biol* **4**: 42-50

Salcedo-Tello P, Ortiz-Matamoros A, Arias C (2011) GSK3 function in the brain during development, neuronal plasticity, and neurodegeneration. *Int J Alzheimers Dis* **2011**: 1-12

Sasaki AT, Chun C, Takeda K, Firtel RA (2004) Localized Ras signaling at the leading edge regulates PI3K, cell polarity, and directional cell movement. *J Cell Biol* **167**: 505-518

Sasaki AT, Firtel RA (2006) Regulation of chemotaxis by the orchestrated activation of Ras, PI3K, and TOR. *Eur J Cell Biol* **85**: 873-895

Sasaki AT, Janetopoulos C, Lee S, Charest PG, Takeda K, Sundheimer LW, Meili R, Devreotes PN, Firtel RA (2007) G protein-independent Ras/PI3K/F-actin circuit regulates basic cell motility. *J Cell Biol* **178**: 185-191

Schrick K, Garvik B, Hartwell LH (1997) Mating in *Saccharomyces cerevisiae*: The role of the pheromone signal transduction pathway in the chemotropic response to pheromone. *Genetics* **147**: 19-32

Schwamborn JC, Puschel AW (2004) The sequential activity of the GTPases Rap1B and Cdc42 determines neuronal polarity. *Nat Neurosci* **7**: 923-929

Segall JE (1993) Polarization of yeast cells in spatial gradients of a mating factor. *Proc Natl Acad Sci USA* **90**: 8332-8336

Servant G, Weiner OD, Herzmark P, Balla T, Sedat JW, Bourne HR (2000) Polarization of chemoattractant receptor signaling during neutrophil chemotaxis. *Science* **287**: 1037-1040

Servant G, Weiner OD, Neptune ER, Sedat JW, Bourne HR (1999) Dynamics of a chemoattractant receptor in living neutrophils during chemotaxis. *Mol Biol Cell* **10:** 1163-1178

Shekarabi M, Kennedy TE (2002) The netrin-1 receptor DCC promotes filopodia formation and cell spreading by activating Cdc42 and Rac1. *Mol Cell Neurosci* **19**: 1-17

Shekarabi M, Moore SW, Tritsch NX, Morris SJ, Bouchard JF, Kennedy TE (2005) Deleted in colorectal cancer binding netrin-1 mediates cell substrate adhesion and recruits Cdc42, Rac1, Pak1, and N-WASP into an intracellular signaling complex that promotes growth cone expansion. *J Neurosci* **25**: 3132-3141

Sherman F, Fink GR, Hicks JB Eds (1986) Laboratory course manual for methods in yeast genetics. Cold Spring Harbor, NY: Cold Spring Harbor Laboratory Press

Sheu YJ, Santos B, Fortin N, Costigan C, Snyder M (1998) Spa2p interacts with polarity proteins and signaling components involved in yeast cell morphogenesis. *Mol Cell Biol* **18**: 4053-4069

Shi SH, Cheng T, Jan LY, Jan YN (2004) APC and GSK-3beta are involved in mPar3 targeting to the nascent axon and establishment of neuronal polarity. *Curr Biol* **14**: 2025-2032

Shi SH, Jan LY, Jan YN (2003) Hippocampal neuronal polarity specified by spatially localized mPar3/mPar6 and PI 3-kinase activity. *Cell* **112**: 63-75

Shimada Y, Wiget P, Gulli MP, Bi E, Peter M (2004) The nucleotide exchange factor Cdc24p may be regulated by auto-inhibition. *EMBO J* **23**: 1051-1062

Skupsky R, Losert W, Nossal RJ (2005) Distinguishing modes of eukaryotic gradient sensing. *Biophys J* **89**: 2806-2823

Slessareva JE, Routt SM, Temple B, Bankaitis VA, Dohlman HG (2006) Activation of the phosphatidylinositol 3-kinase Vps34 by a G protein alpha subunit at the endosome. *Cell* **126**: 191-203

Snetselaar KM, Bolker M, Kahmann R (1996) *Ustilago maydis* mating hyphae orient their growth toward pheromone sources. *Fungal Genet Biol* **20**: 299-312

Song J, Dohlman HG (1996) Partial constitutive activation of pheromone responses by a palmitoylation-site mutant of a G protein alpha subunit in yeast. *Biochemistry* **35**: 14806-14817

Srinivasan S, Wang F, Glavas S, Ott A, Hofmann F, Aktories K, Kalman D, Bourne HR (2003) Rac and Cdc42 play distinct roles in regulating PI(3,4,5)P3 and polarity during neutrophil chemotaxis. *J Cell Biol* **160**: 375-385

Stefan CJ, Overton MC, Blumer KJ (1998) Mechanisms governing the activation and trafficking of yeast G protein-coupled receptors. *Mol Biol Cell* **9**: 885-899

Stein E, Tessier-Lavigne M (2001) Hierarchical organization of guidance receptors: silencing of netrin attraction by slit through a Robo/DCC receptor complex. *Science* **291**: 1928-1938

Stone DE, Cole GM, de Barros Lopes M, Goebl M, Reed SI (1991) N-myristoylation is required for function of the pheromone-responsive G alpha protein of yeast: Conditional activation of the pheromone response by a temperature-sensitive N-myristoyl transferase. *Genes Dev* **5**: 1969-1981

Strickfaden SC, Pryciak PM (2008) Distinct roles for two Gα-Gβ interfaces in cell polarity control by a yeast heterotrimeric G protein. *Mol Biol Cell* **19**: 181-197

Subramanian KK, Narang A (2004) A mechanistic model for eukaryotic gradient sensing: spontaneous and induced phosphoinositide polarization. *J Theor Biol* **231**: 49-67

Suchkov DV, DeFlorio R, Draper E, Ismael A, Sukumar M, Arkowitz R, Stone DE (2010) Polarization of the yeast pheromone receptor requires its internalization but not actin-dependent secretion. *Mol Biol Cell* **21**: 1737-1752

Takeda K, Sasaki AT, Ha H, Seung HA, Firtel RA (2007) Role of phosphatidylinositol 3-kinases in chemotaxis in *Dictyostelium*. *J Biol Chem* **282**: 11874-11884

Terrell J, Shih S, Dunn R, Hicke L (1998) A function for monoubiquitination in the internalization of a G protein-coupled receptor. *Mol Cell* **1**: 193-202

Thiery JP (1984) Mechanisms of cell migration in the vertebrate embryo. *Cell Differ* **15**: 1-15

Tojima T, Hines JH, Henley JR, Kamiguchi H (2011) Second messengers and membrane trafficking direct and organize growth cone steering. *Nat Rev Neurosci* **12**: 191-203

Tranquillo RT, Lauffenburger DA, Zigmond SH (1988) A stochastic model for leukocyte random motility and chemotaxis based on receptor binding fluctuations. *J Cell Biol* **106**: 303-309

Ueda M, Sako Y, Tanaka T, Devreotes P, Yanagida T (2001) Single-molecule analysis of chemotactic signaling in *Dictyostelium* cells. *Science* **294**: 864-867

Vallier L, Segall J, Snyder M (2002) The α-factor receptor C-terminus is important for mating projection formation and orientation in *Saccharomyces cerevisiae*. *Cell Motil Cytoskel* **53**: 251-266

Valtz N, Peter M, Herskowitz I (1995) *FAR1* is required for oriented polarization of yeast cells in response to mating pheromones. *J Cell Biol* **131**: 863-873

Veltman DM, Keizer-Gunnik I, Van Haastert PJ (2008) Four key signaling pathways mediating chemotaxis in *Dictyostelium discoideum*. *J Cell Biol* **180**: 747-753

Veltman DM, Van Haastert PJ (2006) Guanylyl cyclase protein and cGMP product independently control front and back of chemotaxing *Dictyostelium* cells. *Mol Biol Cell* **17**: 3921-3929

Wach A, Brachat A, Pohlmann R, Philippsen P (1994) New heterologous modules for classical or PCR-based gene disruptions in *Saccharomyces cerevisiae*. *Yeast* **10**: 1793-1808

Wahl S, Barth H, Ciossek T, Aktories K, Mueller BK (2000) Ephrin-A5 induces collapse of growth cones by activating Rho and Rho kinase. *J Cell Biol* **149**: 263-270

Wang F, Herzmark P, Weiner OD, Srinivasan S, Servant G, Bourne HR (2002) Lipid products of PI(3)Ks maintain persistent cell polarity and directed motility in neutrophils. *Nat Cell Biol* **4**: 513-518

Wang Y, Chen CL, Iijima M (2011) Signaling mechanisms for chemotaxis. *Develop Growth Differ* **53**: 495-502

Weiner OD (2002) Regulation of cell polarity during eukaryotic chemotaxis: the chemotactic compass. *Curr Opin Cell Biol* **14**: 196-202

Weiner OD, Neilsen PO, Prestwich GD, Kirschner MW, Cantley LC, Bourne HR (2002) A PtdInsP(3)- and Rho GTPase-mediated positive feedback loop regulates neutrophil polarity. *Nat Cell Biol* **4**: 509-513

Wiget P, Shimada Y, Butty AC, Bi E, Peter M (2004) Site-specific regulation of the GEF Cdc24p by the scaffold protein Far1p during yeast mating. *EMBO J* **23**: 1063-1074

Williams MR, Azcutia V, Newton G, Alcaide P, Luscinskas FW (2011) Emerging mechanisms of neutrophil recruitment across endothelium. *Trends Immunol* **32**: 461-469

Xiao Z, Zhang N, Murphy DB, Devreotes PN (1997) Dynamic distribution of chemoattractant receptors in living cells during chemotaxis and persistent stimulation. *J Cell Biol* **139**: 365-374

Xiong Y, Huang CH, Iglesias PA, Devreotes PN (2010) Cells navigate with a local-excitation, global-inhibition-biased excitable network. *Proc Natl Acad Sci USA* **107**: 17079-17086

Xu X, Meier-Schellersheim M, Yan J, Jin T (2007) Locally controlled inhibitory mechanisms are involved in eukaryotic GPCRmediated chemosensing. *J Cell Biol* **178**: 141-153

Xue C, Hsueh YP, Heitman J (2008) Magnificent seven: Roles of G protein-coupled receptors in extracellular sensing in fungi. *FEMS Microbiol Rev* **32**: 1010-1032

Yang L, Garbe DS, Bashaw GJ (2009) A frazzled/DCC-dependent transcriptional switch regulates midline axon guidance. *Science* **324**: 944-947

Yoshimura T, Arimura N, Kawano Y, Kawabata S, Wang S, Kaibuchi K (2006) Ras regulates neuronal polarity via the PI3-kinase/Akt/GSK-3beta/CRMP-2 pathway. *Biochem Biophys Res Commun* **340**: 62-68

Yu L, Qi M, Sheff MA, Elion EA (2008) Counteractive control of polarized morphogenesis during mating by mitogen-activated protein kinase Fus3 and G1 cyclin-dependent kinase. *Mol Biol Cell* **19**: 1739-1752

Zigmond SH (1977) Ability of polymorphonuclear leukocytes to orient in gradients of chemotactic factors. *J Cell Biol* **75**: 606-616

Zmuda JF, Rivas RJ (1998) The Golgi apparatus and the centrosome are localized to the sites of newly emerging axons in cerebellar granule neurons *in vitro*. *Cell Motil Cytoskeleton* **41**: 18-38

Zumbrunn J, Kinoshita K, Hyman AA, Nathke IS (2001) Binding of the adenomatous polyposis coli protein to microtubules increases microtubule stability and is regulated by GSK3 beta phosphorylation. *Curr Biol* **11**: 44-49

VITA

NAME:	Reagan E. DeFlorio
EDUCATION:	B.S. Biology, Butler University, Indianapolis, Indiana, 2003
	Ph.D. Molecular Biology, University of Illinois at Chicago, Chicago, Illinois, 2012
TEACHING EXPERIENCE:	Department of Biological Sciences, University of Illinois at Chicago, Chicago, Illinois: Mendelian and Molecular Genetics, 2006-2012
	Department of Biological Sciences, University of Illinois at Chicago, Chicago, Illinois: Biology of Cells and Organisms, 2005-2006
HONORS:	Programme Eiffel Bourse D'Excellence, September 2010 to July 2011
	EMBO Short-term fellowship ASTF 196-2009, Summer 2009
	Excellence in Teaching Mendelian and Molecular Genetics, University of Illinois at Chicago, Chicago, Illinois: 2010, 2009, 2008, and 2007
	Excellence in Teaching Biology of Cells and Organisms, University of Illinois at Chicago, Chicago, Illinois: 2006
ABSTRACTS:	DeFlorio R, Arkowitz R, Stone D: Gβ phosphorylation plays a role in chemotropic growth during the yeast mating response Yeast Genetics and Molecular Biology Meeting. Vancouver, Canada, 2010.
	DeFlorio R, Eskara J, Stone D: The Role of Gβ phosphorylation during the yeast mating response. Yeast Genetics and Molecular Biology Meeting. Toronto, Canada, 2008.
PUBLICATIONS:	Suchkov D, DeFlorio R, Draper E, Ismael A, Sukumar M, Arkowitz R, Stone D (2010) Polarization of the yeast pheromone receptor requires its internalization but not actin-dependent secretion. *Mol Biol Cell* **21**: 1737-1752